



Ph.D Dissertation

Niousha Taherzadeh

CHRISTIAN-ALBRECHTS-UNIVERSITÄT ZU KIEL

**Phytoplankton Community Response
to Multiple Stressors: a Trait-based
Modeling Approach**

Dissertation

in fulfillment of the requirements for the degree of "Dr. rer. nat."

of the Faculty of Mathematics and Natural Sciences

at Kiel University

Submitted by

Niousha Taherzadeh

Munich, 2018

First referee: Prof. Dr. Kai. W. Wirtz

Second referee: Prof. Dr. Birgit Schneider

Date of the oral examination: 26.10.2018

“If you can imagine it, you can achieve it! If you can dream it, you can become it!”

-William Arthur Ward

To My Lovely Family ♡

Declaration

I hereby declare that this work:

a) apart from the supervisor's guidance the content and design of the thesis is all my own work,

b) the thesis has not already been submitted either partially or wholly as part of a doctoral degree to another examining body and it has not been published or submitted for publication,

c) that the thesis has been prepared subject to the Rules of Good Scientific Practice of the German Research Foundation.

Niousha Taherzadeh

Kiel, 24 July 2018

Abstract

This thesis based on trait-based modeling approach and long term mesocosms data is the first modeling study, which mechanistically and systematically investigated the impact of interplay of multiple stressors and phytoplankton physiological properties on shaping the community size structure.

Using a trait-based modeling approach with assuming cell size as the master trait, this study illustrates (i) how uncertainties in allometric relationship of major growth-nutrient uptake traits influence the size structure of the community, (ii) how community composition responds to bottom up control via nutrient enrichment from deep nutrient rich water, (iii) how nutrient enrichment and removal of grazers as two concurrently occurring multiple stressors reshape the community structure and why/when additive/non-additive interaction types are observed, (iv) how elevated CO₂ and zooplankton (by selective grazing) (in)directly influence the community. A central question then will be how phytoplankton community response to a combination of stressors, and how this response is governed by trade-offs between eco-physiological traits.

The thesis is organized along three interlinked chapters. The first chapter addresses importance of allometric relationship of major growth-nutrient uptake traits, which are introduced into a size-based multi-species nutrient-phytoplankton-detritus model to obtain a more realistic phytoplankton dynamic under periodic nutrient enrichment. Considerable uncertainty in these allometries, hence, limits ones ability to link them to observed changes in phytoplankton community structures. Using the model, this chapter focuses on assessing the sensitivity of the predicted community size structure to variations in allometric coefficients. This work is the first systematic sensitivity study on allometric relationships of physiological traits in phytoplankton. A unimodal pattern of diatoms mean cell size over various nutrient replenishment periods with the maximum at intermediate periods is demonstrated. Lower nutrient subsistence demand of larger diatoms is found to be crucial to promote them under intermediate mixing periodicities. Non-uniform scaling in maximum growth rate is suggested to be helpful in preventing dominance of unrealistically small (diatoms) species.

Secondly, the previously developed model is extended to resolve multi-species phytoplankton-nutrients-detritus-zooplankton dynamics within the upper mixed layer. The data validated model is used to systematically investigate the response of phytoplankton community to a combination of major natural stressors, nutrient enrichment and grazer removal, thus, explain

underlying mechanisms leading to (non)additive interactions of stressors. A novel approach is proposed here to correlated community net growth rate to sudden shifts in the environmental conditions and linking it with trait-mediated adaptive response helped to assess why and when non-additive interactions are observed. Two variables, cross-trait variation (CTV) and the specific multi-stressor sensitivity (SMS), are proposed here to track and predict the community re-organization under the impacts of multiple stressors over time. Our results reveal a relatively uniform relationship between CTV and SMS throughout time, independently whether nutrient or grazing stress has been varied. Synergistic effects exclusively occur at positive cross-variations in traits, thus when effective traits shift to higher values under application of complementary stressors, which here means increased nutrient usage ability under grazing removal and increased grazing susceptibility under nutrient pulses. This study reveals that synergistic effects need time to evolve, thus highlighting the role of duration of experiment. The proposed trait-based explanatory framework can be used to mechanistically assess and probably predict the effects of other stressor combinations and organism groups.

Finally, the extended model is adopted to assess the net impact of elevated CO₂ and selective grazing on the phytoplankton community as experimental studies investigating their impacts are equivocal and model studies rare. The significant impact of ocean acidification on the phytoplankton community under nutrient depletion is highlighted. A critical role of herbivorous grazers is presented as the most important drivers controlling the structure of community under nutrient limitation due to both direct/indirect effects. Direct effects of ocean acidification on the phytoplankton community is illustrated that can either be damped or amplified by indirect effects through higher trophic levels.

Kurzfassung

Diese These basiert auf einem trait-basierten Modellierungsansatz und Langzeit-Mesokosmen-Daten ist die erste Modellierungsstudie, die den Einfluss des Zusammenspiels mehrerer Stressoren und der physiologischen Eigenschaften des Phytoplanktons auf die Gestaltung der Community-Größenstruktur mechanistisch und systematisch untersucht.

Unter Verwendung eines trait-basierten Modellierungsansatzes mit der Annahme der Zellgröße als Hauptmerkmal zeigt diese Studie (i) wie Unsicherheiten in der allometrischen Beziehung der wichtigsten Wachstums-Nährstoff-Aufnahmeigenschaften die Größenstruktur der Gemeinschaft beeinflussen, (ii) wie die Zusammensetzung der Gemeinschaft auf die Bottom-up-Kontrolle durch Nährstoffanreicherung aus tiefem nährstoffreichem Wasser reagiert, (iii) wie die Nährstoffanreicherung und die Entfernung von Weidegängern als zwei gleichzeitig auftretende Mehrfachstressoren die Gemeinschaftsstruktur umgestalten und warum/wenn additive/nicht-additive Interaktionstypen beobachtet werden, (iv) wie erhöhte CO₂ und Zooplankton (durch selektive Beweidung) (in)direkt die Gemeinschaft beeinflussen. Eine zentrale Frage wird dann sein, wie die Phytoplanktongemeinschaft auf eine Kombination von Stressoren reagiert und wie diese Reaktion durch Kompromisse zwischen ökophysiologischen Merkmalen gesteuert wird.

Die Dissertation ist in drei miteinander verknüpfte Kapitel gegliedert. Das erste Kapitel befasst sich mit der Bedeutung der allometrischen Beziehung der wichtigsten Wachstums-Nährstoffaufnahme Merkmale, die in eine Größe-basierte Multi-Spezies Nährstoff-Phytoplankton-Detritus-Modell, um eine realistischere Phytoplankton Dynamik unter periodischen Nährstoffanreicherung. Erhebliche Unsicherheit in diesen Allometrien schränkt daher die Möglichkeit ein, sie mit beobachteten Veränderungen der Phytoplankton-Gemeinschaftsstrukturen zu verknüpfen. Mit Hilfe des Modells konzentriert sich dieses Kapitel auf die Beurteilung der Sensitivität der vorhergesagten Gemeindegroßenstruktur gegenüber Schwankungen der allometrischen Koeffizienten. Diese Arbeit ist die erste systematische Sensitivitätsstudie über allometrische Beziehungen von physiologischen Merkmalen im Phytoplankton. Ein unimodales Muster von Diatomeen zeigt die mittlere Zellgröße über verschiedene Nährstoffnachschiebephasen mit dem Maximum an Zwischenphasen. Ein geringerer Nährstoffbedarf größerer Diatomeen ist entscheidend, um sie unter mittleren Mischperiodizitäten zu fördern. Eine ungleichmäßige Skalierung der maximalen Wachstumsrate wird empfohlen, um die Dominanz von unrealistisch kleinen (Diatomeen) Arten zu verhindern.

Zweitens wird das zuvor entwickelte Modell erweitert, um die Phytoplankton-Nährstoff-Detritus-Zooplankton-Dynamik in der oberen Mischschicht aufzulösen. Das Daten validierte Modell wird verwendet, um systematisch die Reaktion der Phytoplanktongemeinschaft auf eine Kombination von wichtigen natürlichen Stressoren, Nährstoffanreicherung und Weidegang zu untersuchen und so die zugrunde liegenden Mechanismen zu erklären, die zu (nicht-)additiven Wechselwirkungen von Stressoren führen. Ein neuartiger Ansatz wird hier vorgeschlagen, um die Netto-Wachstumsrate der Gemeinschaft mit plötzlichen Veränderungen der Umweltbedingungen in Beziehung zu setzen und sie mit einer durch Merkmale vermittelten adaptiven Reaktion zu verknüpfen, die dazu beiträgt, zu beurteilen, warum und wann nicht-additive Wechselwirkungen beobachtet werden. Zwei Variablen, Cross-Trait-Variation (CTV) und die spezifische Multi-Stressor-Empfindlichkeit (SMS), werden hier vorgeschlagen, um die Reorganisation der Gemeinschaft unter den Auswirkungen von mehreren Stressoren im Laufe der Zeit zu verfolgen und vorherzusagen. Unsere Ergebnisse zeigen ein relativ einheitliches Verhältnis zwischen CTV und SMS über die Zeit, unabhängig davon, ob Nährstoff- oder Beweidungsstress variiert wurde. Synergieeffekte treten ausschließlich bei positiven Kreuzvariationen in Traits auf, also wenn sich effektive Traits unter Anwendung von komplementären Stressoren auf höhere Werte verlagern, was hier eine erhöhte Nährstoffverwertung unter Weidentfernung und eine erhöhte Weideanfälligkeit unter Nährstoffimpulsen bedeutet. Diese Studie zeigt, dass synergistische Effekte Zeit brauchen, um sich zu entwickeln, und unterstreicht damit die Rolle der Dauer des Experiments. Der vorgeschlagene merkmalsbasierte Erklärungsrahmen kann verwendet werden, um die Auswirkungen anderer Stressor-Kombinationen und Organismengruppen mechanistisch zu bewerten und wahrscheinlich vorherzusagen.

Schließlich wird das erweiterte Modell verwendet, um die Nettoauswirkungen von erhöhtem CO₂ und selektiver Beweidung auf die Phytoplanktongemeinschaft zu bewerten, da experimentelle Studien, die ihre Auswirkungen untersuchen, zweideutig und Modellstudien selten sind. Der signifikante Einfluss der Ozeanversauerung auf die Phytoplankton-Gemeinschaft unter Nährstoffzufuhr wird hervorgehoben. Eine kritische Rolle der pflanzenfressenden Gräserfresser wird als die wichtigsten Treiber dargestellt, die die Struktur der Gemeinschaft unter Nährstoffeinschränkung durch direkte/indirekte Effekte kontrollieren. Es werden direkte Effekte der Ozeanversauerung auf die Phytoplanktongemeinschaft dargestellt, die entweder gedämpft oder durch indirekte Effekte durch höhere trophische Ebenen verstärkt werden können.

Contents

Declaration	iv
Abstract	vii
Kurzfassung	i
List of Figures	iv
List of Tables	viii
Acknowledgments	ix
Preface	xi
1. Introduction	1
1.1. Structure of the PhD project	3
1.1.1. Aims	3
1.1.2. Outline	3
2. Can We Predict Phytoplankton Community Size Structure Using Size Scalings of Eco-Physiological Traits?	5
2.1. Abstract	5
2.2. Introduction	6
2.3. Model	7
2.3.1. Model description	7
2.3.2. Model parameterization	10
2.3.3. Model simulation and variation experiments	12
2.4. Results	13
2.5. Discussion	18
2.5.1. Community response to nutrient supply	18
2.5.2. Size structure of marine diatoms	18
2.5.3. Size structure of marine phytoplankton	20

2.5.4. Limitations of our approach	21
2.6. Conclusion	22
3. A trait-based framework for explaining non-additive effects of multiple stressors on plankton communities	24
3.1. Abstract	24
3.2. Introduction	25
3.3. Methods and material	26
3.3.1. Model definition	26
3.3.2. Multi-stressor effects	27
3.3.3. Model initialization and parameterization	28
3.3.4. Validation data and environmental forcings	29
3.3.5. Numerical stressor experiments and interaction traits	29
3.4. Results	30
3.4.1. Model validation	30
3.4.2. Stressor effects	32
3.4.3. Switching off adaptive responses	34
3.4.4. Effect size dependent on adaptive capacity	35
3.4.5. Changes in multi-stressor sensitivity over cross-trait variations	36
3.5. Discussion	37
4. Interplay of ocean acidification with zooplankton towards shaping phytoplankton community	42
4.1. Abstract	42
4.2. Introduction	43
4.3. Method and material	43
4.3.1. Model	43
4.3.2. Numerical experiments	44
4.4. Results	44
4.4.1. The separate effects of grazing and acidification on phytoplankton biomass	44
4.4.2. Changes in the community size structure and biodiversity	48
4.5. Discussion and conclusion	50
Bibliography	54
A. Appendix I	65
A.1. Equilibrium solution to the size-based multi-species model	65
A.2.	67
A.3.	67

B. Appendix II	68
B.1. Model description	68
B.1.1. Model parameters	73
B.2. Allometric relationships of physiological traits	74
B.3. Multi-stressors effect	75
B.3.1. Specific multistressor effect size	75
B.3.2. Effective interaction traits	76
B.3.3. Cross-over trait sensitivity and trade-offs	77
B.4. Supplementary figures	78
B.5. Mono species scenario	78
B.6. Sensitivity analysis	79
C. Appendix III	81
C.1. Individual mesocosms	81
C.2. Cosinodiscus dynamic	82

List of Figures

2.1. Schematic representation of the size-based multi-species model for the surface ocean, which resolves: phytoplankton (Phy), intracellular nutrient quota (Q), nutrient (Nut) and detritus (Det).	8
2.2. Size dependency of maximum growth rate (μ_{\max}) used in this study. Data for μ_{\max} are obtained from [32].	12
2.3. Biomass dynamics of 29 marine diatoms (Di-L0) over 1000 days. Each panel shows the model outcome for a different environmental setting with $\text{Nut}_{\text{in}} = 60 \text{ mmol-N m}^{-3}$ and : a) short , b) intermediate , and c) long replenishment period T	14
2.4. Community composition in terms of mean cell size (a, c) and size variance (b, d) varying over inflow nutrient concentration and nutrient mixing intervals for Di-L1 scenario (a-b); and varying across mixing intervals with a constant $\text{Nut}_{\text{in}} = 60 \text{ mmol-N m}^{-3}$ for different allometric relationships in μ_{\max} (c-d). The μ_{\max} allometries comprise linear (“L”) and non-linear scalings (“NL”) for both diatoms (“Di”) and the entire marine phytoplankton community (“All”): linear scaling for diatoms is applied to either the entire size spectrum (“Di-L0”) or the restricted spectrum above $1 \log_e \text{ESD}$ (“Di-L1”).	15
2.5. Changes in community mean cell size when neglecting allometric relationships one at a time. Thick black line: allometries show in Table B.7 and grey bars: neutral allometry experiment. Di-L0 (a-c) and Di-L1 (d-f): diatom scenarios with linear μ_{\max} over cell volume ranges $1 - 10^7 \mu\text{m}^3$ and $10 - 10^7 \mu\text{m}^3$, respectively., Di-NL: diatom scenario with non-linear μ_{\max} (g-i)., All-L (j-l) and All-NL (m-o): all species community scenarios with assumed linear and non-linear μ_{\max} , respectively. For symbols, see Table 2.2.	17

3.1. Schematic representation of the size-based multi-species model resolving biomass of phytoplankton species (Phy_i with $i=1, \dots, n$), their internal nutrient quotas (Q_i), ambient nutrient concentration (Nut), detritus (Det) and zooplankton, further subdivided into small and large ciliates (Cil-S, Cil-L) and copepods (Cop). N: Nitrogen, P: Phosphorous, C: Carbon, T: Temperature and PAR: Photosynthetically Active Radiation.	27
3.2. Comparison between chlorophyll a (chl_a), dissolved inorganic nitrogen and phosphorous concentration (DIN, DIP) of the reference run and measured data for the control (LpCO_2 , blue) and treated (HpCO_2 , red) mesocosms. Solid lines and diamonds represent model results and measured data respectively. Dashed lines separate different phases of the experiment: initial, first and second spring bloom, and post bloom.	31
3.3. Specific rates and phytoplankton biomass distribution for the reference run under high $p\text{CO}_2$ condition (HpCO_2). Figure A shows total phytoplankton production and loss rates, and figure B represents individual phytoplankton biomass distribution over the time of experiment. Dashed lines denote different phases of the experiment: initial, first and second spring bloom, and post bloom.	32
3.4. Comparison of phytoplankton total production and loss terms between the mono species model configuration (top panels) and the one with multi species (bottom panels) under single/multiple stressors. +Nut and -Zoo represent two stressors corresponding to nutrient enrichment and grazer removal. The solid line shows relative growth rate (production-loss) of the entire community. The dashed line indicates the time of stressor application.	33
3.5. Nitrogen concentration, copepod biomass and phytoplankton biomass distribution under single /multiple stressors. +Nut and -Zoo represent two stressors corresponding to nutrient enrichment and grazer removal. Dashed lines indicate the time of nutrient injection, zooplankton removal or both.	34
3.6. Changes in size dependent characteristics from the state before stressor application: in the contribution of each size class to total net growth rate, in the phytoplankton density distribution, and in interaction traits, the relative nutrient usage ability and susceptibility to copepod grazing. The difference is taken either 2 or 18 days after stressor exertion (see Δt).	36
3.7. Specific multi-stressor sensitivity (SMS) plotted over cross-trait variation (CTV) for 12 multi-stressor experiments. Nutrient input was varied from 0.2, 0.4, 0.8 to 1.6 mmolN m^{-3} and copepod removal from 0.4, 1.3 to 2.5 mmolC m^{-3}	37
4.1. Biomass comparison of copepods and ciliates observed in Kristineberg mesocosms experiment. Solid lines represent mean of each five treated and controlled mesocosms. Dashed line indicates the mean biomass calculated from all 10 mesocosms. Data was interpolated linearly.	45

4.2.	Impact of zooplankton on the phytoplankton biomass distribution. Left: scenario LCO ₂ +LCop with data from control mesocosms for <i>p</i> CO ₂ and grazers. Right: Difference between scenario LCO ₂ +LCop and HCO ₂ +HCop.	47
4.3.	Chl _{<i>a</i>} concentration during the second bloom. Dashed lines indicate simulations with different <i>p</i> CO ₂ conditions but the same values for zooplankton biomass. This zooplankton biomass is obtained from the mean of all 10 mesocosm experiments. Simulations plotted with solid lines were run with mean zooplankton data from treated or control mesocosms only.	48
4.4.	The temporal mean of relative biomass of species smaller than 9 μm ESD for different <i>p</i> CO ₂ conditions and grazing scenarios.	49
4.5.	Evenness, <i>E</i> , as index for biodiversity calculated in simulations for different grazing forcings in high and low <i>p</i> CO ₂ scenarios.	50
A.1.1	Equilibrium nutrient concentration over phytoplankton cell size for different values of equilibrium light intensity (Di-L0).	66
A.2.1	Comparison between simulation time of 1000 days and long term (10000 days) for change of diatom community mean cell size and size diversity (Di-NL, Nut _{in} = 60 mmol-N m ⁻³).	67
A.3.1	Change of diatom community mean size (a, c) and size diversity (b, d) over various inflow nutrient concentrations and mixing intervals for the Di-L0 scenario (a-b) and Di-NL scenario (c-d).	67
B.2.1	Allometric relationships used in the model for major growth-nutrient uptake parameters given in Table B.7.	74
B.5.1	Nitrogen concentration, copepod biomass and phytoplankton biomass distribution under single /multiple stressors. +Nut and -Zoo represent two stressors corresponding to nutrient enrichment and grazer removal. Dashed lines indicate the time of nutrient injection, zooplankton removal or both.	78
B.6.1	Measured Chl- <i>a</i> for 10 Kristineberg mesocosms from [5]. Red and blue indicate High CO ₂ and low CO ₂ conditions respectively.	79
B.6.2	Sensitivity analysis for Chl simulated in the reference configuration for low <i>p</i> CO ₂ condition. Parameters are varied by ±%20 of their original value. Descriptions and reference values of the parameters are listed in Tables B.7 and B.5.	80
C.1.1	Mesocosms with high Chl _{<i>a</i>} show a higher abundance of copepods during the second bloom. Zooplankton abundance data are available for day 49 and 57. We used the mean of both days for copepod abundance and Chl _{<i>a</i>} (μgC m ⁻³). Red dots indicate treated mesocosms, blue dots indicate control mesocosms.	81

C.2.1 Comparison between simulated and measured data for treated (red) and untreated (blue) environments. Simulation results indicate all species larger than 200 μm ESD. Solid lines indicate simulated results and diamonds represent measured data. 82

List of Tables

2.1. Model equations and major functions. Parameters are described in Table 2.2 and Table 2.3.	9
2.2. Model variables and allometric parameters.	10
2.3. Environmental parameters.	10
2.4. Size scaling of physiological parameters for marine diatoms and all marine species.	11
B.1. Model equations. Auxiliary variables and parameters are described in Table B.2– B.7. The subscript i distinguishes phytoplankton size classes and j the three zooplankton classes.	69
B.2. Primary production related rates. Parameters are described in Table B.3 – Table B.7.	70
B.3. Model sub functions and related variable parameters.	71
B.4. Model sub functions and related variable parameters (continue).	72
B.5. Parameters used in the reference run	73
B.6. Parameters used in the reference run	73
B.7. Size scaling of physiological parameters for phytoplankton adapted from [29] and [63]. The subscript ' i ' represents each phytoplankton species, V is the phytoplankton cell volume and L the natural logarithm of Equivalent Spherical Diameter.	74

Acknowledgments

This thesis would have not been possible without the support, friendship, dedication and assistance of numerous people. Foremost, I would like to thank my advisor Prof. Dr. Kai W. Wirtz for his constant and excellent support (scientific and psychological). I feel enormously privileged to have him as my advisor. Dear Kai, thank you for always being nice and patient, and encouraging me to be more strong to handle life negativities. You are one of the people who influenced my life in a positive way and I am always grateful to had the opportunity to work with you. I would like to thank my second advisor Dr. Onur Kerimoglu for his great support. My deepest gratitude goes to my colleague Dr. Carsten Lemman for his kindness and support. Dear Carsten, thank you for always accepting me with a smile whenever I needed help. Special thanks is for my dear ex-colleague and work partner Dr. Michael Bengfort, with whom I did great works. I would like to thank also my other colleagues Dr. Anja Singer, Dr. Wenyan and Dr. Richard Hofmeister for bringing positivity to my Ph.D life. I am just curious to know that, from now on who will eat half of my lunch!!

A special thanks goes to my second family here, Franz and Anja, who accepted me as a member of their family and supported me always.

My best childhood friends Hoda, Shirin, Asal, Atena and Elnaz! Thank you for being in happy and sad moments with me despite miles of distance. Dear Rahul, thank you so much for being with me whenever I reached to you and for listening to my complains! You are one of the nice and kind persons I have ever met.

Most importantly I thank my parents Lotfollah and Shamsi who always support me with their loves through these years, and tolerate their loneliness just for my sake to reach these days. Love you both!

Soulmaz, my beautiful sister and best friend, thank you for all your support and love. You bring smile on my face whenever I talk with you! I miss you every single moment! Howard, my lovely brother-in-law, thank you for your support specially in checking language mistakes despite of being so stranger with the topic! Welcome to our family!

Masha, my beautiful sister-in-law, thank you for your kindness and being always supportive. I am so happy to have you in my life as another sister and best friend.

Danial, my brother, my life mentor, I cannot find words to express my feelings toward you, since no words can describe them! I just want to say thank you thousands and thousands of

times for always supporting me and showing me the right path and encouraging me to leave my comfort zone! I am just wondering what would be the next challenge?!

And finally for sure challenging Ph.D life would not be tolerable without two sweet persons: my lovely nephew Elias and niece Sarah, who give an extra meaning to my life. You are Auntie's world! My loves of life!

Preface

This thesis is based on the following works:

- Taherzadeh, N., Kerimoglu, O., and Wirtz, K. W. (2017). Can we predict phytoplankton community size structure using size scalings of eco-physiological traits? *Ecological Modelling* 360, 279 – 289.

The idea originates from all authors. The model development, including coding, parameterization and numerical experiments were done by myself. I wrote the manuscript, which was improved by the second and last authors.

- Taherzadeh, N., Bengfort, M., and Wirtz K. W. (2018). A trait-based framework for explaining non-additive effects of multiple stressors on plankton communities, Submitted to *Frontier journal*.

The initial idea originates from the last author and myself. The model development, including coding, parameterization and validation were done by second author and myself; and partially was done by last author. I wrote the manuscript, which was improved by the last author.

- Taherzadeh, N., Bengfort, M., and Wirtz K. W. (2018). Interplay of ocean acidification with zooplankton towards shaping phytoplankton community

The initial idea originates from all authors. The model development, including coding, parameterization and validation were done by second author and myself; and partially was done by last author. Numerical experiments were done by second author. Second author wrote the manuscript, which was improved by myself and last author.

In preparation of this work several free and open source tools and resources have been used. I used Latex for writing, Python for model development and data post-processing, Bitbucket for source control.

1

Introduction

Marine phytoplankton, unicellular photosynthetic organisms, are responsible for approximately half of the primary production on earth [31] and are recognized as crucial indicators for alteration in the marine environment, as they usually respond quickly to a shift in environmental conditions. Every day, phytoplankton fix more than a hundred million tons of carbon; which is subsequently transferred into the aquatic ecosystem, sustaining secondary production in all higher trophic levels [20]. They, therefore, play a key role in ecological functioning and biogeochemical cycling of major elements such as carbon, nitrogen and phosphorous in aquatic ecosystems [40]. Hence, any alteration in phytoplankton community composition due to natural/anthropogenic stressors can in turn affect the success and composition of subsequent trophic levels, resulting in cascading consequences on aquatic ecosystems such as changes in food web dynamics [9, 47], total primary production [8] and biogeochemical cycling [40]. The importance of these consequences make studying of phytoplankton a prominent topic in plankton research, helping scientists to predict and understand the adaptive capabilities of natural communities to shifts in environmental conditions.

Although, empirical studies on phytoplankton in general investigate the effects of a single environmental variable at a time, in nature phytoplankton communities concurrently confront multiple environmental changes, i.e., stressors, such as nutrient enrichment, excessive grazing or ocean acidification. The net effect of such stressors usually cannot be predicted based only on their individual impacts, as stressors can moderate the effect of each other through unforeseen interactions, leading to "ecological surprises" [17]. The interactions between stressors typically involve net impacts that significantly vary from the sum of their individual effects (i.e. an additive effect) [35] defined as antagonistic or synergistic interactions where the net effects of stressors are lesser/greater than the additive effect. Despite the increase in research interest, large knowledge gap exists regarding to understand and predict the impact of multi-stressors on the phytoplankton communities and explaining when and where such stressors interactions are observed. In particular, It is difficult to fundamentally describe why interactions between

stressors are usually context dependent or varies over time/space [11]. Moreover, our knowledge is also limited due to lack of enough studies on assessing the effects of multi-stressors at the community level.

In particular, how phytoplankton communities restructure themselves under environmental perturbations depends on their flexibility in eco-physiological traits [58, 32]. The increase in availability of phytoplankton traits data stimulate the growing interest of ecologists in the assessing of responses of species traits to changes in environmental conditions [29].

"The existence of so great a diversity of species on Earth remains a mystery, ... the answer may lie in quantifying the trade-offs that organisms face in dealing with the constraints of their environment."

-David Tilman

Within this context, trait can be defined as any characteristic of phytoplankton that determines its fitness via its impact on production, growth and survival. Examples of such traits for phytoplankton are resource uptake, susceptibility to grazer or predator avoidance and morphological traits such as cell size [58]. Empirical studies suggest that the competitive abilities of species are constrained by various trade-offs [58, 29]. A significant portion of such relationships between traits are predicted by the phytoplankton cell size as a 'master trait' [32, 59, 62], as it has a very large influence on the individual eco-physiological traits. Existence of trade-offs explains why not everything can be maximized at the same time. For example, nutrient acquisition in phytoplankton is linked with the cell size, whereby small cells are dominant in low nutrient environments while big cells occupy nutrient rich environments [3]. On the other hand, bigger cell size enhances survival chances against predators. Such a trade-off between competitive ability versus grazer susceptibility is one of the most researched topics on understanding the community composition. Therefore, understanding the mechanisms controlling size structure of the community are, thus, of crucial importance for predicting the impact of climate change in the future.

Despite the increasing interest, our knowledge of phytoplankton community composition is still limited by lack of powerful numerical methods for analysing the effects of such traits on structure of the community [21]. The central theme of this thesis is thus to develop a trait-based plankton model that covers the trait-environment relationships. Whereas earlier work on phytoplankton resource competition focused on individual species or phytoplankton types, trait-based representations of phytoplankton communities are becoming increasingly popular [34]. Current nutrient-phytoplankton-zooplankton (NPZ) ecosystem models suffer from various problems. These models mechanistically describe specific species by grouping them into functional types (e.g. zooplankton, fish) and classifying the size (e.g. pico-, nano) which results in countless parameters. Thus, due to need for many fixed parameters and very few variables (adaptive ones), such models demonstrate the real systems in a static way. However, in nature, organisms and their environment are extremely adaptive entities, capable of responding to alteration in environmental conditions by adjusting behavior or regulating physiological traits. Therefore, popular alternative models to traditional NPZ models are trait-based models

as they are based on the eco-physiological traits of individual species and aim to reduce over-parameterizations problem by taking into account the trade-offs associated with key traits. The traits in these models are able to adapt to temporal environment by regulating their values, while arising trade-offs through balancing gains and costs prevent them from becoming unrealistic. Hence, the trait-based models allows a better representation of reality and can help to predict the responses of marine systems to ongoing global changes more accurately.

1.1. Structure of the PhD project

1.1.1. Aims

In the context of this work, we focused on the phytoplankton community response to shifts in environmental conditions governed by underlying phytoplankton eco-physiological traits and trade-offs between them. Accordingly, the scope of this thesis was divided into three phases:

1. tackling the uncertainty in allometric relationships of eco-physiological traits and effect of bottom-control via nutrient enrichment on the multi-species phytoplankton community,
2. gaining more insight about the underlying mechanisms leading to observation of non-additive interactions of multiple stressors.
3. systematically investigating the interplay of ocean acidification and selective grazing on shaping the phytoplankton community.

This thesis based on trait-based and multi-species modeling approach and long term mesocosms data is the first modeling study, which mechanistically and systematically investigated the impact of interplay of stressors and phytoplankton physiological properties on shaping the community size structure. In addition, it can be used as a guideline for the development of future size-structured ecosystem models and providing important insights for the interpretation of observed successional shifts in phytoplankton communities.

1.1.2. Outline

This work is composed of three chapters, where each is stand-alone manuscript having its own research question, methods and results.

Chapter 2 demonstrates the impact of uncertainties in size scalings of phytoplankton major nutrient-growth traits on the phytoplankton community under temporal changes in ambient nutrient concentration. For this study a size-based multi-species phytoplankton-detritus-nutrient model is developed and sets of numerical experiments were defined to systematically investigate the response of phytoplankton community at environments subjected to periodically nutrient enrichment. This study is the first study what systematically assesses the importance of allometric relationships of traits used in marine ecosystem models.

Chapter 3 presents response of the phytoplankton community to concurrently exerted multiple stressors and introduces a novel trait framework to link shifts in environmental conditions to underlying traits to assess when and where non-additive interactions of multi-stressors is observed. This work considers nutrient addition and grazer removal as two main stressors acting simultaneously on the community. Here, the previously developed model is extended to cover zooplankton dynamics and other external factors such as temperature, CO₂. The extended phytoplankton-nutrient-detritus-zooplankton model is validated by long term mesocosms experiments data from Kristineberg.

In the **Chapter 4**, the model, which, also includes size allometries for trophic interactions and for the sensitivity of primary production to ocean acidification, is adopted to assess the net impact of elevated CO₂ and selective grazing on the phytoplankton community as experimental studies investigating their impacts are equivocal and model studies rare.

2

*Can we predict phytoplankton community size structure using size Scalings of Eco-Physiological Traits?*¹

2.1. Abstract

Cell size is an important determining factor for predicting the physiological and ecological properties of phytoplankton. Size dependencies in eco-physiological properties are in general reported as log-log linear scaling relationships. Considerable uncertainty in these allometries, hence, limits our ability to link them to observed changes in phytoplankton community structures. In this study, we develop a size-based multi-species phytoplankton model and assess the sensitivity of the predicted community size structure to variations in allometric coefficients. The model describes the nutrient-phytoplankton-detritus dynamics within the upper mixed layer for a matrix of habitats, which are characterized by the deep layer nutrient concentration and mixing frequency. Predicted diatom community mean cell size becomes maximal at intermediate mixing frequencies, which confirms the importance of storage capacity (relative to the subsistence demand) at intermittent nutrient supplies. Smaller subsistence demand of large diatoms makes a critical factor in shaping the community size structure, while in environments with either short or long nutrient replenishment periods, maximum growth rate gains similar or more importance. Notably, in these environments, the diatom community converges towards unrealistically small species when we assumed a uniform (log-log linear) allometry in maximum growth rate. Independent theoretical and empirical arguments motivated the usage of non-uniform growth scaling, with which the minimal diatom cell size actually observed in nature is realized in long-term simulations. Using allometries parameterized for the entire

¹Taherzadeh, N., Kerimoglu, O., and Wirtz, K. W. (2017). Can we predict phytoplankton community size structure using size scalings of eco-physiological traits? *Ecological Modelling* 360, 279 – 289.

phytoplankton community, the subsistence advantage of the larger species becomes insignificant, leading to a ubiquitous dominance of smaller species, even when assuming non-uniform scaling in maximum growth rate. This finding corresponds with the observed dominance of pico-phytoplankton in many parts of the ocean. All combinations of physiological allometries for diatom or mixed communities, however, underestimate both the mean cell size of the community and also size diversity. This may indicate a significant role of other ecological selection mechanisms, such as arising from size-selective grazing. The approach outlined in this paper helps to better assess the limits and the potential of size based phytoplankton models as an increasingly important tool in plankton research.

Key words

Allometric scaling, Non-uniform scaling, Size-based model, Multi-species model, Community structure, Subsistence quota

2.2. Introduction

Unicellular photosynthetic organisms in the ocean are responsible for roughly half of the primary production on Earth [31], therefore, making a prominent subject of environmental research. Phytoplankton communities display high diversity with regard to the size of individual organisms, with cell volumes spanning more than nine orders of magnitude, from smallest cyanobacteria ($\sim 0.1 \mu\text{m}^3$) to the largest diatoms ($> 10^8 \mu\text{m}^3$) [32]. Phytoplankton cell size influences a large number of physiological traits as reviewed below and therefore plays a key role in ecological functioning and biogeochemical cycling of major elements such as carbon, nitrogen and phosphorous in aquatic ecosystems [40].

Given the importance of phytoplankton community structure in functioning of marine ecosystems, a better understanding of the factors controlling the structure of those communities is needed. Whereas earlier work on phytoplankton resource competition focused on individual species or phytoplankton types, trait-based representations of phytoplankton communities are becoming increasingly popular [34]. Empirical studies suggest that the competitive abilities of species are constrained by various trade-offs [58, 29]. A significant portion of such relationships between traits are predicted by the phytoplankton cell size as a ‘master trait’ [32, 59, 62], as it has a very large influence on the individual eco-physiological traits. For major physiological traits such as maximum growth rate (μ_{max}), maximum uptake rate (v_{max}), nutrient uptake affinity (A), and minimum and maximum intracellular nutrient quotas ($Q_{\text{min}}, Q_{\text{max}}$), power law functions of cell volume had been fitted based on collected data [e.g. 58, 29]:

$$y = \beta V^\alpha \tag{2.1}$$

where y represents the physiological trait, V phytoplankton cell volume (μm^3), β the intercept

(minimum or maximum value for the smallest cell size) and α the scaling exponent describing the size dependency of the trait. Using cell size for predicting eco-physiological traits in ecosystem models [e.g., 108, 111, 100, 1] helps reducing the parameterization complexity considerably. However, high uncertainties exist regarding the quantitative, and in some cases, qualitative form of these allometric relationships. For example, major uncertainties exist related to size scaling of maximum growth rate (μ_{\max}). For μ_{\max} reported size scaling exponents range from; -0.32 [86], -0.25 [29] similar to a specific metabolic rate [12], -0.13 for diatoms [84], -0.17 for dinoflagellates [6], -0.08 for Antarctic phytoplankton [95] to small values such as -0.06 for all marine phytoplankton [32]. In contrast to these fitted linear relationships between μ_{\max} and cell size, theoretical work by Wirtz [110], in agreement with the data compilation by Finkel et al. [32], proposed a unimodal function of μ_{\max} over cell size. Also, the recent experimental work of Marañón et al. [63] supports a unimodal, thus non-uniform allometry, with size scaling exponent of 0.19 for species with cell volume less than $300 \mu\text{m}^3$ and -0.15 for the ones with cell volume larger than $40 \mu\text{m}^3$.

Until now, no modeling study has performed a systematic investigation of the impact of uncertainties in allometric relationships on the prediction of the community composition and dynamics. It is also unclear to what extent physiological aspects can explain the observed size structure; or when other (ecological) aspects become major determinants. The purpose of the model study presented here is, first, to investigate the influence of various μ_{\max} size scalings (linear/non-linear) on the predicted community size structure in typical environments characterized by different nutrient availability and disturbance frequencies. Second, we extend our analysis to assess the importance of size scalings in other physiological traits (v_{\max} , A , Q_{\min} and Q_{\max}) for phytoplankton community dynamics. This sensitivity study should from a methodological point of view reveal the importance of each size scaling relationship for assembling size-based ecosystem models.

To address these objectives, we describe a size-based multi-species model where each species is assigned a cell size, which in turn determines the resource competition abilities of each species according to various allometric relationships regarding the diatoms only and the entire community of unicellular autotrophs. We then systematically assess the relative importance of size scaling of each eco-physiological trait under consideration.

2.3. Model

2.3.1. Model description

Our model describes phytoplankton community dynamics within a 0-dimensional box representing the surface layer of marine system. The model resolves the interactions between nutrient (Nut), detritus (Det), and multiple phytoplankton species (Phy_i) and the variability of the internal nutrient store of each phytoplankton species (Q_i) (Eq.1-Eq.4) (Figure 3.1 and

Table B.1). The model box is assumed to be perturbed at certain frequencies to describe the loss of phytoplankton form, and incorporation of the nutrient-rich deep water to the surface layer during mixing events (e.g., Gargett [36]). The mixing frequencies and the nutrient concentration at the bottom layer (Nut_{in}) were considered here as environmental sensitivity parameters.

Phytoplankton is further subdivided into n species, according to a standard approach of modeling intra-compartment changes [82, 26, 53]. To each phytoplankton (Phy_i with $i=1, \dots, n$) a certain cell size is assigned, which in turn determines the parameters for growth and nutrient uptake kinetics following allometric relationships (see Table 2.2 and Table B.7).

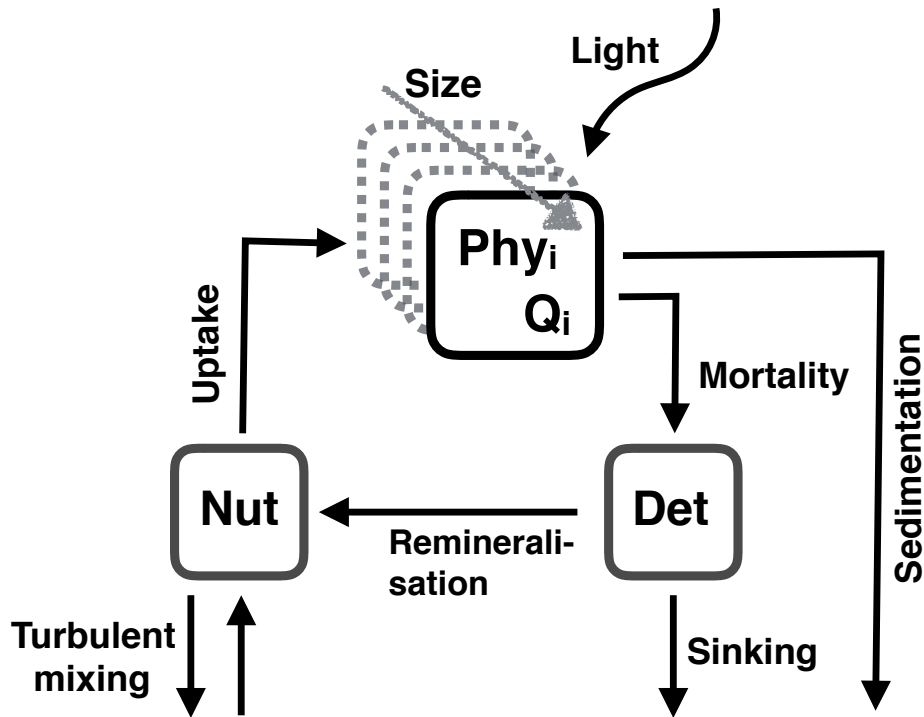


Figure 2.1.: Schematic representation of the size-based multi-species model for the surface ocean, which resolves: phytoplankton (Phy), intracellular nutrient quota (Q), nutrient (Nut) and detritus (Det).

Phytoplankton growth in the model depends on intracellular nutrient quota according to Droop [22] (Table B.1, Eq.5). The formulation relates growth to the availability of internal nutrients rather than directly to external nutrient concentration (Monod model, [25]). Consequently, the Droop formulation is better applicable to fluctuating conditions compared to, e.g., the Monod model [38, 94]. Changes in the internal nutrient pool reflect an imbalance between nutrient uptake and dilution by growth (Table B.1, Eq.2). Nutrient uptake increases with ambient nutrient concentration and is down-regulated when the intracellular pool reaches a maximum (Q_{max}) (Table B.1, Eq.7) [71]. A Monod-type saturation function is considered to define phytoplankton growth as a function of light intensity [45, 102, 88] and describes how photosynthesis rate increases with light intensity and saturates at high irradiance. The average

light intensity over the mixed layer is obtained by the Lambert-Beer law (Table B.1, Eq.6) which, is commonly used in resource competition studies to express the attenuation of light due to background particles and phytoplankton biomass [45]

Constant phytoplankton mortality fuels the detritus pool, while detritus is remineralized to inorganic nutrients and removed from the surface ocean by both mixing and sinking (Table B.1, Eq.4). To describe periodical mixing events the surface layer experiences nutrient enrichment by upwelling of deep water, which is realized by a modification of the dilution rate.

Table 2.1.: Model equations and major functions. Parameters are described in Table 2.2 and Table 2.3.

1. $\frac{d\text{Phy}_i}{dt} = \mu_i(Q_i, \bar{I})\text{Phy}_i - (m + D)\text{Phy}_i$
2. $\frac{dQ_i}{dt} = V_i(\text{Nut}, Q_i) - \mu_i(Q_i, \bar{I})Q_i$
3. $\frac{d\text{Nut}}{dt} = D(\text{Nut}_{\text{in}} - \text{Nut}) + \phi\text{Det} - \sum_{i=1}^n V_i(\text{Nut}, Q_i)\text{Phy}_i$
4. $\frac{d\text{Det}}{dt} = \sum_{i=1}^n m\text{Phy}_i Q_i - (\phi + D + \frac{v_{\text{Det}}}{z})\text{Det}$
5. Growth: $\mu_i(Q_i, \bar{I}) = \left(\frac{\mu_{\max,i} Q_{\max,i}}{Q_{\max,i} - Q_{\min,i}} \right) \left(1 - \frac{Q_{\min,i}}{Q_i} \right) \left(\frac{\bar{I}}{K_I + \bar{I}} \right)$
6. Average light intensity: $\bar{I}(z) = \frac{1}{z} \int_0^z I_0 e^{-kz'} dz' = \frac{I_0}{kz} (1 - e^{-kz})$, $k = \kappa + \epsilon \sum_{i=1}^n (\text{Phy}_i Q_i)$
7. Nutrient uptake: $V_i(\text{Nut}, Q_i) = \left(\frac{v_{\max,i} \text{Nut} A_i}{v_{\max,i} + \text{Nut} A_i} \right) \left(\frac{Q_{\max,i} - Q_i}{Q_{\max,i} - Q_{\min,i}} \right)$

An aggregate representation of the multi-variate model outcome was used for better assessing community dynamics. We specifically employ the three macro-ecological properties (1) total biomass, (2) mean size, and (3) size diversity:

$$\text{Phy}_T = \sum_{i=1}^n \text{Phy}_i \quad (2.2)$$

$$\langle L \rangle = \frac{1}{\text{Phy}_T} \sum_{i=1}^n L_i \cdot \text{Phy}_i \quad (2.3)$$

$$\delta L = \frac{1}{\text{Phy}_T} \sum_{i=1}^n (L_i - \langle L \rangle)^2 \cdot \text{Phy}_i \quad (2.4)$$

where Phy_T is the total phytoplankton biomass, L_i the size of "species" i , $\langle L \rangle$ the mean size of the community and δL the size diversity.

Table 2.2.: Model variables and allometric parameters.

Symbol	Value	Unit	Description
State variables			
Phy_i		mmol-C m^{-3}	Phytoplankton biomass
Q_i		mol-N mol-C^{-1}	Intracellular nutrient quota
Nut		mmol-N m^{-3}	Nutrient concentration
Det		mmol-N m^{-3}	Detritus concentration
Physiological parameters *			
μ_{\max}	Allom. scaled	d^{-1}	Maximum growth rate
Q_{\min}	Allom. scaled	mol-N mol-C^{-1}	Minimum internal cell quota
Q_{\max}	Allom. scaled	mol-N mol-C^{-1}	Maximum internal cell quota
v_{\max}	Allom. scaled	$\text{mol-N (mol-C d)}^{-1}$	Maximum nutrient uptake rate
A	Allom. scaled	$\text{m}^3 (\text{mmol-C d})^{-1}$	Nutrient affinity
Q_c	Allom. scaled	pgC cell^{-1}	Cell carbon content

* see Table B.7

2.3.2. Model parameterization

The initial phytoplankton biomass concentration is uniformly distributed among model species and set to 10 mmol-C m^{-3} . Furthermore, the initial intracellular nutrient quota is assumed to be at its maximum and the initial ambient nutrient concentration matches the inflow nutrient concentration. All parameters are summarized in Table 2.2 and Table 2.3. Their values were chosen identical or close to published values for similar models or represent typical environmental conditions.

Table 2.3.: Environmental parameters.

Symbol	Value	Unit	Description	Source
L		$\log_e \text{ESD } (\mu\text{m})$	Cell size	
m	0.1	d^{-1}	Phytoplankton mortality rate	Sarthou et al. [84]
κ	0.2	m^{-1}	Background turbidity	Edwards and Brindley [28]
z	25	m	Mixed layer depth	Kara et al. [48]
ϵ	0.05	$\text{m}^2 \text{mmol-N}^{-1}$	Specific light attenuation	
D	0.15	d^{-1}	Mixing rate	Fasham et al. [30]
I_0	80	W m^{-2}	Light intensity at surface	
K_I	25	W m^{-2}	Half saturation constant for light	
ϕ	0.01	d^{-1}	Remineralization rate of detritus	Edwards [27]
v_{Det}	7	m d^{-1}	Detritus sinking velocity rate	Fasham et al. [30]
T	5 – 60	d	Mixing period	Gargett [36]
Nut_{in}	5 – 80	mmol-N m^{-3}	Deep water nutrient concentration	NODC [74]
\bar{I}		W m^{-2}	Average light intensity	

Size scalings of eco-physiological parameters: The following phytoplankton growth and nutrient uptake parameters are linked to cell size (master trait) through the power law function (Equation (2.1)): maximum uptake rate (v_{\max}), maximum growth rate (μ_{\max}), nutrient affinity

(A), minimum and maximum cell quotas (Q_{\min} and Q_{\max}). The employed allometric scaling relationships for diatoms and all species (diatom included) are drawn from recently published studies and are summarized in Table B.7. Reported mass specific scaling parameters for v_{\max} , Q_{\min} and Q_{\max} on a per cell basis are converted to a per mol carbon basis using allometric coefficients for the carbon content per cell.

To investigate the effect of differences in reported size scalings of μ_{\max} [e.g. 6, 12, 57, 29, 63] on the predicted community size structure, we first referred to data digitized from Finkel et al. [32], as only rather complete compilation of existing literature data, and then chose five scenarios (Figure 2.2). We considered three different allometric relationships for μ_{\max} of diatoms: a non-linear scaling relationship with a peak at cell volume of $500 \mu\text{m}^3$ (Figure 2.2, a, [110]) (Di-NL) and two linear scaling relationships, one for the full range of cell volumes (Di-L0), the other constrained by the observed diatom cell size range (Di-L1). In addition, we compared two allometric relationships for the entire community: a non-uniform (All-NL) and a linear scaling relationships (All-L) (Figure 2.2, b). The non-linear μ_{\max} of diatom is fitted by eye as upper envelope of the data set and linear ordinary least squares regression of the \log_{10} transformed data yields estimates for β and exponent α in Equation (2.1) (Table B.7).

Table 2.4.: Size scaling of physiological parameters for marine diatoms and all marine species.

Species	Parameter	Unit	$\log_{10}\beta$	α	Source
Diatoms	Q_{\min}	$\mu\text{mol-N cell}^{-1}$	-8.59 ± 0.30	0.56 ± 0.12	Litchman et al. [57]
	Q_{\max}	$\mu\text{mol-N cell}^{-1}$	-8.39 ± 0.04	0.81 ± 0.01	Montagnes and Franklin [68]
	v_{\max}	$\mu\text{mol-N (cell d)}^{-1}$	-7.80 ± 0.32	0.67 ± 0.11	Litchman et al. [57]
	A^*	L (cell d)^{-1}	-7.31 ± 0.84	0.50 ± 0.92	Litchman et al. [57]
	Q_c	pg-C cell^{-1}	-0.54 ± 0.01	-0.81 ± 0.03	Menden-Deuer and Lessard [67]
	μ_{\max} (linear)	d^{-1}	0.50 ± 0.06	-0.16 ± 0.02	
	μ_{\max} (non-linear)	d^{-1}			
$V_{\text{cell}} < 500 \mu\text{m}^3$			0.31	0.02	
$V_{\text{cell}} > 500 \mu\text{m}^3$			0.96	-0.24	
<hr/>					
All species	Q_{\min}	pg-N cells^{-1}	-1.47 (-1.78, -1.26)	0.84 (0.77, 0.92)	Marañón et al. [63]
	Q_{\max}	pg-N cells^{-1}	-1.26 (-1.35, 0.99)	0.93 (0.83, 0.96)	Marañón et al. [63]
	v_{\max}	$\mu\text{mol-N (cell d)}^{-1}$	-8.10 (-8.80, -7.30)	0.82 (0.65, 1.00)	Edwards et al. [29]
	A^*	L (cell d)^{-1}	-7.31 (7.56, -6.86)	0.49 (0.41, 0.55)	Edwards et al. [29]
	Q_c	pg-C cell^{-1}	-0.69 (-0.83, -0.58)	0.88 (0.83, 0.94)	Marañón et al. [63]
	μ_{\max} (linear)	d^{-1}	0.11 (0.01, 0.20)	-0.08 (-0.12, -0.05)	
	μ_{\max} (non-linear)	d^{-1}	-0.10 (-0.24, 0.04)	0.10 (-0.05, 0.22)	
$V_{\text{cell}} < 500 \mu\text{m}^3$			0.38 (0.14, 0.62)	-0.15 (-0.22, -0.09)	
$V_{\text{cell}} > 500 \mu\text{m}^3$					

* Calculated as $\frac{v_{\max}}{K_n}$ [43, 93], where K_n denotes the half-saturation concentration of nutrient uptake (mmol-N m^{-3}) with $\log_{10}\beta = -0.49 \pm 0.07$ and $\alpha = 0.17 \pm 0.03$ for diatoms adopted from Litchman et al. [57] and $\alpha = 0.33$ (0.24, 0.45) for all species from Edwards et al. [29].

The number of virtual phytoplankton species is set to $n=29$. The size classes are distributed evenly over fixed cell volumes range from 1 to $10^7 \mu\text{m}^3$ corresponding to a range of 0.22 to $5.58 \log_e \text{ESD} (\mu\text{m})$ (ESD: Equivalent Spherical Diameter), which provides a representative size spectrum of phytoplankton observed in nature [32]. The original allometric coefficients are

based on cell volume and thus need to be rescaled to ESD ($V = \frac{\pi}{6} \text{ESD}^3$). Trait values for each model species then follow from substituting the converted allometries into $y = \beta' e^{\alpha' L}$, where α' and β' are the ESD-based allometric coefficients, and L the natural logarithm of ESD. While published allometries are often expressed in terms of cell volume, we choose $L = \log_e \text{ESD}$ as a mechanistically more sound size unit, since, relevant ecological and physiological traits in the phytoplankton can be linked to ESD using biophysical arguments [110, 111]. Nevertheless, we provided both scales in Figure 2.2 for convenience.

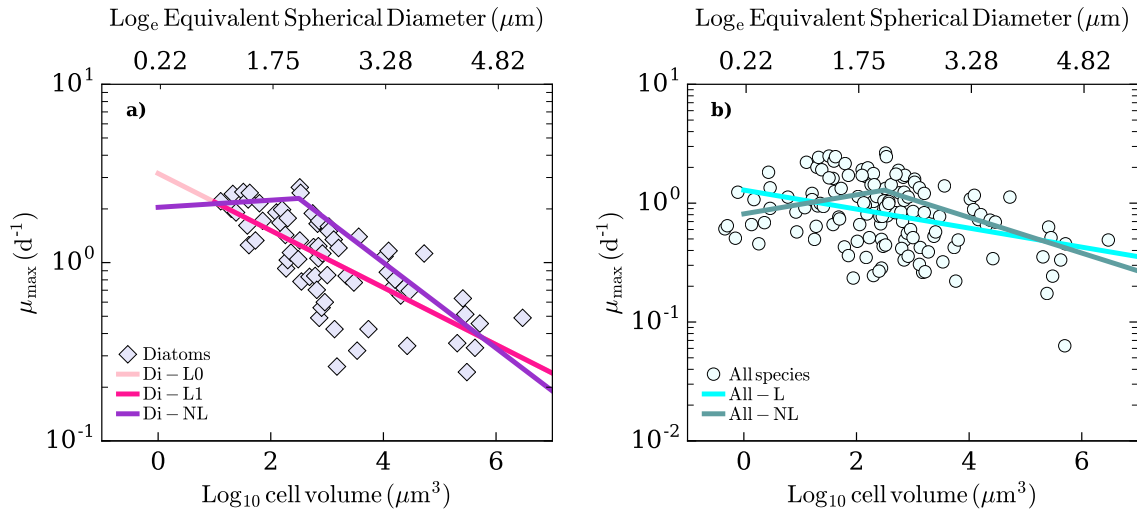


Figure 2.2.: Size dependency of maximum growth rate (μ_{\max}) used in this study. Data for μ_{\max} are obtained from [32].

2.3.3. Model simulation and variation experiments

Differential equations (Table B.1, Eq.1-Eq.4) were solved numerically by using the Scipy Odeint² solver (Python package) which is based on lsoda from the FORTRAN library ODEPACK. The simulation time was set to 1000 days, within which simulations reached equilibrium. The community mean size and size diversity were averaged for the last 200 days. Since this study emphasizes the ecological time-scale, termination after 1000 days neglected changes in the target variables mean cell size $\langle L \rangle$ and diversity δL below 0.5% per year. The long term simulations (10000 days) prove also qualitative consistency with 1000 days simulations (see Section A.2). The size structure of the community was investigated across various inflow nutrient concentrations (Nut_{in} : 5–80 mmol-N m^{-3}) and mixing intervals (T : 5–60 days). The values were selected from the typical ranges observed in nature [36, 74]. To assess the importance of each size scaling relationship for shaping the community, the size constraint of each physiological trait defined in Table B.7 was individually removed, while the remaining traits were kept size dependent. The average of data obtained from Finkel et al. [32] (Figure 2.2) were assigned to size independent μ_{\max} and for other traits, the trait value at median cell size were used.

²<https://docs.scipy.org>

2.4. Results

Under absence of temporal heterogeneities caused by mixing events, equilibrium residual nutrient concentration (Nut^*) of smaller phytoplankton remains always lower than that for larger phytoplankton. This indicates the unconditional dominance of smaller species independent of light intensity and nutrient supply rate (Di-L0 scenario, see Section A.1). Hence, smaller phytoplankton species emerge as unconditional winners according to the resource competition theory [103]. However, when this system is periodically perturbed by introducing nutrients and removing phytoplankton from the model box, analogous to the effect of wind-induced mixing of a stratified water column, a niche for larger diatoms emerge (Figure 2.3).

All diatom scenarios (Di-L0, Di-L1 and Di-NL) result in a unimodal distribution of community mean size across mixing periodicities (Figure 2.4, c). For short and long mixing intervals ($T < 15$ and $T > 35$ days) few smaller phytoplankton become dominant while the others vanish, so that mean size of the community reaches to $\sim 2.5 \log_e ESD$ (μm) and the size diversity declines. At these periodicities, the community mean size decreases towards values above the existing minimal cell size of diatom ($\geq 1.0 \log_e ESD$ (μm) for both Di-L1 and Di-NL scenarios, and below this minimal size for Di-L0 case (Figure 2.4, c). Conversely, intermediate mixing periodicities ($T : 15 \sim 35$ days) favor larger cells as expressed by a community mean cell size of up to $\sim 3.5 \log_e ESD$ (μm) for all diatom scenarios (Figure 2.4, c). Also, community size diversity displays a moderate unimodal dependency over mixing intervals with sustained elevated diversity at intermediate mixing intervals (Figure 2.4, d).

Community compositions remain relatively small and do not show significant changes to Nut_{in} concentration at short and long mixing intervals, representing larger species outcompeting smaller species (Figure 2.4, a-b; and see Section A.3). Whereas, at intermediate periodicities, community mean size and size diversity peak at intermediate Nut_{in} concentration resulting in a unimodal distribution across various inflow nutrient concentrations.

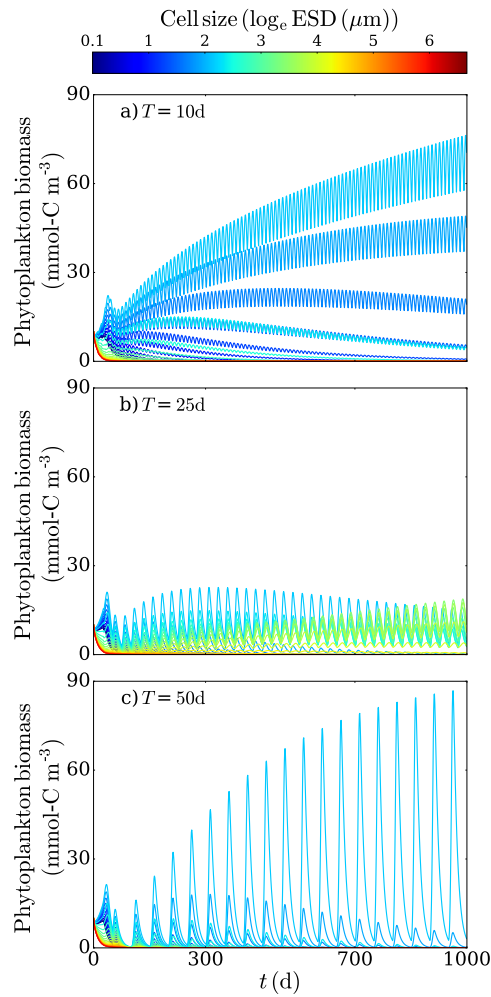


Figure 2.3.: Biomass dynamics of 29 marine diatoms (Di-L0) over 1000 days. Each panel shows the model outcome for a different environmental setting with $\text{Nut}_{\text{in}} = 60 \text{ mmol-N m}^{-3}$ and : a) short , b) intermediate , and c) long replenishment period T .

The mean cell size of all species community displays a relatively uniform pattern across various inflow nutrients/mixing intervals (Figure 2.4, c). Uniform μ_{max} size scaling for the entire community of marine species (All-L) induces dominance of the smallest species at all environmental settings (Figure 2.4, c) . However, a non-uniform μ_{max} allometry slightly shifts the community mean cell size up to $2.1 \log_e \text{ESD} (\mu\text{m})$ (All-NL, Figure 2.4, c), which is close to where the μ_{max} peaks (Figure 2.2, b).

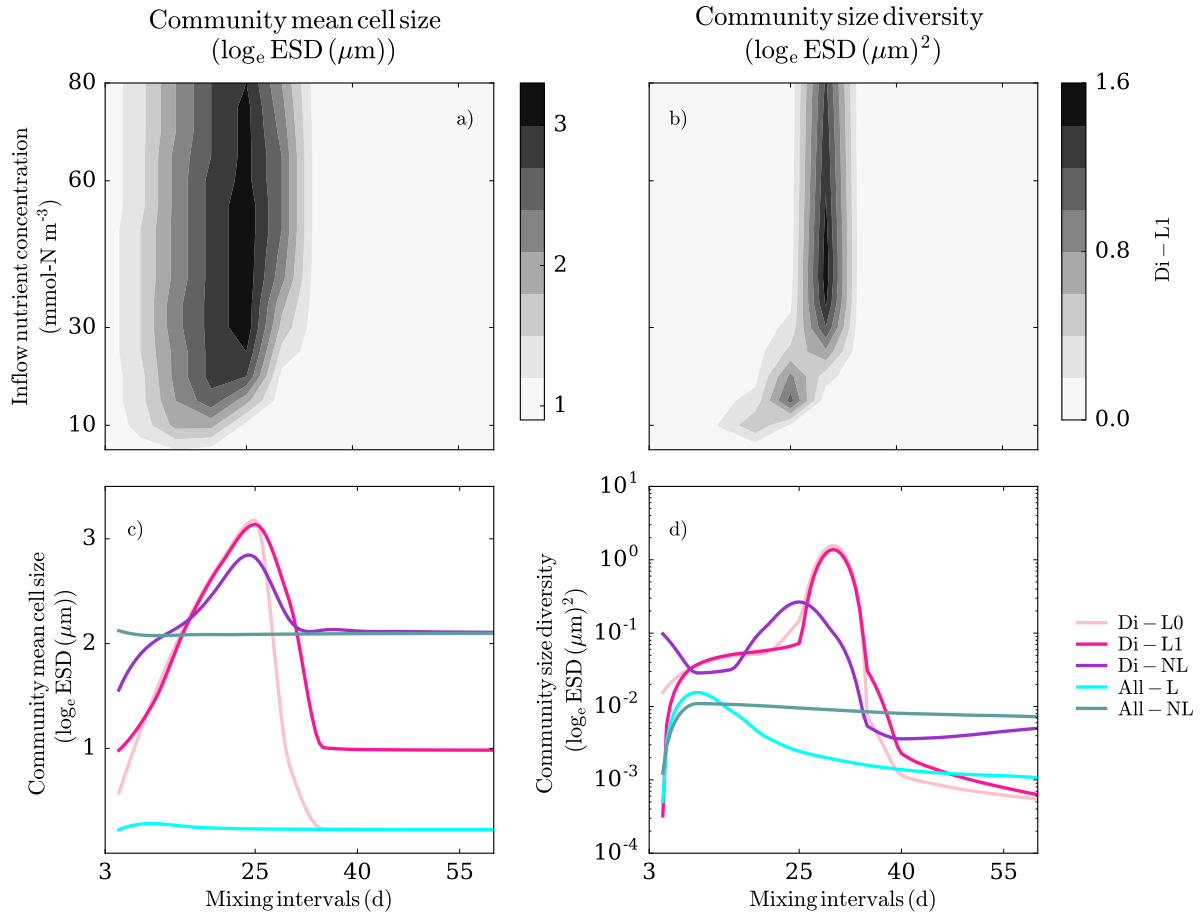


Figure 2.4.: Community composition in terms of mean cell size (a, c) and size variance (b, d) varying over inflow nutrient concentration and nutrient mixing intervals for Di-L1 scenario (a-b); and varying across mixing intervals with a constant $\text{Nut}_{\text{in}} = 60 \text{ mmol-N m}^{-3}$ for different allometric relationships in μ_{max} (c-d). The μ_{max} allometries comprise linear (“L”) and non-linear scalings (“NL”) for both diatoms (“Di”) and the entire marine phytoplankton community (“All”): linear scaling for diatoms is applied to either the entire size spectrum (“Di-L0”) or the restricted spectrum above $1 \log_e \text{ESD} (\mu\text{m})$ (“Di-L1”).

To investigate the relevance of the size scaling relationship for each physiological parameter considered in this study (Table B.7), we performed experiments where the allometry for each physiological parameter was assumed size-neutral, while keeping the other parameters intact. As the major variation was observed across the mixing intervals, we show here the results obtained under three environment setups characterized by a constant $\text{Nut}_{\text{in}} = 60 \text{ mmol-N m}^{-3}$ and three different mixing periodicities, $T = 10, 25, 60$ days (Figure 2.5).

For all three environmental settings, the size scaling of Q_{min} appears to be the most important determinant of the community size structure under short and intermediate mixing intervals for all diatom scenarios (Di-L0, Di-L1 and Di-NL), as removing the size dependency of Q_{min} leads to a collapse of community mean cell size down to $\sim 0.25 \log_e \text{ESD} (\mu\text{m})$. At short and long mixing periodicities, our results also highlights a major role of μ_{max} scaling for all diatom scenarios. In Di-NL scenario, the community mean size at these periodicities, which is lower

than that in the intermediate intervals, but higher than that obtained by linear allometries for μ_{\max} , turns out to be sustained also by Q_{\min} allometries (Figure 2.5, a-i).

During intermediate mixing intervals, four size scalings of traits are at least required to sustain the community at its maximum mean cell size, the ones in maximum growth rate, minimum intracellular quota, affinity and maximum uptake rate. The model results reveal a minor or negligible role of size scalings in two traits: maximum uptake rate (v_{\max}) and maximum intracellular quota (Q_{\max}) in shaping community size structure (Figure 2.5, b, e, h). Finally, our findings indicate the relatively important role of size scaling of affinity under low inflow nutrient concentrations ($<10\text{mmol-N m}^{-3}$) regardless of any mixing intervals (results not shown). Contrary to the diatom community, the community with all species (All-L and All-NL) displays an insignificant response to removal of the size constraint in individual physiological traits, which indicates the persistence of small species at any nutrient/mixing regime (Figure 2.5, m-o). The model outcome reveals that only μ_{\max} size scaling plays a major role in shaping the size structure of the species community.

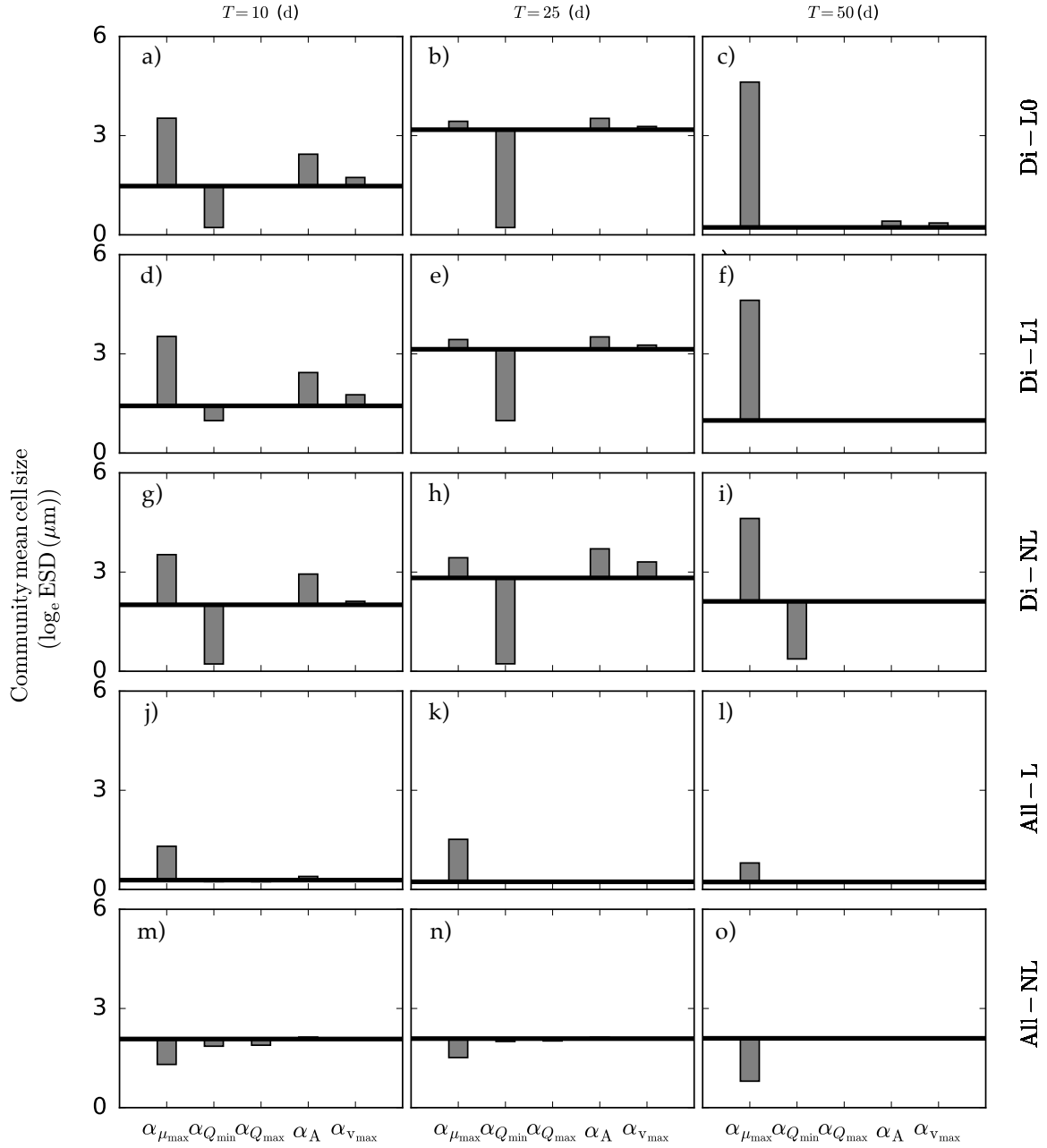


Figure 2.5.: Changes in community mean cell size when neglecting allometric relationships one at a time. Thick black line: allometries show in Table B.7 and grey bars: neutral allometry experiment. Di-L0 (a-c) and Di-L1 (d-f): diatom scenarios with linear μ_{\max} over cell volume ranges $1 - 10^7 \mu\text{m}^3$ and $10 - 10^7 \mu\text{m}^3$, respectively., Di-NL: diatom scenario with non-linear μ_{\max} (g-i)., All-L (j-l) and All-NL (m-o): all species community scenarios with assumed linear and non-linear μ_{\max} , respectively. For symbols, see Table 2.2.

2.5. Discussion

2.5.1. Community response to nutrient supply

The relevance of nutrient supply rate for the phytoplankton composition has been long recognized [103]. By explicitly addressing the nutrient concentrations at the bottom layers and continuity in the supply rate we account for two major determinants of the overall supply rate observed in aquatic ecosystems. In the ocean, nutrient enrichment of the surface water is affected by various physical processes such as internal waves, mesoscale eddies and vertical convective mixing [66]. The duration of these nutrient injections vary from the hours to several days in coastal waters, and to monthly and even longer periods in the open ocean [36].

Effects of these two drivers on the phytoplankton community structure has been previously explored. Based on numerical simulations of pairwise competition experiments, [38] demonstrated that phytoplankton cells with a large storage capacity can gain a competitive advantage at intermediate pulsing frequencies, which was experimentally confirmed by [23]. For the case of nitrogen utilization, the larger allometric scaling coefficient for Q_{\max} than that for Q_{\min} leads to a storage advantage for the larger cells, and to their competitive dominance under intermediate mixing frequencies, as suggested by a pairwise invasibility analysis applied to a simple box model of upper mixed layer dynamics [57]. By using the allometric relationships provided by [57], and applying the invasibility analysis to an idealized model of an incompletely mixed water column, [49] demonstrated that, whereas too low and too high mixing intensities favor small cells, intermediate turbulent mixing intensities favor large cells. The study also shows the storage advantage concept becomes relevant whenever spatial heterogeneities exist, which is often the case in real ecosystems.

In the above mentioned studies, only the size of the most dominant species was used as a proxy for the phytoplankton community [38, 57, 49]. In this study, we used two aggregate properties of the community for a more complete description of the community size structure, the mean cell size and size diversity. This would have also been possible with a moment closure modeling approach [e.g., 100, 1], which would have been computationally more efficient as well. However, multi-species models can provide further potentially relevant information if the size distribution deviates from normality, such as in the case of multi-modalities [e.g., 16], although in this study this was not necessary, as such behavior was not observed.

2.5.2. Size structure of marine diatoms

The absence of perturbations always favored small cells (see Section A.1). However, when periodic mixing events are introduced, all three diatom scenarios (Di-L0, Di-L1 and Di-NL) predict dominance of relatively large diatoms at intermediate mixing intervals ($T : 15 \sim 35$ days) particularly in periodically mixed environments. The qualitative response of phytoplankton species to fluctuating nutrient conditions is in accordance with the outcome of previous studies

[57, 49]. This response leads therefore to a unimodal pattern of the community mean cell size (Figure 2.4, c) across mixing intervals. The unimodal relationship between size diversity and mixing intervals for the diatom community as suggested by our simulation results (Figure 2.4, d), is also consistent with the intermediate disturbance hypothesis, which predicts that species diversity is maximum at intermediate frequency of disturbance [81, 96]. This unimodality arises because of, firstly competitive exclusion following resource depletion, which reduces the number of species under (nearly) undisturbed conditions, and secondly, slow extinction rates of species at intermediate mixing periodicities such that only a few species will manage to survive [81, 96, 15, 55].

Both the mean community size and diversity rapidly increases with inflow nutrient concentrations (Figure 2.4, a-b and see Section A.3) over intermediate mixing periodicities, and tend to decrease again at very high nutrient concentrations. This pattern agrees with the modeling study of [108] for the global ocean, who found regional variations in phytoplankton size, with larger cells being rare in oligotrophic waters and relatively abundant in areas of high nutrients supplies. At short ($T < 15$ days) and long ($T > 35$ days) periodicities, inflow nutrient concentration does not affect the community composition significantly.

Choice of different size scalings for the diatom maximum growth rate becomes more critical during short and long mixing intervals. With uniform (log-log linear) allometry in maximum growth rate over the entire size spectrum (1 to $10^7 \mu\text{m}^3$) (Di-L0, Figure 2.4, c), the diatom community always converges towards the smallest species represented in the model, whereas in nature no diatom species with cell size below $V=10 \mu\text{m}^3$ can be found [32]. Hence, the physiological trade-offs alone can not sustain the community within the window of observed diatom cell size in nature. This convergence towards non-existing diatoms can be recovered by restricting the size range above $10 \mu\text{m}^3$ (Di-L1, Figure 2.4, c). However, by considering the entire size spectrum but reducing the unrealistically high maximum growth rates of the smallest species using non-uniform μ_{max} (Di-NL, Figure 2.4, c), the model captures both the minimum observed diatom size and provides a bottom up explanation for the absence of diatom $< 10 \mu\text{m}^3$, in addition to other potential mechanisms that we did not consider in this study such as selective grazing or sinking, to keep diatom sizes within observed ranges in nature.

Among all size scalings of traits, the allometric relationships for minimum intracellular nutrient quota (Q_{min}) is found to be the key trait shaping the community size structure at short and intermediate mixing intervals (Di-L0, Di-L1 and Di-NL, Figure 2.5, a-i), whereas at long periodicities it becomes important only in Di-NL case. Without size dependency of the minimum quota, the community collapses to very small, thus non-existing diatom species regardless of any mixing periodicities. Furthermore, during both short and long mixings, size scaling of maximum growth rate also play a major role in shaping the community size structure for all diatom scenarios (Di-L0, Di-L1 and Di-NL, Figure 2.5, a-i). While size scalings of maximum uptake rate (v_{max}) and maximum nutrient quota (Q_{max}) play a minor role in sustaining community composition in any nutrient/mixing regime, allometric relationship of nutrient affinity (A) becomes relevant at very low inflow nutrient concentrations (results not shown)

such as in oligotrophic open oceans and/or in regions characterized by deep stratification and poor nutrient delivery to the surface [108, 7], respectively.

Although, the effect of size scalings of mol-C based traits: Q_{\min} , Q_{\max} and v_{\max} on the predicted community size structure depends on the chosen size scaling of carbon quota of phytoplankton (Q_c), our results using different Q_c allometric relationships ($\alpha = 0.712$, $\log_{10}\beta = -0.314$) [97] indicate the similar overall final outcomes (results not shown) regarding to v_{\max} and Q_{\min} . However, size scaling of Q_{\max} becomes relevant as difference in size scaling exponents becomes larger ($\alpha_{Q_{\max}} = 0.81 > \alpha_{Q_c} = 0.712$). Survival of intermediate size species and a relatively large size diversity can only be simulated using allometric relationships of a set of (at least) four physiological traits (maximum growth rate and uptake rate, minimum intracellular nutrient quota and nutrient affinity). Indeed, in eutrophic coastal upwelling zones and regions of enhanced turbulent mixing larger phytoplankton becomes more dominant [108, 7]. The outcome also calls for attention when developing size based models, which need to address a larger and ideally complete spectrum of trade-offs and allometries to avoid strong unrealistic bias in predicted size structures.

2.5.3. Size structure of marine phytoplankton

Allometries for the entire phytoplankton community result in small mean size and size diversity (Figure 2.4, c, d), thus creating a uniform pattern over nutrient concentrations/mixing periodicities. Unlike the case for diatom only, difference between Q_{\max} and Q_{\min} slopes for the entire phytoplankton community is small (Table B.7), therefore the storage (Q_{\max}/Q_{\min}) advantage that larger diatoms benefit from does not hold when considering all species. Recent theoretical work of [110] and the experimental study of [63] suggested a unimodal function of μ_{\max} over cell size as additional mechanism maintaining larger cells. Contrary to the linear allometric relationship, the decline of phytoplankton μ_{\max} (Figure 2.2, b) for cell sizes decreasing from approximately $1.5 \log_e \text{ESD} (\mu\text{m})$ may result in a trade-off between small cells with higher nutrient affinity and slightly larger cells with faster growth rates, which may help larger species to survive in variable environments [38]. Our model outcomes demonstrate that, linear size dependency in maximum growth rate results in species with highest maximum growth rate to be the unconditional winners. However, even though non-uniformity in maximum growth rate prevents unrealistically high growth rate of the smallest species, non-uniformity alone cannot explain the existence of larger species where the role of size scalings of Q_{\max} and Q_{\min} is minor or top-down control is absent. Furthermore, we found an insignificant change in the community mean cell size compared to the diatom community, where the size constraint of traits were removed (Figure 2.4, g-o). The model outcomes point to the major role of maximum growth rate in shaping the all species community size structure at any nutrient/mixing regime.

The outcome of comparison for these two communities, can be used to predict any community size structure based on different sets of allometric relationships. The model in this study is developed based on the assumption that nitrogen is the only limiting nutrient, given similar

size scaling exponents for minimum and maximum intracellular phosphorus quotas for marine diatoms ($\alpha_{Q_{\min}} = 0.79$ and $\alpha_{Q_{\max}} = 0.8$) by Litchman et al. [57], P-limitation will likely result in the overall too drastic dominance of small species regardless of other physiological allometries.

2.5.4. Limitations of our approach

The low complexity of our model structure allowed us to focus on the bottom-up factors, and the relevance of eco-physiological traits for community composition across aquatic ecosystems. However, the model suffers from a number of shortcomings such as the loss of size diversity in nearly all scenarios, the likewise fast disappearance of large species, especially of larger diatoms, and too little variation in the size structure in mixed (diatom plus non-diatom) communities. These shortcomings point to the relevance of other factors, which are likely to be relevant.

Water temperature has often been proposed to impact size structure of marine phytoplankton communities [95, 68, 32]. The study by Sommer [95] on Antarctic phytoplankton reveals a weak size dependency of maximum growth rate on cell size, indicating more favorable conditions for larger species under cold temperature. Indeed, later work of Montagnes and Franklin [68] also points to an increase in organisms size and decline in specific maximum growth rate with decrease in temperature. If all physiological rates slow down, the supremacy of small cells might become less persistent in general.

Recent size-based models highlight the importance of zooplankton grazing for the phytoplankton size structure [78, 108, 85, 1]. The model of Wirtz and Sommer [114] reproduces shifts in mean size L observed in mesocosm studies with high precision. Their quantitative analysis of driving forces behind changes in L revealed a pre-dominant role of selective grazing, promoting of larger species in particular in the blooming phase. Similarly, in nutrient rich regions, small phytoplankton flourish but intense grazing pressure by smaller zooplankton prevent their excessive growth [85, 108, 1]. This top-down control thus shifts the community mean cell size towards higher values. As in this study the aim is to understand fully the effect of bottom-up control, we deliberately did not consider grazing in our model. Due to this simplification, the dominance of small species is possibly overestimated, especially at nutrient rich regions.

Sinking of individual cells should according to Stoke's law further accentuate the dominance of small species. However, the actual effect of sinking on the community (size) structure is difficult to assess due to the control of excess density and buoyancy by the physiological state of cells. The advantage of small species at high sedimentation rates for physiologically impaired cells may therefore turn to a lacking size dependency of physiologically competent cells [57]. Recent work of Wirtz [111], based on data of Bienfang et al. [10] and Waite et al. [107], provides a mechanistic formulation for positive buoyancy of larger diatom, which may further explain the strong competitive loss of large and very large diatoms in our numerical experiments.

2.6. Conclusion

Allometric relationships of phytoplankton major traits are increasingly incorporated into size-based prognostic ecosystem models [108, 111, 100, 1]. However, to date no study has explicitly considered the uncertainties in the underlying scaling rules and systematically investigated the importance of size scaling of each eco-physiological trait. In this study, we quantified the effect of bottom-up control and various size scaling relationships of phytoplankton physiological traits on community size structure. The model outcomes reveal a unimodal distribution of community mean size, as already suggested by previous theoretical studies [57, 49], and size diversity across nutrient mixing periodicities or inflow nutrient concentrations (at intermediate nutrient replenishment periods). Both properties remain relatively unchanged at short or long periodicities due to the persistence of small species. Contrary to the diatom community, when all taxonomic groups are considered the model always reveals this dominance of smaller species regardless of any nutrient/mixing regime.

Another major finding is the critical importance of the functional shape in allometries for modeling. Non-uniformity in maximum growth rate over the entire size spectrum leads to more realistic outcomes by reducing the unrealistic maximum growth rates of smallest species, hence preventing the community mean size to collapse below minimum diatom size as observed in uniform maximum growth scenario (Di-L0). For the all marine phytoplankton species community, non-uniformity alone can not alleviate the lack of larger species, which reflects a too weak influence of the size scalings of minimum and maximum quotas or lacking of other mechanisms.

Along different habitats, different sets of trait allometries seem to sustain community composition. For diatoms, size scaling of minimum nutrient quota plays a major role at short and intermediate mixing periodicities, while allometric relationships of maximum growth rate gains importance at short and long periodicities. Under low inflow nutrient concentrations, the size scaling of affinity becomes relevant at any mixing interval. For the community of all species, size scaling of maximum growth rate is the most important feature for shaping the community size structure.

These findings help to critically assess limits and potentials of size-based ecosystem models. We emphasize the importance of resolving the allometries for at least nutrient affinity, maximum growth rate, and subsistence quota in these models. Finally, we conclude that physiological size constraints alone cannot provide realistic simulations of phytoplankton size structure, which implies a high relevance of other mechanisms such as selective grazing and sinking. Having gained fundamental insights into the relevance of a large set of size scaling relationships in physiological traits, adding other processes such as aggregation, size dependent sinking and grazing remains to be a future task. Such as an extended model may become a useful tool to investigate the dynamics of community size structure under multiple stressors such as: nutrient limitation, shallowing of the mixed surface layer, and size selective grazing. The control of primary production by bottom-up (nutrient limitation) and top-down (grazing) factors has been

for decades a relevant topic in marine ecosystem research, but a quantitative understanding of the interaction between them - in particular as mediated by structural changes - is still lacking.

To sum up, our size-based model served as a conceptual framework contributing to a better understanding of how the rich size structure of phytoplankton is influenced by scaling relationships in eco-physiological traits. It can guide the development of future size-structured ecosystem models and provides important insights for the interpretation of observed successional shifts in phytoplankton communities. As the empirical evidence for testing this (or other) size-based model is still scarce, our study also calls for the conduct of specific experiments which allow insight into the making of phytoplankton size distributions or for increased efforts in deriving size allometries from homogeneous data sets [e.g., as in 63].

Acknowledgments

We thank two anonymous reviewers for helpful and constructive comments on the manuscript. This work was supported by the Helmholtz society via the program PACES, by the German Research Foundation (DFG) within the Priority Program DYNATRAIT, by the German Federal Ministry of Research and Education in the framework projects MOSSCO and BIOACID.

3

*A trait-based framework for explaining non-additive effects of multiple stressors on plankton communities*¹

3.1. Abstract

Phytoplankton communities are increasingly subjected to multiple stressors from natural or anthropogenic sources. The cumulative effect of these stressors, however, may vary considerably from the sum of impacts from individual stressors. Nonlinear effects such as changes in community traits can either boost up (synergistic) or weaken (antagonistic) single stressors. Despite previous empirical studies and meta analyses on the interaction types of various multiple stressors, a more fundamental understanding of nonlinear effect accumulation is lacking. To fill this gap, we here propose a new theoretical framework that is centered on the concept of interaction traits and their trade-offs. The framework is applied to a novel size-based plankton model resolving multi-species phytoplankton-nutrients-detritus-zooplankton dynamics within the upper mixed layer. The model is validated using data from a series of outdoor mesocosm experiments. In the direct aftermath of single perturbations that increase net growth rate, here nutrient enrichment and grazer removal, the simulated phytoplankton community undergoes structural changes as visible in altered community traits. These temporal variations explain why the multiple stressor interaction switches from antagonistic to synergistic as compensatory trait variations reduce over time of the experiment. This finding can be generalized within our trait-based explanatory framework, which should be capable to mechanistically assess and predict effects of other stressor combinations and for other organism groups.

¹Taherzadeh, N., Bengfort, M., and Wirtz, K. W. (2018). A trait-based framework for explaining non-additive effects of multiple stressors on plankton communities

Key words

Phytoplankton, multiple stressors, grazing removal, nutrient enrichment, multi-species, antagonistic, synergistic

3.2. Introduction

Phytoplankton communities are responsible for half of the primary production on earth [31] and form the base of aquatic food-webs, but are also subject to accelerated shifts in their growth environment. These shifts add to natural variations and derive from a suite of processes starting from many aspects of climatic change and comprising direct anthropogenic interventions such as fertilizing the global ocean with inorganic carbon and the coastal ocean with nutrients. It is thus rather the norm than the exception that phytoplankton communities undergo a broad combination of environmental perturbations in parallel [104]. If any of those alterations in a growth factor induces a decrease in fitness, it is called a "stressor" [35]. In the following, this popular definition is here extended to alterations with positive growth effects: arbitrary but simultaneously changing growth factors are in the following termed "multiple stressors". According to this neutral definition, for example, a (beneficial) temperature rise together with nutrient enrichment act as "multiple stressors" [14]. Experimental studies of plankton eco-physiology in general investigate the effects of a single stressor at a time. However, multiple stressors may have an impact that differs from the sum of effects of each stressor in isolation. If the impact exceeds the sum of individual effects, the stressors are called synergistic, while in the case of a lower total impact these are termed antagonistic [17]. Non-additive impacts represent 'ecological surprises' that can counteract our (linear) understanding of ecosystem functioning. For example, experimental studies of [50] and [106] suggest that acidification shifts freshwater phytoplankton communities towards larger dinoflagellates, filamentous green algae, and larger eukaryotic phytoplankton that all grow slower under higher temperature [2], which indicate a synergistic (negative) effect of acidification and environmental warming.

How phytoplankton communities restructure themselves under environmental perturbations depends on their flexibility in eco-physiological traits [58, 32]. Major eco-physiological traits such as maximum growth rate or minimum nutrient demand determine competitive processes and interaction with the biotic and abiotic environment (e.g., grazing susceptibility or nutrient acquisition capacity). Most of these traits are correlated through trade-offs due to which an adaptation in one trait results in shifts of other traits [112, 58], with direct and indirect consequences on resource usage strategies [113]. Species that have an advantage under one stressor (e.g., elevated temperature) may not perform well when a second stressor (e.g., elevated CO₂) is acting simultaneously [60]. Hence, the specific response of characteristic traits to both single and combined stressors makes a central part of the overall growth and structural response of phytoplankton communities to concurrently changing growth factors. These specific trait

shifts are in turn rooted in eco-physiological trade-offs, an idea that provides the starting point of the work presented here. Previously, impacts of multiple stressors on phytoplankton have been investigated by empirical works [e.g. 106, 33, 89] and meta-analysis of experimental studies [e.g. 35, 14]. Multiple stressors were in particular not systematically connected to phytoplankton traits and trade-offs. To fill this gap, we introduce a new theoretical framework which aims to explain the community response to the multiple stressors taking into account structural, trait-related changes. For doing so, we define (1) a response specific effect size to quantitatively link main features of the community such as total net growth rate to alteration in environmental conditions, and (2) trait-mediated adaptive growth response quantifying the contribution of structural changes to the overall community response. A major goal of our study is to unravel the relation between this adaptive capacity and the effect size. We will address this challenge by building and validating a fully trait-based plankton model that resolves flexibility and adaptive responses. The model will enable systematic stressor experiments to investigate how trait shifts buffer or amplify the response impacts of multiple perturbations.

3.3. Methods and material

3.3.1. Model definition

Almost all eco-physiological traits in unicellular autotrophs are linked to cell size [58, 32, 111]. To represent a major share of the adaptive capacity in phytoplankton, we therefore adopt a previously developed size-based model, which is extended to a simple ecosystem model by supplementing dynamic equations for zooplankton, detritus and two nutrients. The model is based on the multi-species model presented by [98], and adds more physiological detail such as CO₂ sensitivity and, most of all, ecological detail by incorporating size-based trophic relations derived by [111]. The model describes ecosystem dynamics within a zero-dimensional box representing the surface layer of a water column and resolves a full ensemble of phytoplankton species or groups, resp. (Phy_i with $i=1, \dots, n$), and their internal nutrient quotas ($Q_{N,i}, Q_{P,i}$), three zooplankton groups (Z_j with $j=1, 2, 3$), two nutrients (nitrogen and phosphorous) ($\text{Nut}_N, \text{Nut}_P$) and detritus ($\text{Det}_N, \text{Det}_P$) (see Supplementary Material, Table S1, Eq.1–9) (Figure 3.1). Each phytoplankton group (Phy_i) is characterized by its fixed cell size, which in turn determines the growth-nutrient uptake parameters (see Table S7), primary production, mixotrophy and loss terms (see Supplementary Material, Table S2–S4). Zooplankton is divided into small and large ciliates, and copepods. A comprehensive model description is given in the Supplementary Material (SI).

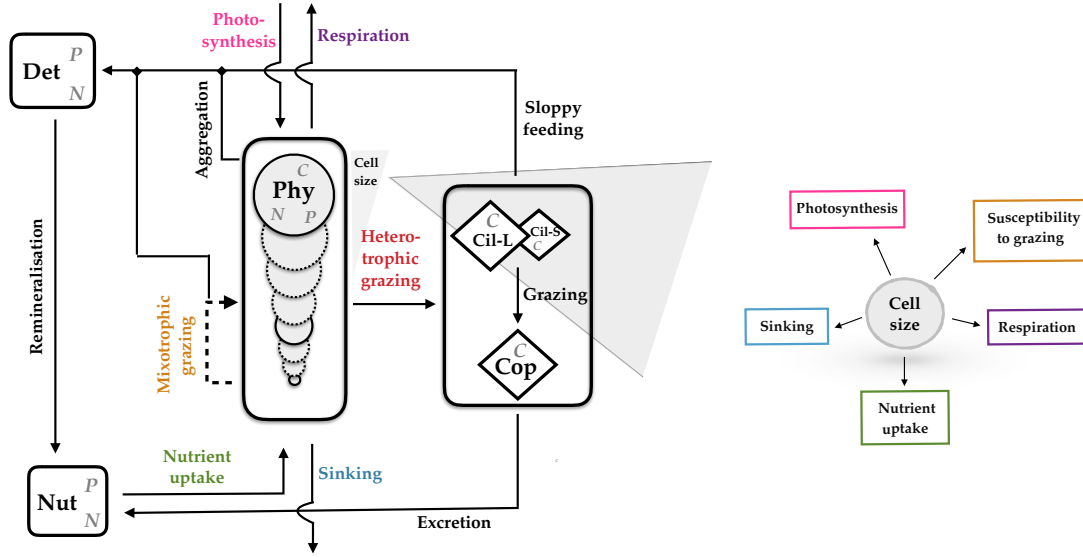


Figure 3.1.: Schematic representation of the size-based multi-species model resolving biomass of phytoplankton species (Phy_i with $i=1, \dots, n$), their internal nutrient quotas (Q_i), ambient nutrient concentration (Nut), detritus (Det) and zooplankton, further subdivided into small and large ciliates (Cil-S, Cil-L) and copepods (Cop). N: Nitrogen, P: Phosphorous, C: Carbon, T: Temperature and PAR: Photosynthetically Active Radiation.

3.3.2. Multi-stressor effects

Our study seeks to develop a more general and mechanistic approach to study, quantify and predict multi-stressor effects on functional groups in ecosystems. The generic formalism should describe arbitrary stressor effects in complex systems such as phytoplankton communities or marine food-webs. Let E_n and E_m denote two external variables or stressors such as nutrient input and grazing pressure. For relating (known) effects of perturbing E_n and E_m to (unknown) multi-stressor effects, we pinpoint possible determinants of the non-linear interaction between stressor reactions. A special focus is laid on internal re-organization of biological agents, termed adaptive trait dynamics, and the trade-offs ruling that dynamics. We define as the first determinant the specific multi-stressor sensitivity (SMS) being the sensitivity of the community growth rate μ to parallel changes in E_n and E_m :

$$\text{SMS} = \frac{\delta^2 \mu}{\delta E_n \delta E_m} \quad (3.1)$$

This combined sensitivity to both stressors n and m can be shown to approach a function of observed single stressor shifts ΔE_n and ΔE_m , their growth effects $\Delta \mu_n$ and $\Delta \mu_m$, and the observed multi-stressor effect $\Delta \mu_{nm}$ (see SI; B.3)

$$\text{SMS} = \frac{\Delta \mu_{nm} - \Delta \mu_n - \Delta \mu_m}{\Delta E_n \Delta E_m} \quad (3.2)$$

When the SMS is zero, the single stressor effects sum up to the multi-stressor effect ($\Delta\mu_{nm}=\Delta\mu_n + \Delta\mu_m$), which reflects additive effects. Analogously, the SMS is positive for synergistic and negative for antagonistic effects.

Similar to the definition of the specific multi-stressor sensitivity, we introduce the interaction trait x_n with respect to stressor n as the marginal dependency of the growth rate on the (perturbed) environmental variable E_n :

$$x_n = \frac{\partial\mu}{\partial E_n} \quad (3.3)$$

and analogously x_m for stressor m . x_m and x_n denote biomass weighted community traits that best characterize the response of the community to stressors m and n such as susceptibility to grazing in case of trophic control or nutrient usage ability for limitations in nutrient supply (see SI). In the frequent case of a linear dependency of μ on E_n , the interaction trait is equivalent to the specific proportionality factor. Usually, x_n changes upon alteration in E_n owing to, e.g., phenotypic plasticity or species resorting. For the same reasons, interaction traits may also change under application of other stressors (e.g. E_m) such as susceptibility to grazing can alter due to nutrient stress. We hence introduce the cross-trait variation (CTV) that describes how the effective interaction traits are modified by other stressors.

$$\text{CTV} = \frac{x_{m,n} - x_m}{\Delta E_m} + \frac{x_{n,m} - x_n}{\Delta E_n} \quad (3.4)$$

where ΔE_n and ΔE_m again denote the magnitude in each perturbation, and $x_{m,n}$ the interaction trait x_m under combined application of stressor n and m ($x_{n,m}$ the interaction trait x_n in the same case). The cross-trait variation quantifies the extent of how effective interaction traits are modified by other stressors such as alteration in susceptibility to grazing due to nutrient stress and the alteration in nutrient usage ability due to grazing. Inherent to these changes are trade-offs, thus morphological or physiological relations between different traits. If these trade-offs are absent and other stressors do not affect the dynamics in each specific trait ($x_{n,m}=x_n$, $x_{m,n}=x_m$), the CTV is zero.

3.3.3. Model initialization and parameterization

Initial conditions: Phytoplankton cell sizes in the model range from 0.1 to $10^7 \mu\text{m}^3$ (0.6 – 107 μm ESD) corresponding to -0.5 to 6.2 \log_e ESD (μm) (ESD: Equivalent Spherical Diameter), which provides a representative size spectrum of phytoplankton observed in nature [32]. The number of virtual phytoplankton species is set to $n=17$, which has been tested to leave qualitative results unchanged compared to higher resolutions in size classes. The initial distribution of phytoplankton biomass over cell size equals a Gaussian function with mean at 2.8 \log_e ESD (μm), standard deviation at 2 \log_e ESD (μm) and a constant offset of 1 mmol-C m^{-3} for each size bin. Initial intracellular nutrient quotas for both nitrogen and phosphorous are at their maximum.

The initial ambient dissolved nitrogen (N) and phosphorous (P) concentration are set to 7 mmol-N m⁻³ and 0.8 mmol-P m⁻³, respectively. Both small and large ciliates are assumed to have equal initial values (0.25 mmol-C m⁻³), while the biomass concentration of copepods start at 5 mmol-C m⁻³, detritus N and P at 1.8 mmol-N m⁻³ and 0.005 mmol-P m⁻³. All model parameters used in the reference run are summarized in SI (Table S5–S6).

Physiological parameters: As explained in more detail by [98], phytoplankton growth and nutrient uptake parameters are linked to cell size (master trait) through the power law function ($y = \beta V^a$). These size allometries result in group specific values for maximum uptake rate (v_{\max}), maximum growth rate (μ_{\max}), nutrient affinity (A), minimum and maximum cell quotas (Q_{\min} and Q_{\max}). The employed allometric scaling relationships are drawn from recently published studies and are summarized in Table S7.

3.3.4. Validation data and environmental forcings

To test the model skill, we compiled and used data from the Kristineberg mesocosm experiments, conducted in the Gullmar Fjord (Kristineberg, Sweden) between March and July 2013 (113 days) as part of the BIOACID (Biological Impacts of Ocean ACIDification) project phase II. The ten mesocosm bags of 55.5 m³ volume contained the natural plankton spectrum after passing a 1mm mesh. Five control treatments were held at present day CO₂ conditions ($\sim 380 \mu\text{atm } p\text{CO}_2$, here termed LpCO₂), whereas the other five were enriched with CO₂-saturated water to emulate the expected end-of-the-century carbonate chemistry conditions ($\sim 760 \mu\text{atm } p\text{CO}_2$, HpCO₂). A comprehensive description of experimental design and technical details are given by [5]. For the validation runs, time-series of $p\text{CO}_2$, temperature, mixing layer depth (MLD), PAR, and measured zooplankton data were used as forcing. We converted copepod abundance data to biomass by multiplying with a constant factor of $4 \cdot 10^{-4}$ mmol-C/Ind.

We averaged the data of the LpCO₂ and HpCO₂ replicates to yield time-series in chlorophyll a (Chl_a), dissolved inorganic nitrogen (DIN), and dissolved inorganic phosphorous (DIP) concentrations as reference for calibration. All model parameters were identical in the two scenarios.

3.3.5. Numerical stressor experiments and interaction traits

Numerical stressor experiments were run at low $p\text{CO}_2$ and low grazing pressure on the community structure. The relatively strong size selective grazing pressure in the validation runs owing to elevated copepod abundance was lowered by reducing the prey affinity of copepods to allow for moderate co-existence of all phytoplankton size classes. This implies that in the experiments zooplankton was dynamically resolved as state variable. We considered two perturbations (here termed stressors) prevalent in pelagic ecosystems: nutrient enrichment (+Nut) and zooplankton removal (-Zoo). Variations in nutrient levels and zooplankton grazing are commonly perceived as most important for phytoplankton dynamics [24, 51, 39]. Nutrient enrichment (+Nut) may

originate, e.g., from mixing events while zooplankton removal (-Zoo) follows, e.g., from the passage of a swarm of small fish, the major predator of mesozooplankton. Both stressors can be thought to indirectly reflect anthropogenic and climatic changes such as increased storm frequency or the down-harvesting of large pelagic fish and concomitant rise in small fish. The respective states (N and Z) were perturbed at day 57, when nutrients were limited and also the fluctuation in total phytoplankton biomass was negligible for a short time. These shifts were applied individually and also simultaneously at distinct intensities.

All experiments were repeated using a single phytoplankton size class only, with cell size of $3.5 \log(\text{ESD})$, which corresponds to a time- and community- average in most multi-species simulations. This setting emulates state-of-the-art models neglecting trait dynamics and adaptive capacity. Using both the multi- and mono-species configuration, the response of total net growth rate of the community to both single and combined stressors were traced over time and averaged for distinct periods depending on the nutrient state.

From the definition of the two stressors, we deduced the relevant interaction traits following the rationale given in the SI and summarized in Eq.B.6. Each interaction trait represents the growth dependency on a specific ambient factor (stressor). In case of nutrient limitation, the interaction trait quantifies the nutrient usage ability of species. Species that are most sensitive to limiting nutrients are characterized by low nutrient usage ability. These weakest competitors benefit most from the nutrient addition. In case of losses due to copepod grazing, the interaction trait of species can be interpreted as the susceptibility to grazing. The most edible species gain most from zooplankton removal. The community mean of both traits, are inherently related due to their dependencies on the size distribution, which is an example for an indirect size-related trade-off.

3.4. Results

3.4.1. Model validation

The multi-species simulation features a pronounced bloom in Chl_a parallel to a complete draw-down in DIN and DIP, followed by a second bloom at deplete nutrient conditions (Figure 3.2). This dynamics corresponds to the observed (average) time evolution of Chl_a , DIN and DIP concentration. Using measured zooplankton as external forcing leads to a nearly precise reconstruction of the second phytoplankton bloom, including the differences between control and treated $p\text{CO}_2$ environments (Figure 3.2), which approves a high skill in particular of the phytoplankton model.

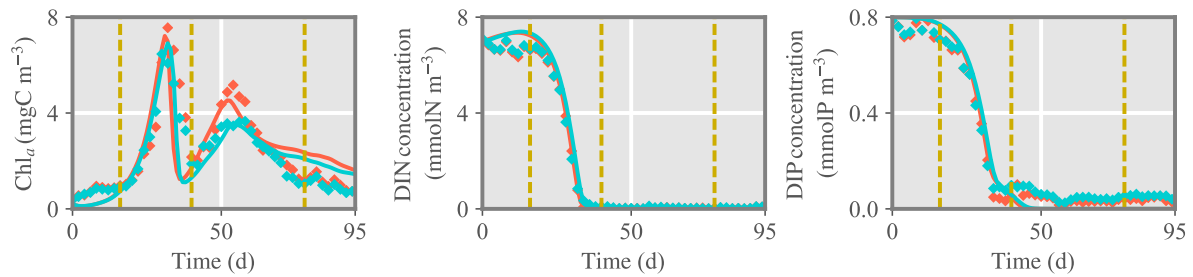


Figure 3.2.: Comparison between chlorophyll a (chl_a), dissolved inorganic nitrogen and phosphorous concentration (DIN, DIP) of the reference run and measured data for the control ($LpCO_2$, blue) and treated ($HpCO_2$, red) mesocosms. Solid lines and diamonds represent model results and measured data respectively. Dashed lines separate different phases of the experiment: initial, first and second spring bloom, and post bloom.

The variations in individual process rates shown in Figure 3.3 disclose possible mechanisms underlying the observed phytoplankton dynamics and how their relevance is changing through the different growth phases. During the initial phase of the simulation, phytoplankton biomass decreases slightly due to aggregation until day ~ 10 for both pCO_2 scenarios. Later around day 30, with gradual drawdown of nutrients (Figure 3.2, B and C), phytoplankton pigment and biomass concentration peaks and abruptly declines upon depletion of nutrients around day 40, because of aggregation together with ongoing grazing (Figure 3.3, A). This reduction appears earlier in the simulation than the data suggest. At this time, strong copepod grazing pressure on intermediate size phytoplankton ($\sim 3 \log_e ESD$) creates a bimodal size distribution with two distinct size groups of small ($2-15\mu m$ ESD) and large model species ($150-500\mu m$ ESD) (Figure 3.3, B). Following the collapse of the first bloom, remineralized nutrients and direct excretion of nutrients by zooplankton enable the formation of a second bloom. Respiratory carbon losses prevail over grazing losses in the first half of the simulation, thus until the second bloom. The effect of high and low pCO_2 becomes visible during the second bloom, under elevated pCO_2 mainly due to higher copepod biomass and thus faster nutrient regeneration in that treatment, which leads to higher phytoplankton biomass especially in the size class representing large and nearly inedible *Coscinodiscus sp.* (Figure 3.3, B). Towards the end of simulation, ongoing grazing pressure together with mixotrophic grazing and sinking result in the collapse of the second bloom.

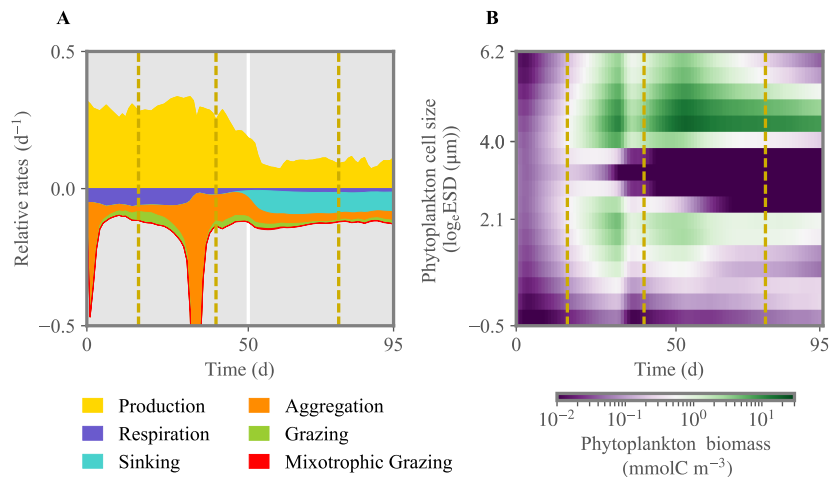


Figure 3.3.: Specific rates and phytoplankton biomass distribution for the reference run under high $p\text{CO}_2$ condition (Hp CO_2). Figure A shows total phytoplankton production and loss rates, and figure B represents individual phytoplankton biomass distribution over the time of experiment. Dashed lines denote different phases of the experiment: initial, first and second spring bloom, and post bloom.

Modified reference run: As a reference to the numerical experiments, the model dynamically resolved zooplankton. The resulting grazing pressure turns out lower compared to the zooplankton imposed from mesocosm measurements (in the calibration run), which prevented intermediate size classes from extinction in the simulation. Although, less herbivores led to a diminished second Chl $_a$ bloom, but the modified reference run still captured the first bloom, which is the main seasonal event in most marine systems (results not shown).

3.4.2. Stressor effects

Nutrient enrichment: Directly after injection of nitrogen, total net growth rate of the model community increases, resulting in higher phytoplankton biomass production (Figure 3.4, I; Figure 3.5, H). After a short delay, also simulated zooplankton starts to grow. The higher biomass level of copepods translate to increased top-down control of both ciliates and phytoplankton. Biomass of small and large ciliates does not change pronouncedly as being already at a very low level. When the injected nitrogen pulse diminishes around days 60-70, aggregation and grazing turn the total net growth rate negative, lowering community biomass production. Owing to the increased copepod biomass, size separation at phytoplankton species with cell size of $\sim 3 \log_e \text{ESD}$ intensifies around day 65 (Figure 3.5, H). A greater copepod stock also leads to biomass enhancement of small species, which make the optimal prey for ciliates. After total drawdown of the injected nitrogen, excretion of nutrients by the decreasing copepod stock and nutrient remineralization fuel the production of mostly small species with cell size $\sim 2\text{--}3 \log_e \text{ESD}$.

Grazer removal: Removal of much of the zooplankton standing stock at day 56 (Figure 3.5, D) results in higher total net growth rate, thus higher biomass production (Figure 3.4, H). However,

the gain in primary production is lower compared to the one in the nutrient enrichment scenario, as during the time of relieved grazing pressure, phytoplankton remains much limited by nutrients. The removal of grazers slightly favors intermediate size classes, so that these smoothly recover from very low biomass levels (Figure 3.5, I), while larger species outside the size grazing kernel of copepods remain unaffected. However, removal of mesozooplankton relieves the ciliates. Their growth slightly reduces the biomass of small species until copepods start to recover shortly after application of the stressor. At that point, total phytoplankton biomass declines. Further mixotrophic grazing, sinking and aggregation also contribute to the decrease of total net growth rate enduring from approximately day 60 towards the end of simulation.

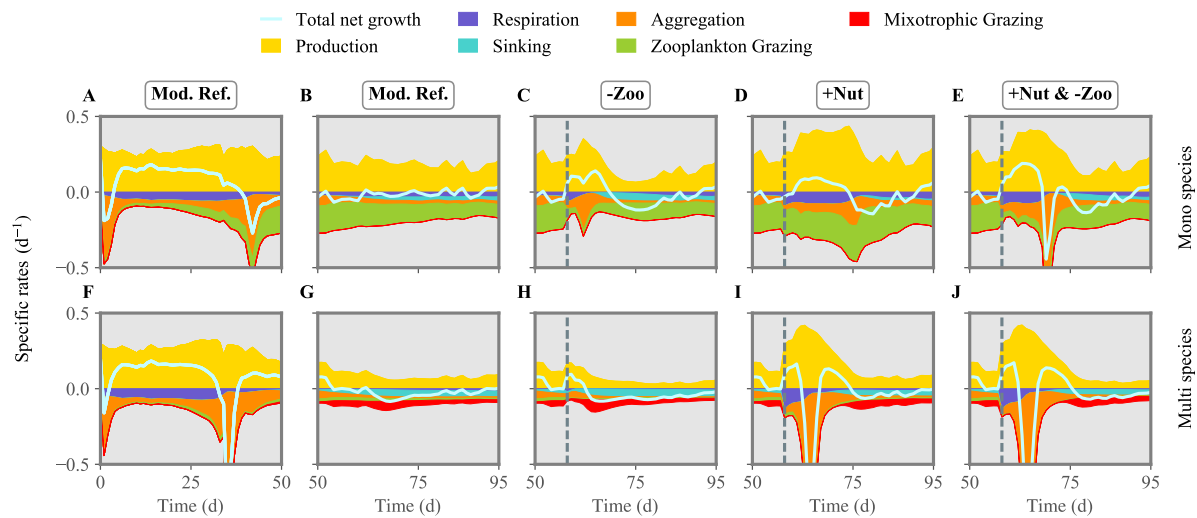


Figure 3.4.: Comparison of phytoplankton total production and loss terms between the mono species model configuration (top panels) and the one with multi species (bottom panels) under single/multiple stressors. +Nut and -Zoo represent two stressors corresponding to nutrient enrichment and grazer removal. The solid line shows relative growth rate (production-loss) of the entire community. The dashed line indicates the time of stressor application.

Nutrient injection and grazer removal: Both nitrogen injection and zooplankton removal, when acting as single stressors, increase the phytoplankton standing stock directly after exposure as explained above. Also when both are applied at the same time, net growth rates increases (Figure 3.5, E). The first 20 days after exposure, changes in the phytoplankton community dynamics are similar to the ones in the nutrient enrichment scenario (Figure 3.5 and 3.4, J). Thereafter, as nutrients are again depleted and zooplankton biomass stays relatively constant but lower compared to the nutrient injection scenario, the phytoplankton community reacts similar to the scenario of (only) zooplankton removal. Hence, although both stressors are applied at the same time, their dominant impact is organized sequentially, here first similar to nutrient enrichment then to zooplankton removal.

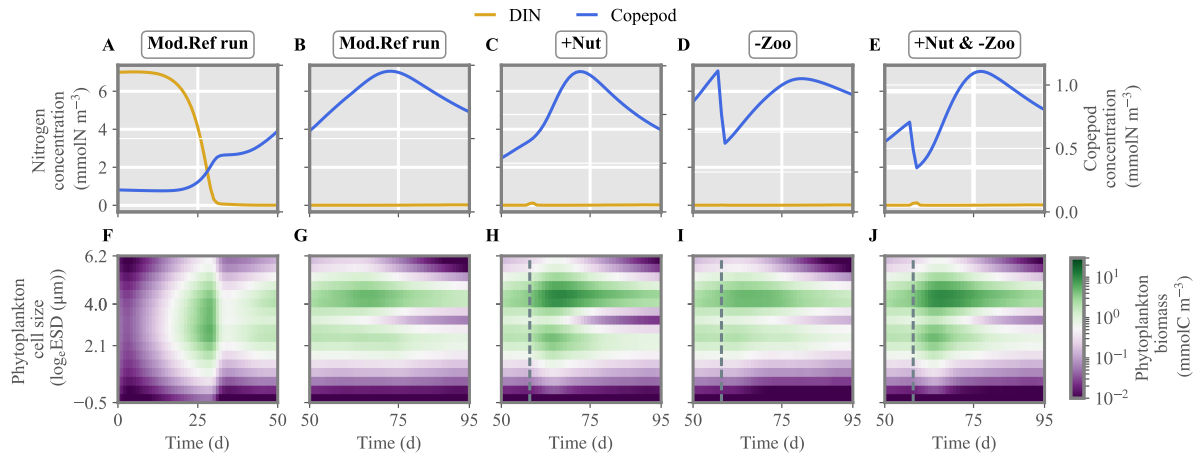


Figure 3.5.: Nitrogen concentration, copepod biomass and phytoplankton biomass distribution under single / multiple stressors. +Nut and -Zoo represent two stressors corresponding to nutrient enrichment and grazer removal. Dashed lines indicate the time of nutrient injection, zooplankton removal or both.

3.4.3. Switching off adaptive responses

We compared the results of the multi species model with a mono species scenario to highlight the importance of species sorting and structural changes. In the reference run and all scenarios, the non-adaptive phytoplankton reaches in average higher primary production rates and is much more top-down controlled compared to the multi-species set-up (Figure 3.4). There, mixotrophic grazing and occasionally aggregation make the major loss processes. The mono species phytoplankton compartment experiences a positive net growth rate until day 45, when both aggregation and copepod grazing terminate the bloom and turn the net growth rate negative (Figure 3.4, A and B). Non-adaptive phytoplankton responds to nutrient enrichment more moderately compared to a community with full adaptive capacity. This pattern is mostly due to limited aggregation losses in the aftermath of the nutrient injection (Figure 3.4, D). The lack of competition and thus of a best adapted species with maximal nutrient usage ability extends the period of nutrient replete conditions. This situation further leads to higher copepod biomass. Removal of the copepods increases both production and aggregation of non-adaptive phytoplankton, but the relieve from the major loss factor stimulates a stronger biomass gain in relation to the adaptive case (Figure B.5, SI). Subsequently, copepods start to recover and graze down the phytoplankton (Figure 3.4, C). Simultaneously injecting nutrients and removing copepods (Figure 3.4, E) strongly enhance positive growth rates until day ~ 65 , where a short phase of intense aggregation terminates the bloom. This pattern is qualitatively similar to the multi-species case, but differs from the non-adaptive response to single stressors.

3.4.4. Effect size dependent on adaptive capacity

Changes in the phytoplankton community composition as induced by single and multiple stressors are displayed in Figure 3.6. Size dependent alterations are shown for two characteristic periods after exerting the stressors, i.e. under nitrogen replete (day 59) and deplete (day 75) conditions. At nutrient replete condition, stressor induced changes in biomass weighed net growth rate are maximal at small and large cell sizes (around 2 and 4 \log_e ESD), thus creating a bimodal size distribution as observed also in Figure 3.5.

The fitness landscape under combined perturbation in nutrient and grazing levels is similar to the one under nutrient injection, which reflects stronger growth stimuli compared to the zooplankton removal scenario. This pattern reappears in the modification of the biomass size spectrum (Figure 3.6, B) as well as of the nutrient usage ability (Figure 3.6, C). The latter increases for small model species because of their higher nutrient affinity and for very large size classes because of their lower subsistence demand. Nutrient usage ability declines for intermediate size phytoplankton but, averaged over the entire community, increases in the "+Nut" and the combined stressor scenario. In the intermediate size range, the susceptibility to copepod grazing slightly decreases under all three stressor scenarios (Figure 3.6, D). In the subsequent nutrient deplete phase, most effects on growth rate and interaction traits are roughly reverted with respect to the initial nutrient replete phase, which indicates a relaxation of the community structure to the original state. Average community growth rates are close to zero after the multiple stressor application and negative in the single stressor experiments, and so are biomass changes. Nutrient usage ability has increased under the "-Zoo" perturbation, while becoming negative for the "+Nut" and the combined scenario. Also susceptibility to grazing has increased in the "-Zoo" case, whereas in the other cases it approaches zero. To sum up, changes in the two interaction traits are in general negatively correlated immediately after stressor application while positively correlated around two weeks thereafter. Trait and growth effects after the onset of a combined stressor with few exceptions resemble the ones in the "+Nut" case.

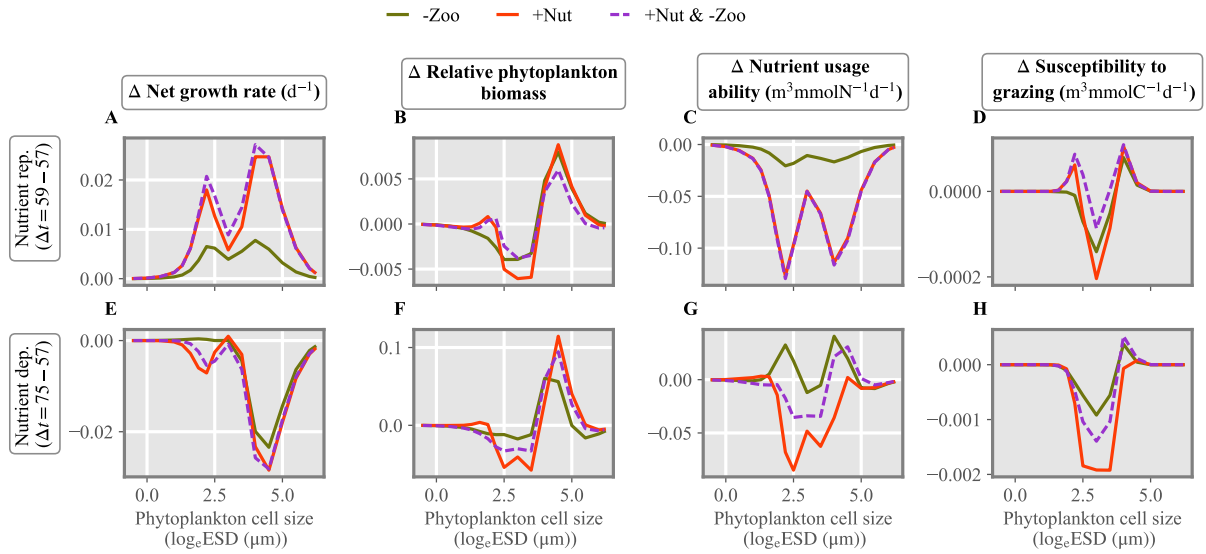


Figure 3.6.: Changes in size dependent characteristics from the state before stressor application: in the contribution of each size class to total net growth rate, in the phytoplankton density distribution, and in interaction traits, the relative nutrient usage ability and susceptibility to copepod grazing. The difference is taken either 2 or 18 days after stressor exertion (see Δt).

3.4.5. Changes in multi-stressor sensitivity over cross-trait variations

When the numerical stressor experiments are run with distinct intensities of nutrient pulses and copepod removals, we obtain a striking pattern in the relation between the cross-trait variation (CTV) and the specific multi-stressor sensitivity (SMS) (Figure 3.7). First, both the SMS and CTV increase over time and the SMS switches from antagonistic to synergistic few days after parallel application of the two stressors. Our results reveal a relatively uniform relationship between CTV and SMS throughout time, independently whether nutrient or grazing stress has been varied. Synergistic effects exclusively occur at positive cross-variations in traits, thus when effective traits shift to higher values under application of complementary stressors, which here means increased nutrient usage ability under grazing removal and increased grazing susceptibility under nutrient pulses.

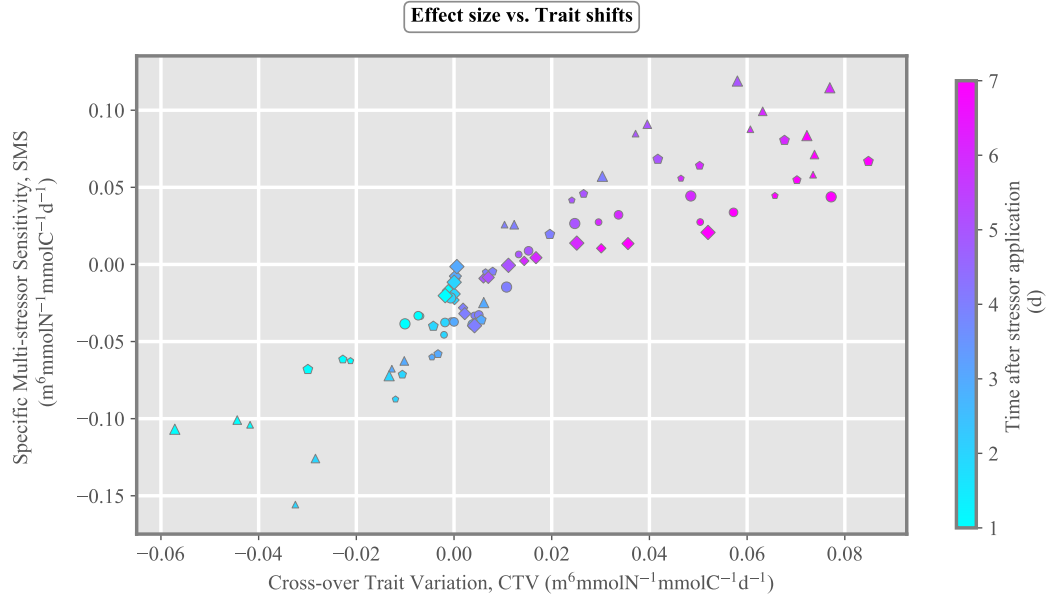


Figure 3.7.: Specific multi-stressor sensitivity (SMS) plotted over cross-trait variation (CTV) for 12 multi-stressor experiments. Nutrient input was varied from 0.2, 0.4, 0.8 to 1.6 mmolN m^{-3} and copepod removal from 0.4, 1.3 to 2.5 mmolC m^{-3} .

3.5. Discussion

Model performance: Our size-based model demonstrates high skills in reproducing average trajectories of Chl_a , DIN and DIP observed during the Kristineberg mecososm experiments. This is remarkable since, model equations and parameters including allometric scalings were chosen in accordance with mechanistic theories of phytoplankton growth [71, 111]. However, some model coefficients describing relevant processes such as aggregation or the fraction of dissolved nutrients released by mesozooplankton could not be constrained by theory or data and thus had to be calibrated. As a result, the model well captures the first and second Chl_a bloom including their decay and the speed of the nutrient drawdown. Furthermore, it also reproduces the observed bi-modal size structure of the phytoplankton community. As described by [5], the most important species contributing to the Chl_a build-up were the small (2–5 μm) silicifying species *Arcocellulus* sp., *Minidiscus* sp. (both diatoms), and *Tetraparma* sp. (Chrysophyte) as well as the very large (>200 μm) diatom *Coscinodiscus* sp. In addition, the main taxa contributing to the second bloom were small (2–5 μm) diatoms (*Minidiscus* sp., *Arcocellulus* sp.), a large variety of small green flagellates (0.8–5 μm) and *Coscinodiscus* sp. Initial (<day 20) moderate mismatches between observed and simulated states may reflect weaknesses in our assumptions on nutrient uptake. Another small discrepancy between data and model appears in the collapse of the first bloom. The function describing phytoplankton TEP production and concomitant particle aggregation has been tested within the model calibration phase to emulate a necessary strong

amplification of aggregation at the onset of nutrient limitation. However, it may still neglect dynamic aspects including delays in aggregate formation. And despite the physiological and ecological detail rarely considered *en suite* in state-of-the-art models, not all processes relevant to achieve full consistency between observations and simulations, are taken into account. For example, viral infection may influence phytoplankton mortality rate [13, 64] and variable sinking velocity [111] can lead to a different reduction of Chl_a .

Processes shaping community dynamics: The phytoplankton dynamics in the model turns out rather robust against $\pm 20\%$ variations in the most relevant parameters; large alterations were only found for the simulated second bloom, which in particular is most sensitive against changes in allometric coefficients of physiological traits (Figure S2). The importance of such size scaling relationships on shaping the phytoplankton community structure and dynamics was previously investigated by [98] using a predecessor model variant. Taherzadeh et al. also demonstrated that physiological size constraints alone cannot provide realistic simulations of phytoplankton size structure, which implies a high relevance of other mechanisms such as selective grazing, aggregation and sinking. The extended model presented here confirms this finding and emphasizes the role of such processes for shaping ecosystem dynamics especially after the first spring bloom peak, which agrees with previous studies [4, 78, 114, 109]. Selective grazing can reduce the ability of the strongest competitors to dominate the community, a mechanism also been termed "killing the winner" [101]. Ongoing grazing of intermediate size species by copepods and of small ones by ciliates allows larger phytoplankton species to grow despite their inferior uptake and growth capabilities. The balance between many size dependent growth and loss factors, most of all nutrient uptake, growth and grazing, has led to coexistence of most size classes in nearly all simulations.

Perturbations in nutrient and grazing levels: In the global ocean, intermittent enrichment of surface water by deep water nutrients is one of the major natural perturbations affecting phytoplankton growth and community composition. Such nutrient additions are generated by various physical processes like internal waves, mesoscale eddies and vertical convective mixing [66]. The injections can vary in their duration from hours to few days in coastal waters, and to monthly or even longer periods in the open ocean [36]. Our nutrient injection experiments emphasize the role of grazing in nutrient rich waters as major process buffering the effect of nutrient addition and hence, keeping the size structure of the community within an observed typical range [32]. Thus, although larger species gain an advantage under nutrient additions, mesozooplankton limits their excessive growth. Conversely, small species with high area-to-volume ratios and high nutrient affinity are in general favoured in oligotrophic oceans [70].

Copepod mortality through consumption by higher trophic levels such as jellyfish and fish larvae or juveniles often makes the second most important natural stressor influencing the lower marine food-web [39]. The results of our individual stressor studies suggest that both, nitrogen enrichment and copepod removal enhance the total net growth rate and biomass production for all phytoplankton size classes, even though not with equal share. Concurrent application of

these two stressors indeed leads to higher positive net growth rate directly after exertion. The growth stimulus is not additive, thus smaller than the sum of the effect of the single stressors. It also triggers a major loss event by amplified aggregation about ten days after the perturbation, and buffers a part of the environmental improvement to the subsequent period.

Role of trait responses: Buffered responses are different to the picture produced by the mono-species model neglecting adaptive trait shifts. Here, the multiple stressors application does not lead to sustaining positive growth effects. Persistent exploitation of growth stimuli even during the nutrient deplete phase therefore seems to require a memory effect mediated by steady re-organization of the phytoplankton community structure, which is most pronounced under multiple stressors application. This finding emphasizes the usefulness of our size-based modeling approach when assessing impacts of multiple stressors on the phytoplankton community. The lack of response buffering through internal re-organization in the mono species scenario results in excessive primary production, which subsequently is strongly counteracted by zooplankton grazing mostly because the susceptibility of phytoplankton remains constant over time. As a consequence, the mono-species phytoplankton compartment is much more top-down controlled compare to multi-species case. Removing internal degrees of freedom not only fails to track observed community size distribution in nature but also leads to the inability of the simulated community biomass to respond realistically to sudden shifts in environmental conditions.

When applied simultaneously, the two stressors act as a single intense perturbation event on the multi-species community that was expected to result in a synergistic community response [41]. However, our results show the opposite. The model outcomes demonstrate that, during the initial phase the overall net effect of combined stressors on the community is similar to the one of nutrient enrichment in isolation. Therefore, based on the additive model proposed by [17], the combined stressor impact cancels single nutrient enrichment stressor effects, resulting in a combined net effect smaller than the sum of individual stressors. About a week after exertion of stressors, the net effect of multiple stressors on the total net growth rate and phytoplankton biomass becomes larger than the sum of two single stressors, hence, combined stressors interact synergistically on the response variables (Figure 3.6, bottom panel).

Our finding on the combined effect of two major environmental stressors for phytoplankton growth points to a possibly more general temporal sequence of accompanying changes at the community and ecosystem level. Over time, the response to nitrogen injection and copepod removal switches from antagonistic to synergistic as traits evolve along a trade-off, here induced by shifts in the size distribution that in turn affect nutrient usage ability and susceptibility to copepod grazing. After a delay, the nutrient usage ability is higher under in "removal" scenarios compared to the "pulse only" scenario. Likewise, edibility becomes lower in "pulse" scenarios compared to the "removal only" case. This positive cross-variation in the major interaction traits mediates a temporal change in the interaction type.

From antagonism to synergy: This change from an antagonistic to a synergistic response is also in agreement with previous studies. For example, the meta analysis of [19] indicated

that experimental duration might be associated with the interaction type, or [80] suggested that the net effect is shifted from antagonistic to synergistic over the course of a six-year experiment when analyzing the interaction between effects of nitrogen availability and CO₂ addition on total plant biomass. In general, directly after exertion of any multiple stressor, new environmental condition can restructure a community constrained by trade-offs. However, over time competitive exclusion following resource depletion reduces the number of species such that only a few (superior) species will manage to survive [81, 96, 15, 55]. Therefore, we observe a synergistic interaction between multiple stressors resulting in a detrimental impact on the diversity in the community.

Multi-stressor sensitivity explained by cross-over trait variation: A first major finding of this study is the emergent proportionality between specific multi-stressor sensitivity and cross-over variations in effective traits:

$$\text{SMS} \approx \text{CTV} \quad (3.5)$$

This relation can be theoretically justified using linear perturbation theory within the new formalism introduced in this work. This framework thus proved ability to link single stressor effects and trait dynamics to multi-stressor effects. It allows to identify possible determinants of the non-linear interaction between stressor reactions with special focus on internal re-organization of biological agents, which in turn is ruled by trade-offs. These trade-offs reflect bio-mechanic constraints, related to morphology or bioenergetics. They are inherent in variations to interaction traits, which in turn incorporate the response specific stressors such as the nutrient usage ability (w.r.t. nutrient limitation) or the susceptibility to grazing. The two new measures SMS and CTV may serve as powerful tools when understanding or even predicting often diverging responses of complex systems under multiple stressors

Conclusion

Phytoplankton communities are increasingly subject to natural or anthropogenic stressors. As effects of each stressor may vary due to the current state of eco-physiological traits and also due to properties of the stressor itself (intensity and duration), it remains one of the most challenging problems to determine the impacts of combined stressors on marine ecosystems. The approach proposed in this study proved its ability to explain when impacts become additive or non-additive. One prerequisite was a new size-based plankton model resolving major dependencies of plankton growth and interaction rates. We specifically illustrated that a mono-species model without size dependencies in eco-physiological traits does not have the ability to track realistic responses of planktonic ecosystems to environmental changes. A second prerequisite is our new formalism that features two measures of often puzzling multi-stressor responses in complex systems: specific multi-stressor sensitivity and cross-trait variation. The novel formalism helped to reveal that those two measures are closely correlated as apparent from a systematic investigation of the influence of multiple stressors on a model plankton

community. The approach thus offers a way to mechanistically explain the variety of responses and interaction types observed in natural systems with special consideration of community re-organization.

Trade-offs between interaction traits can infer positive cross-variations over time such that the impact of multiple stressors switches from antagonistic to synergistic. Our work highlights role of the duration of experiments for the occurrence of synergistic responses. Thus, to be more general, directly after exertion of any (positive) stressors, the newly created environment can favor various groups of species leading to coexistence of different size classes. Later, as conditions becomes severe only superior species are able to withstand and survive. Hence, we observe a switch from antagonistic and synergistic interaction over time.

To sum up, our size-based model in combination with our new trait-based formalism can relate community responses and trait shifts under imposed stressors, and can be used to understand and assess the impacts of various multiple stressors on marine ecosystems.

Acknowledgments

We thank Onur Kerimoglu, Lennart T. Bach, Tim Boxhammer, Maria Moreno de Castro, Henriette Horn, Carsten Lemmen, Markus Schartau, Ulrich Sommer and Jan Taucher and who helped us within fruitful discussions to work on this interesting research. This work was supported by the Helmholtz society via the program PACES, by the German Research Foundation (DFG) within the Priority Program DYNATRAIT, by the German Federal Ministry of Research and Education in the framework projects MOSSCO and BIOACID.

4

*Interplay of ocean acidification with zooplankton towards shaping phytoplankton community*¹

4.1. Abstract

Oceanic uptake of anthropogenic CO₂, thus, consequent reduction in pH level of seawater, known as ocean acidification, is considered as a crucial stressor affecting composition of marine communities. However, net impact of elevated CO₂ remains unclear, as experimental results are equivocal and model studies rare. To gain more understanding about how planktonic communities response to the expected end of century CO₂ ($\sim 380 \mu\text{atm}$), we adopted a mechanistic trait-based plankton, which includes size allometries in eco-physiological properties, such as for trophic interactions or for the sensitivity of primary production to ocean acidification. The model results compare well with a series of observations from long-term mesocosms experiment. Our findings suggest that a significant impact of ocean acidification on the phytoplankton community can only be observed under nutrient repletion. The model outcomes highlights the key role of herbivorous grazers, which can either be reduced or promoted by increased CO₂, as the most important drivers controlling the structure of community under nutrient limitation due to both direct/indirect effects. Zooplankton, directly via size-selective grazing determines the phytoplankton community size structure and biodiversity or indirectly through nutrient excretion into the surface layer extends growth of phytoplankton in time. Direct effects of ocean acidification on the phytoplankton community can either be damped or amplified by indirect effects through higher trophic levels. The positive effect of increased CO₂ on the production of total phytoplankton biomass is amplified by zooplankton community alteration, while changes

¹Taherzadeh, N., Bengfort, M., and Wirtz, K. W. (2018). Interplay of ocean acidification with zooplankton towards shaping phytoplankton community.

in the phytoplankton size-structure are dominated by grazing effects, which act oppositely to the direct CO₂ effects.

4.2. Introduction

Reduction in the pH level of the seawater due to oceanic uptake of anthropogenic CO₂, known as ocean acidification (OA), is commonly believed to be a major threat for marine communities associated with the ongoing climatic change [46]. Despite recent studies on assessing the effect of OA on the phytoplankton [56, 105, 52, 61], it is still poorly known that how OA play a role in shaping marine phytoplankton communities. Most of these studies are limited their investigation to single or a few species, as experimental studies using natural communities are difficult to run and therefore rare or likely too short to unravel system wide modifications [73, 83, 87, 42]. Notwithstanding these caveats, most studies suggest that OA has a limited direct impact on bacterial and plankton communities, especially, when compared to other growth factors or to indirect OA effects. This finding has been substantiated by one of the long-term mesocosms studies, which was conducted in a coastal site in Sweden, using natural plankton communities [5, 44]. The study demonstrated a significant difference for phytoplankton biomass under high $p\text{CO}_2$ and low nutrient conditions that can not unambiguously be linked to CO₂ fertilization alone. An important difference is changes in the food-web structure, here the increase of copepod biomass under high $p\text{CO}_2$, most probably stimulated by enhanced growth of their phytoplankton prey [99]. In addition, this study and a number of community experiments point to larger differences of the response within the community as often pico-phytoplankton or large diatoms were favored under high $p\text{CO}_2$. Clearly, the quantification of such indirect effects requires employment of mechanistic models. These models should also be able to represent structural differences in the response as major driving factors for post-bloom plankton dynamics such as for CO₂-dependent primary production, nutrient uptake, and grazing (or its avoidance). To analyze direct and indirect responses of the community to elevated $p\text{CO}_2$, we adopted a size-based phytoplankton model (Figure 3.1). We concentrated on simulating two size-selective stressors, size-selective grazing and the (indirect) effect of CO₂ fertilization. The aim of this study is to quantitatively attribute observed changes in plankton dynamics in OA experiments to either direct and indirect effects of CO₂ on shaping phytoplankton communities.

4.3. Method and material

4.3.1. Model

We adopted the previously developed size-based model to systematically investigate the impacts of ocean acidification on the size structure of marine phytoplankton communities (Figure 3.1). Comprehensive description of model equations, parameterization and validation data is given

in Section ?? and Appendix B.

4.3.2. Numerical experiments

To test how the model reproduces the experimental results, we distinguish between four different scenarios:

1. **HCO₂+HCop**: High $p\text{CO}_2$ conditions with mean zooplankton abundance from the five treated mesocosms (indicated as red solid line in the following figures).
2. **LCO₂+LCop**: Low $p\text{CO}_2$ conditions with mean zooplankton abundance from the five control mesocosms (blue solid line in figures).
3. **HCO₂+MCop**: High $p\text{CO}_2$ conditions with mean zooplankton abundance from all ten mesocosms (red dashed line in Fig in Figures).
4. **LCO₂+MCop**: Low $p\text{CO}_2$ conditions with mean zooplankton abundance from all ten mesocosms (blue dashed line in Fig in figures).

In order to analyze the impact of selective grazing and acidification on the phytoplankton biodiversity, we looked at the evenness E , which is defined as normalized Shannon index [90]:

$$E = -\frac{\sum_{i=1}^n p_i \ln(p_i)}{\ln n}. \quad (4.1)$$

Here p_i is the proportion of individuals belonging to the i th class of species and n is the total number of different size classes of species. E gives the uncertainty in predicting the species identity of an individual that is taken at random from the dataset.

4.4. Results

4.4.1. The separate effects of grazing and acidification on phytoplankton biomass

There are different studies investigating the effect of ocean acidification on meso-zooplankton species. Some indicate a positive effect on meso-zooplankton abundances [37], some a negative [65, 18, 91, 92]. Most studies agree that direct effects of ocean acidification on copepods for reasonable $p\text{CO}_2$ values are negligible. Nevertheless, indirect effects as changing food quality and quantity might effect meso-zooplankton species abundance. Without modeling the underlying mechanisms in detail we are able to investigate the direct effects of grazing and acidification on the phytoplankton community. This will help us to understand and estimate the potential impact of the combination of both stressors. In the Kristineberg experiment, copepods and

ciliates have a higher and lower biomass respectively, during the second Chl_a bloom in elevated CO_2 experiments than in the control mesocosms (see Fig. 4.1).

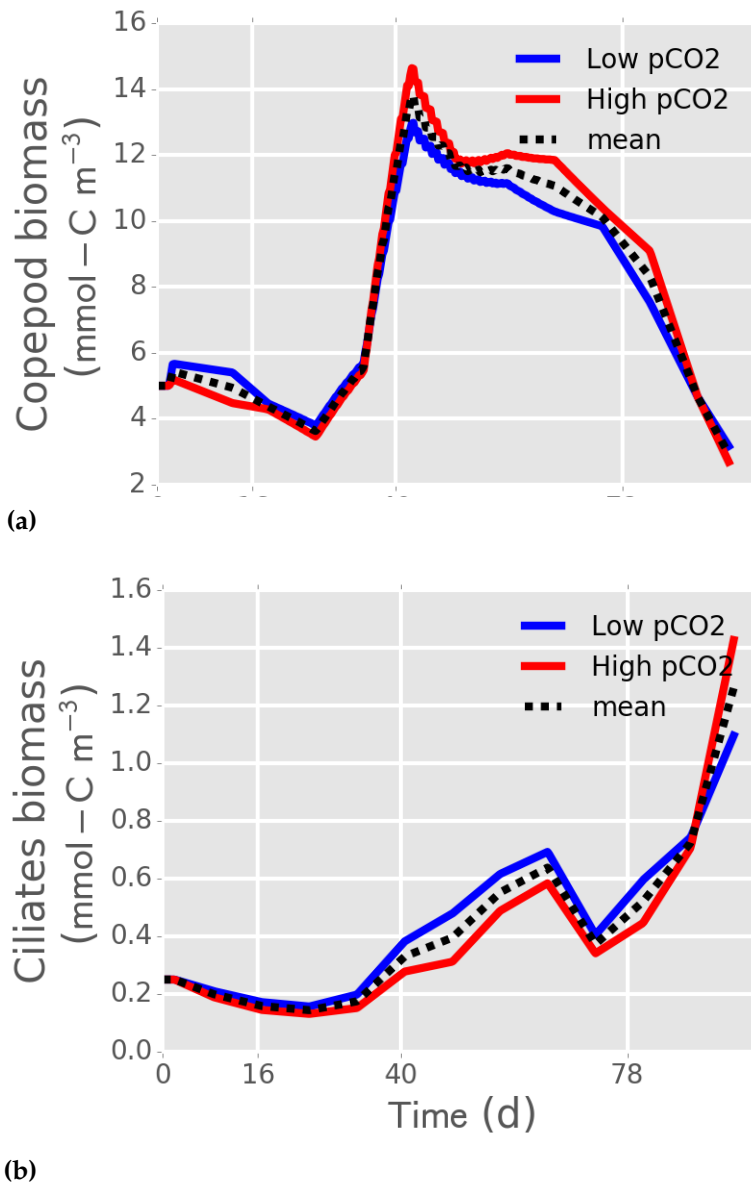


Figure 4.1.: Biomass comparison of copepods and ciliates observed in Kristineberg mesocosms experiment. Solid lines represent mean of each five treated and controlled mesocosms. Dashed line indicates the mean biomass calculated from all 10 mesocosms. Data was interpolated linearly.

Figure 4.2 displays the simulated biomass distribution for the phytoplankton community over time. The positive values in the left figures refer to the case that, a simulation with high $p\text{CO}_2$ conditions and high copepod concentration results in an increment of biomass, while negative values indicate the opposite case. The model outcome without zooplankton (Figure 4.2, b) shows that the zooplankton keeps nutrients and biomass in the system. Without them the particulate organic nutrient pool is depleted soon after the first bloom due to detritus sinking

and hence, no second bloom occurs. The dominant phytoplankton species have a medium size ($\sim 2.7\mu\text{m log}_{\text{ESD}}$) because of their high μ_{max} and being the maximum size class for mixotrophic grazers in the model. For the case where zooplankton grazes on phytoplankton, but does not excrete any nutrients into the system (Figure 4.2 c), the second phytoplankton bloom is not as pronounced as in the experimental observations. All simulations demonstrate that large species benefit from high $p\text{CO}_2$ during the first bloom. The higher amount of biomass results in a higher biomass reduction due to aggregation. Therefore, we observe negative effects of elevated $p\text{CO}_2$ on phytoplankton biomass directly after the first bloom. This effect is more strong for medium sized phytoplankton species.

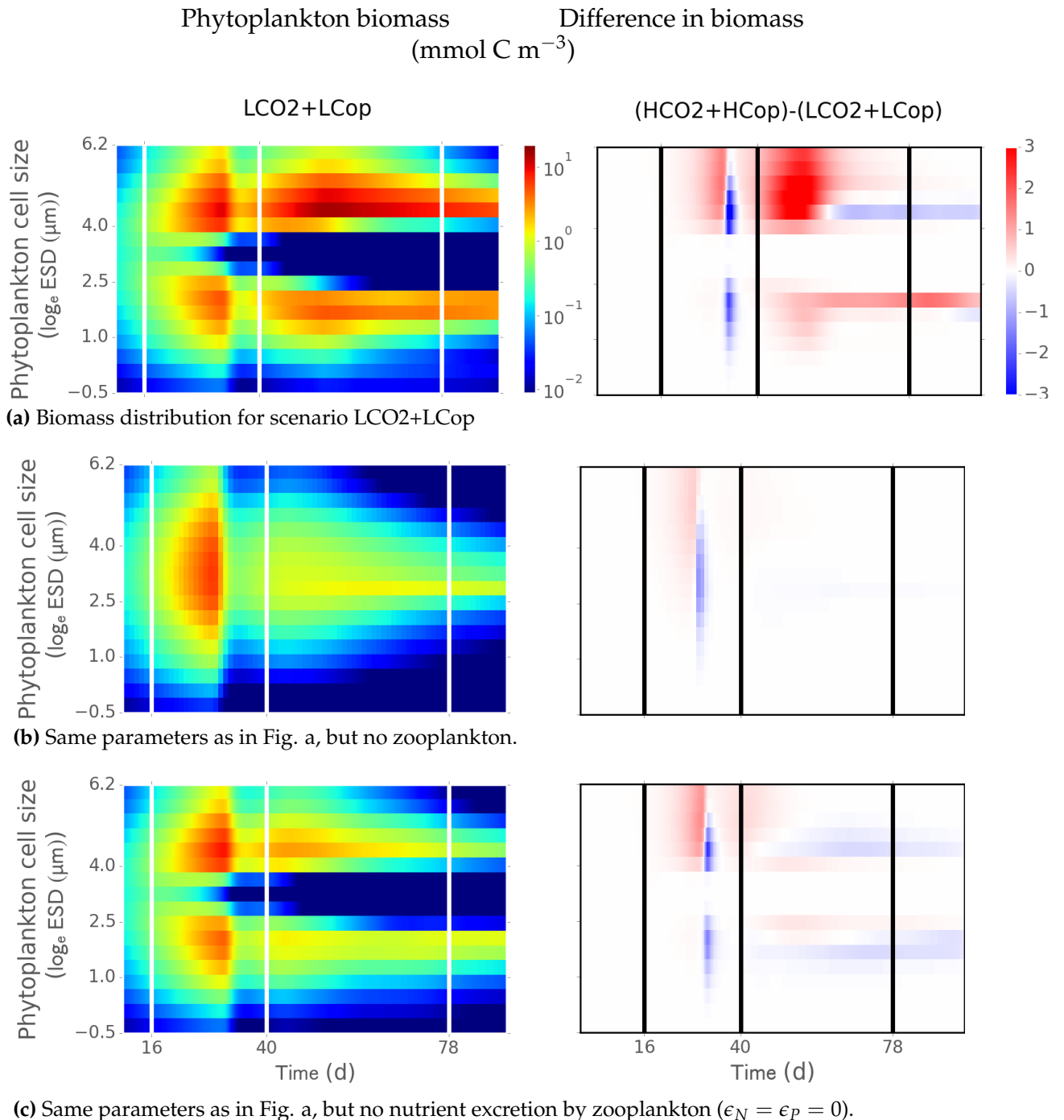


Figure 4.2.: Impact of zooplankton on the phytoplankton biomass distribution. Left: scenario LCO₂+LCop with data from control mesocosms for $p\text{CO}_2$ and grazers. Right: Difference between scenario LCO₂+LCop and HCO₂+HCop.

The amplifying effect of copepods on phytoplankton biomass during the second bloom of the experiments is shown in Figure 4.3. In the case of scenario 3 (HCO₂+MCop) and 4 (LCO₂+MCop) (dashed lines in Figure 4.3), the difference in Chl_a concentration is caused by higher phytoplankton growth under elevated $p\text{CO}_2$ conditions. This effect is even amplified in scenario 1 (HCO₂+HCop) and 2 (LCO₂+LCop) (solid lines in Figure 4.3), as the higher copepod

biomass results in an increased nutrient input in the high $p\text{CO}_2$ scenario. Nutrient excretion by zooplankton is proportional to their biomass. Therefore, copepods have a much stronger effect on the total phytoplankton biomass than ciliates.

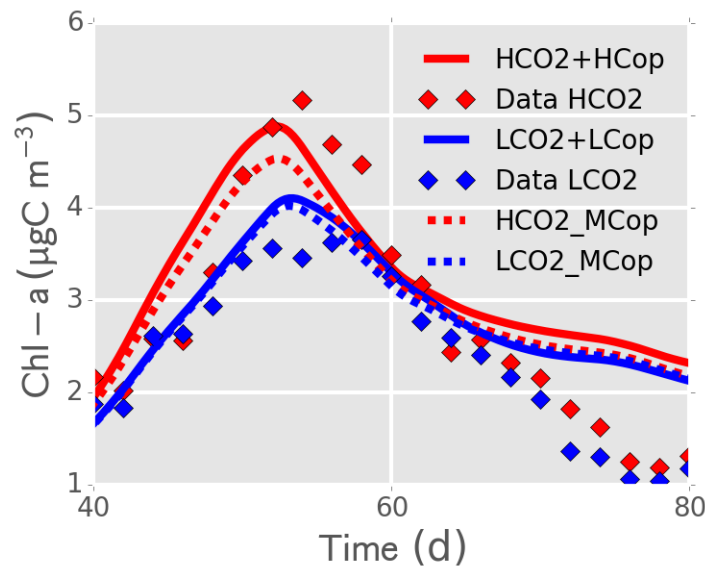


Figure 4.3.: Chl_a concentration during the second bloom. Dashed lines indicate simulations with different $p\text{CO}_2$ conditions but the same values for zooplankton biomass. This zooplankton biomass is obtained from the mean of all 10 mesocosm experiments. Simulations plotted with solid lines were run with mean zooplankton data from treated or control mesocosms only.

4.4.2. Changes in the community size structure and biodiversity

In the previous section, we presented that copepods have a positive effect on the total phytoplankton biomass. As copepods do not only consume phytoplankton but also ciliates, which in turn are predators of smaller phytoplankton species, the effect of changing abundance in grazers on the size distribution of the phytoplankton community is more difficult to analyze. Figure 4.4 shows how the temporal mean of the relative biomass of small phytoplankton species ($\text{ESD} < 9\mu\text{m}$) changes for different $p\text{CO}_2$ conditions and grazing scenarios. The left of the x-axis hereby represent the scenario with low copepod and high ciliat concentration taken from the experiments under low CO_2 conditions (see Fig. 4.1). The right side of the x-axis represent the scenario with high copepod and low ciliate concentration. In the middle of the x-axis we used the mean zooplankton concentration from all 10 mesocosm experiments. $p\text{CO}_2$ is kept constant on different values (y-axis) during the single simulations. The relative biomass of small species decreases with increasing CO_2 pressure. This is caused by the fact that, large species have the strongest direct benefit from increased $p\text{CO}_2$ in our model. An increase of copepods leads to a decrease in ciliates biomass, the reduced grazing pressure on small phytoplankton species enables an increase of their biomass as well. If small species benefit from this indirect effects, large species have a disadvantage as they compete for the same nutrients. In terms of direct CO_2

effects, major changes occur for low values of $p\text{CO}_2$. The model outcome suggests that, above approximately $500 \mu\text{atm}$ any further increase of $p\text{CO}_2$ will not result in significant direct effects. Direct effects are even more stronger, if we simulate a change to preindustrial CO_2 conditions ($< 300 \mu\text{atm}$).

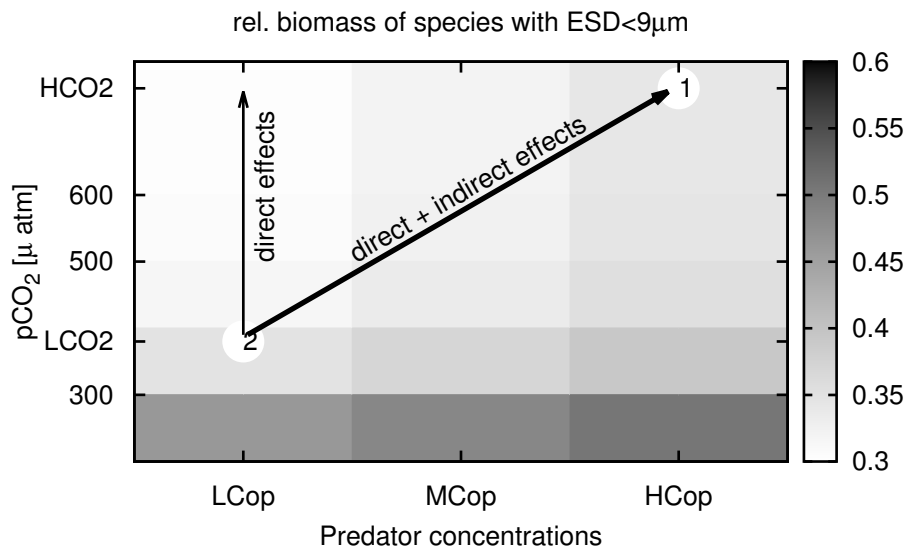


Figure 4.4.: The temporal mean of relative biomass of species smaller than $9 \mu\text{m}$ ESD for different $p\text{CO}_2$ conditions and grazing scenarios.

In our reference scenarios we observe that, initially evenness increases as phytoplankton biomass increases. This is independent from CO_2 treatment and grazing as long as nutrients are available and predators are rare. In the high $p\text{CO}_2$ scenario with high copepod concentration evenness reaches higher values than under low $p\text{CO}_2$ conditions (Figure 4.5). Using the same grazing pressure for both scenarios, the difference between the high and low $p\text{CO}_2$ scenario is very small and opposite to the scenarios with different copepod concentrations under high and low $p\text{CO}_2$ conditions. Large species benefit from increased $p\text{CO}_2$ independent from the predator biomass used for the simulation. Consequently, the relative biomass of small species decreases with increased $p\text{CO}_2$ if the same predator concentrations are used in both scenarios (see Figure 4.4). If copepods increase their biomass with increasing $p\text{CO}_2$, as it was the case in the Kristineberg experiments, the direct CO_2 effect on the phytoplankton community distribution can be damped or even inverted by the reduced grazing pressure from ciliates. When small species grow under nutrient depleted conditions, mixotrophic grazing transports biomass to larger size-classes. This leads to an increased evenness under high copepod concentrations (Fig. 4.5).

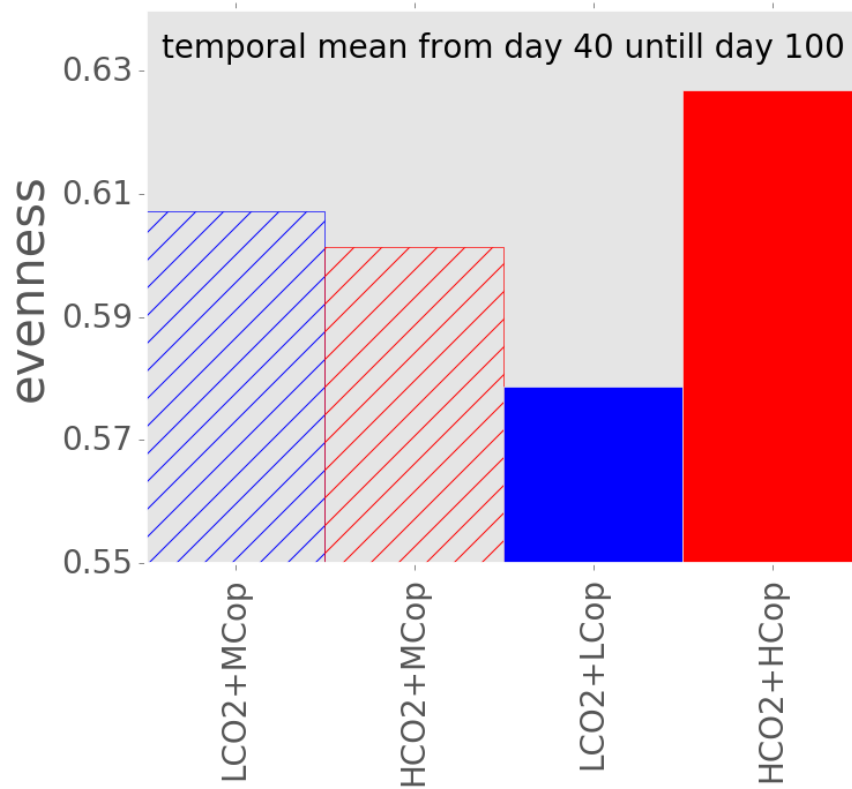


Figure 4.5.: Evenness, E , as index for biodiversity calculated in simulations for different grazing forcings in high and low $p\text{CO}_2$ scenarios.

4.5. Discussion and conclusion

Despite the fact that, we used the mean data from all CO_2 enriched and control mesocosms respectively, the individual experiments performed a bit differently in each case. Our finding that, copepod biomass increases the total phytoplankton biomass in case of nutrient depletion during the second bloom, remains true for the individual experiments as well. Looking at measurements from individual mesocosm experiments instead of mean results from treated and untreated mesocosms, we see that there is a positive correlation between Chl_a concentration and copepod abundance during the second bloom (Appendix C, Figure C.1.1). This correlation seems to be independent from the CO_2 treatment. In general, grazers have a negative effect for species that fit in their feeding kernel, but they can have a positive effect for the total phytoplankton biomass. Following our stressor definition, zooplankton are more a subsidy than a stressor for the phytoplankton community in the system we have studied here. While, an increased CO_2 pressure caused by anthropogenic climate change follows the classic stressor definition.

In terms of size structure within the phytoplankton community, our model indicates an increase of larger species biomass with increasing atmospheric $p\text{CO}_2$. Although, the model reproduces the general pattern in the biomass development of *Coscinodiscus sp.*, the timing of the blooms is shifted in relation to the measured data. In addition, the model seems to

overestimate the amplitude of these blooms (Appendix C, Figure C.2.1). This is partly may be due to the model results showing the biomass of all species larger than 200 μm ESD, while the data point are calculated only from *Coscinodiscus sp.* abundance. Therefore, a direct comparison of simulated relative biomass of *Coscinodiscus sp.* (see Fig. 4.5) with empirical data is difficult and would probably lead to a misinterpretation of the results. In summary, our simulations suggest that, zooplankton not only changes the phytoplankton community size distribution by selective grazing, but promotes phytoplankton growth by providing nutrients.

Large phytoplankton species dominate blooms, because they benefit most from direct CO_2 effects and do not suffer from grazing. This direct effect can be outweighed by indirect effects like a decrease of ciliates through intermediate grazing, which favors small phytoplankton species. This is in line with previous results from experimental data analysis by Langer *et al.* [54] who conclude that top-down effects from predators, rather than bottom-up effects from food source determine the composition of small-sized plankton communities. Indirect effects of copepods on microphytoplankton and bacterial communities via a trophic cascade have been studied in detail by Zöller *et al.* [115]. Similar mesocosms experiments in Finland in 2015, showed comparable results [75]. Paul *et al.* demonstrated that the positive effect of increased $p\text{CO}_2$ on the chlorophyll concentration is caused by organic matter which is longer available as a nutrient pool for phytoplankton under high $p\text{CO}_2$ than under current conditions. They correlate this observation with a decreased respiration and bacterial production rate under acid conditions. The complexity arising from interactions on different trophic levels makes it difficult to extrapolate the results from small-scale experiments or simulation to larger scales. In order to evaluate the effect of climate change on the plankton community, it is important to point out that ocean acidification is not an alone-standing effect. Rather, it is accompanied by an increase in temperature, which is supposed to have a strong effect on most species [76].

Acknowledgments

We thank Lennart T. Bach, Tim Boxhammer, Maria Moreno de Castro, Henriette Horn, Onur Kerimoglu, Carsten Lemmen, Markus Schartau, Ulrich Sommer and Jan Taucher and who helped us within fruitful discussions to work on this interesting research. This work was funded by the German Federal ministry of Science and Education (BMBF) in the framework of BIOACID III project (FKZ 03F0728B). It was also funded by the Deutsche Forschungsgemeinschaft (DFG) within the Priority Programme 1704 Flexibility matters: Interplay between trait diversity and ecological dynamics using aquatic communities as model systems (DynaTrait).

General conclusion

Phytoplankton communities are increasingly subject to natural or anthropogenic stressors. As effects of each stressor may vary due to the current state of eco-physiological traits and also due to properties of the stressor itself (intensity and duration), it remains one of the most challenging problems to determine the impacts of combined stressors on marine ecosystems. The main aim of this thesis was to understand the influence of these stressors on the phytoplankton community by systematically assessing the underlying mechanisms and eco-physiological traits and trade-offs between them. For doing so, a trait-based modeling approach as a powerful tool to link trait changes to temporal variability in environment have been used with phytoplankton cell size as a key trait linking other major eco-physiological traits. As it is not possible to investigate all types of stressors, for this work nutrient enrichment, grazer removal, elevated CO₂ and selective grazing have been selected as major stressors threatening the community.

This thesis explicitly for the first time considered the uncertainties in underlying scaling rules and systematically investigated the importance of size scaling of each eco-physiological trait in ecosystem models. Using a size-based multi species nutrient-phytoplankton-detritus model forced periodically by deep nutrient rich water, in particular it is found that the diatom community mean size and size diversity follow a unimodal distribution across nutrient mixing periodicities. Conversely, when all taxonomic groups are considered the model always reveals dominance of smaller species regardless of any nutrient/mixing regime. The lower nutrient subsistence demand of larger diatoms is indicated as a key trait sustaining them at intermediate mixing periodicities and high maximum growth rate of smaller cells as the main determinant of their success at too stable and too unstable environments. Non-uniform scaling in maximum growth rate is revealed to be crucial in preventing dominance of unrealistically small (diatoms) species. However, for the all marine phytoplankton species community, it is found that non-uniformity alone can not alleviate the lack of larger phytoplankton, which reflects weaker influence of allometries of minimum and maximum quotas or lacking of other possible processes such as sinking, grazing, aggregation and etc (chapter 2).

Extending the previously developed model to resolve multi-species phytoplankton-nutrients-detritus-zooplankton dynamics within the upper mixed layer and introducing mentioned missing processes, this work aimed to address the influence of simultaneously occurring multiple stressors, nutrient enrichment and grazing removal, on the phytoplankton community. A novel

approach proposed here to link community net growth rate to shift in the environmental conditions and correlating it with trait-mediated adaptive response helped to assess why and when non-additive interactions are observed. In this approach we introduced two new terms: cross-trait variation (CTV) and the specific multi-stressor sensitivity (SMS) to assess the multi-stressors dynamics. Result of various numerical stressor experiments in this study with distinct intensities nutrient pulses and copepod removals reveals a striking pattern in the relation between the CTV and the SMS. First, both the SMS and CTV increase over time and the SMS switches from antagonistic to synergistic few days after parallel application of the two stressors. The results also highlight a relatively uniform relationship between CTV and SMS throughout time, independently whether nutrient or grazing stress has been varied. Synergistic effects exclusively occur at positive cross-variations in traits, thus when effective traits shift to higher values under application of complementary stressors, which here means increased nutrient usage ability under grazing removal and increased grazing susceptibility under nutrient pulses. This work demonstrated that synergistic effects need time to evolve, thus highlighting the role of duration of experiment. This thesis moreover emphasis on the importance of size-based models as a mono-species model without size differentiation does not have the power to track shifts in environment and thus, adaptation of species to their habitats to maintain community composition as observed in nature (chapter 3).

In this thesis, it is in particular found that ocean acidification has significant impact on the phytoplankton community only under nutrient replete condition. It is also pinpoint the critical role of herbivorous grazers as the most important drivers controlling the structure of community under nutrient limitation due to its both direct/indirect effects. Zooplankton, directly via size-selective grazing determines the phytoplankton community size structure and biodiversity or indirectly through nutrient excretion into the surface layer extends growth of phytoplankton in time. Direct effects of ocean acidification on the phytoplankton community is shown that it can be damped or amplified by indirect effects through higher trophic levels. The positive effect of elevated CO_2 on the production of total phytoplankton biomass is amplified by the changes in zooplankton community, while alteration in the phytoplankton size-structure are dominated by grazing effects, which act oppositely to the direct CO_2 effects (chapter 4).

The model presented in this thesis contain simplifications and assumptions as any model, but powerful enough to capture real community dynamics as observed in long term outdoor Kristineberg mesocosms experiments. In addition, all numerical experiments are chosen as close to events observed in nature. To sum up, this work with the presented size-based model (validated with data) and performed numerical experiments, is the first modeling study which, mechanistically and systematically investigated the impact of interplay of stressors and phytoplankton physiological properties on shaping the community size structure. This trait-based framework can be further be used to understand and assess the impacts of other multiple stressors such as global warming threatening marine ecosystems.

Bibliography

- [1] Esteban Acevedo-Trejos, Gunnar Brandt, Jorn Bruggeman, and Agostino Merico. Mechanisms shaping size structure and functional diversity of phytoplankton communities in the ocean. *Scientific Reports*, 5:8918, 2015.
- [2] Nona S. R. Agawin, Carlos M. Duarte, and Susana Agustí. Nutrient and temperature control of the contribution of picoplankton to phytoplankton biomass and production. *Limnology and Oceanography*, 45(8):1891–1891, 2000. ISSN 1939-5590. doi: 10.4319/lo.2000.45.8.1891a. URL <http://dx.doi.org/10.4319/lo.2000.45.8.1891a>.
- [3] DL Aksnes and JK Egge. A theoretical model for nutrient uptake in phytoplankton. *Marine Ecology Progress Series*. Oldendorf, 70(1):65–72, 1991.
- [4] Robert A. Armstrong. Grazing limitation and nutrient limitation in marine ecosystems: Steady state solutions of an ecosystem model with multiple food chains. *Limnology and Oceanography*, 39(3):597–608, 1994. ISSN 1939-5590. doi: 10.4319/lo.1994.39.3.0597. URL <http://dx.doi.org/10.4319/lo.1994.39.3.0597>.
- [5] Lennart T. Bach, Jan Taucher, Tim Boxhammer, Andrea Ludwig, The Kristineberg KOSMOS Consortium, Eric P. Achterberg, María Algueró-Muñiz, Leif G. Anderson, Jessica Bellworthy, Jan Büdenbender, Jan Czerny, Ylva Ericson, Mario Esposito, Matthias Fischer, Mathias Haunost, Dana Hellemann, Henriette G. Horn, Thomas Hornick, Jana Meyer, Michael Sswat, Maren Zark, and Ulf Riebesell. Influence of ocean acidification on a natural winter-to-summer plankton succession: First insights from a long-term mesocosm study draw attention to periods of low nutrient concentrations. *PLOS ONE*, 11(8):1–33, 08 2016.
- [6] Karl Banse. Cell volumes, maximal growth rates of unicellular algae and ciliates, and the role of ciliates in the marine pelagial. *Limnology and Oceanography*, 27(6):1059–1071, 1982. ISSN 1939-5590. doi: 10.4319/lo.1982.27.6.1059.
- [7] Andrew D. Barton, Andrew J. Pershing, Elena Litchman, Nicholas R. Record, Kyle F. Edwards, Zoe V. Finkel, Thomas Kiørboe, and Ben A. Ward. The biogeography of marine plankton traits. *Ecology Letters*, 16(4):522–534, 2013.

- [8] John Beardall and John A Raven. The potential effects of global climate change on microalgal photosynthesis, growth and ecology. *Phycologia*, 43(1):26–40, 2004.
- [9] John Beardall and Slobodanka Stojkovic. Microalgae under global environmental change: implications for growth and productivity, populations and trophic flow. *ScienceAsia*, 32(s1):001–010, 2006.
- [10] P. K. Bienfang, P. J. Harrison, and L. M. Quarmby. Sinking rate response to depletion of nitrate, phosphate and silicate in four marine diatoms. *Marine Biology*, 67(3):295–302, 1982. ISSN 1432-1793. doi: 10.1007/BF00397670.
- [11] Andrew R Blaustein and Joseph M Kiesecker. Complexity in conservation: lessons from the global decline of amphibian populations. *Ecology letters*, 5(4):597–608, 2002.
- [12] James H. Brown, James F. Gillooly, Andrew P. Allen, Van M. Savage, and Geoffrey B. West. Toward a metabolic theory of ecology. *Ecology*, 85(7):1771–1789, 2004. ISSN 1939-9170. doi: 10.1890/03-9000.
- [13] Corina PD Brussaard. Viral control of phytoplankton populations—a review. *J. Eukaryotic Microbiol.*, 51(2):125–138, 2004.
- [14] John Cairns. Stress, environmental. 2014.
- [15] Scott L Collins and Susan M Glenn. Intermediate disturbance and its relationship to within-and between-patch dynamics. *New Zealand Journal of Ecology*, pages 103–110, 1997.
- [16] Renato Mendes Coutinho, Toni Klauschies, and Ursula Gaedke. Bimodal trait distributions with large variances question the reliability of trait-based aggregate models. *Theoretical Ecology*, (4):389–408, 2016. ISSN 1874-1746. doi: 10.1007/s12080-016-0297-9.
- [17] Caitlin Mullan Crain, Kristy Kroeker, and Benjamin S. Halpern. Interactive and cumulative effects of multiple human stressors in marine systems. *Ecology Letters*, 11(12):1304–1315, 2008. ISSN 1461-0248. doi: 10.1111/j.1461-0248.2008.01253.x. URL <http://dx.doi.org/10.1111/j.1461-0248.2008.01253.x>.
- [18] Gemma Cripps, Penelope Lindeque, and Kevin J Flynn. Have we been underestimating the effects of ocean acidification in zooplankton? *Global Change Biology*, 20(11):3377–3385, 2014.
- [19] Emily S Darling and Isabelle M Côté. Quantifying the evidence for ecological synergies. *Ecology letters*, 11(12):1278–1286, 2008.
- [20] Scott C Doney, Victoria J Fabry, Richard A Feely, and Joan A Kleypas. Ocean acidification: the other co2 problem. 2009.

- [21] Stéphane Dray and Pierre Legendre. Testing the species traits environment relationships: The fourth-corner problem revisited. 89:3400–3412, 12 2008.
- [22] M. R. Droop. Some thoughts on nutrient limitation in algae. *Journal of Phycology*, 9(3): 264–272, 1973. ISSN 1529-8817. doi: 10.1111/j.1529-8817.1973.tb04092.x.
- [23] Helene Ducobu, Jef Huisman, Richard R. Jonker, and Luuc R. Mur. Competition between a prochlorophyte and a cyanobacterium under various phosphorus regimes: Comparison with the droop model. *Journal of Phycology*, 34(3):467–476, 1998. ISSN 1529-8817. doi: 10.1046/j.1529-8817.1998.340467.x.
- [24] J Emmett Duffy. Biodiversity loss, trophic skew and ecosystem functioning. *Ecology Letters*, 6(8):680–687, 2003.
- [25] R. C. Dugdale. Nutrient limitation in the sea: Dynamics, identification, and significance. *Limnology and Oceanography*, 12(4):685–695, 1967. ISSN 1939-5590. doi: 10.4319/lo.1967.12.4.0685.
- [26] Wolfgang Ebenhoeh. Temporal organization in a multi-species model. *Theoretical Population Biology*, 42(2):152–171, 1992. ISSN 0040-5809. doi: [http://dx.doi.org/10.1016/0040-5809\(92\)90010-Q](http://dx.doi.org/10.1016/0040-5809(92)90010-Q).
- [27] Andrew M. Edwards. Adding detritus to a nutrient-phytoplankton-zooplankton model: a dynamical-systems approach. *Journal of Plankton Research*, 23(4):389–413, 2001. doi: 10.1093/plankt/23.4.389.
- [28] Andrew M. Edwards and John Brindley. Oscillatory behaviour in a three-component plankton population model. *Dynamics and Stability of Systems*, 11(4):347–370, 1996. doi: 10.1080/02681119608806231.
- [29] Kyle F. Edwards, Mridul K. Thomas, Christopher A. Klausmeier, and Elena Litchman. Allometric scaling and taxonomic variation in nutrient utilization traits and maximum growth rate of phytoplankton. *Limnology and Oceanography*, 57(2):554–566, 2012. ISSN 1939-5590. doi: 10.4319/lo.2012.57.2.0554.
- [30] M. J. R. Fasham, H. W. Ducklow, and S. M. McKelvie. A nitrogen-based model of plankton dynamics in the oceanic mixed layer. *Journal of Marine Research*, 48(3):591–639, 1990.
- [31] Christopher B. Field, Michael J. Behrenfeld, James T. Randerson, and Paul Falkowski. Primary production of the biosphere: Integrating terrestrial and oceanic components. *Science*, 281(5374):237–240, 1998. ISSN 0036-8075. doi: 10.1126/science.281.5374.237.
- [32] Zoe V. Finkel, John Beardall, Kevin J. Flynn, Antonietta Quigg, T. Alwyn V. Rees, and John A. Raven. Phytoplankton in a changing world: cell size and elemental stoichiometry. *Journal of Plankton Research*, 32(1):119–137, 2010. doi: 10.1093/plankt/fbp098.

- [33] Sabine Flöder and Helmut Hillebrand. Species traits and species diversity affect community stability in a multiple stressor framework. *Aquatic Biology*, 17(3):197–209, 2012.
- [34] Michael J. Follows and Stephanie Dutkiewicz. Modeling diverse communities of marine microbes. *Annual Review of Marine Science*, 3(1):427–451, 2011. doi: 10.1146/annurev-marine-120709-142848.
- [35] CL Folt, CY Chen, MV Moore, and J Burnaford. Synergism and antagonism among multiple stressors. *Limnol. Oceanogr*, 44(3 part 2):864–877, 1999.
- [36] Ann E. Gargett. Physical processes and the maintenance of nutrient-rich euphotic zones. *Limnology and Oceanography*, 36(8):1527–1545, 1991. ISSN 1939-5590. doi: 10.4319/lo.1991.36.8.1527.
- [37] Jessica Garzke, Thomas Hansen, Stefanie MH Ismar, and Ulrich Sommer. Combined effects of ocean warming and acidification on copepod abundance, body size and fatty acid content. *PloS one*, 11(5):e0155952, 2016.
- [38] James P. Grover. Resource competition in a variable environment: Phytoplankton growing according to the variable-internal-stores model. *The American Naturalist*, 138(4):811–835, 1991.
- [39] Daniel S Gruner, Jennifer E Smith, Eric W Seabloom, Stuart A Sandin, Jacqueline T Ngai, Helmut Hillebrand, W Stanley Harpole, James J Elser, Elsa E Cleland, Matthew ES Bracken, et al. A cross-system synthesis of consumer and nutrient resource control on producer biomass. *Ecology letters*, 11(7):740–755, 2008.
- [40] Lionel Guidi, Lars Stemann, George a. Jackson, Frédéric Ibanez, Hervé Claustre, Louis Legendre, Marc Picheral, and Gabriel Gorsky. Effects of phytoplankton community on production, size, and export of large aggregates: A world-ocean analysis. *Limnology and Oceanography*, 54(6):1951–1963, 2009. ISSN 0024-3590. doi: 10.4319/lo.2009.54.6.1951.
- [41] Alex R. Gunderson, Eric J. Armstrong, and Jonathon H. Stillman. Multiple stressors in a changing world: The need for an improved perspective on physiological responses to the dynamic marine environment. *Annual Review of Marine Science*, 8(1):357–378, 2016. PMID: 26359817.
- [42] Christiane Hassenrück, Artur Fink, Anna Lichtschlag, Halina E Tegetmeyer, Dirk de Beer, and Alban Ramette. Quantification of the effects of ocean acidification on sediment microbial communities in the environment: the importance of ecosystem approaches. *FEMS microbiology ecology*, 92(5), 2016.
- [43] F. P. Healey. Slope of the monod equation as an indicator of advantage in nutrient competition. *Microbial Ecology*, 5(4):281–286, 1980. doi: 10.1007/BF02020335.

- [44] Henriette G. Horn, Nils Sander, Annegret Stuhr, María Algueró-Muñiz, Lennart T. Bach, Martin G. J. Löder, Maarten Boersma, Ulf Riebesell, and Nicole Aberle. Low co2 sensitivity of microzooplankton communities in the gullmar fjord, skagerrak: Evidence from a long-term mesocosm study. *PloS one*, 11(11):e0165800, 2016.
- [45] J. Huisman and F.J. Weissing. Competition for nutrients and light among phytoplankton species in a mixed water column: Theoretical studies. *Water Science and Technology*, 32(4): 143–147, 1995. ISSN 0273-1223. doi: [http://dx.doi.org/10.1016/0273-1223\(95\)00691-5](http://dx.doi.org/10.1016/0273-1223(95)00691-5).
- [46] IPCC. Impacts, adaptation and vulnerability. contribution of working group ii to the fourth assessment report of the intergovernmental panel on climate change. 2007. *ML, Canziani, OF, Palutikof, JP, van der Linden, PJ, Hanson, CE (eds) Cambridge University Press, Cambridge, 2007.*
- [47] Andrew J. Irwin, Zoe V. Finkel, Oscar M. E. Schofield, and Paul G. Falkowski. Scaling-up from nutrient physiology to the size-structure of phytoplankton communities. *Journal of Plankton Research*, 28(5):459–471, 2006. doi: 10.1093/plankt/fbi148. URL <http://dx.doi.org/10.1093/plankt/fbi148>.
- [48] A. Birol Kara, Peter A. Rochford, and Harley E. Hurlburt. Mixed layer depth variability over the global ocean. *Journal of Geophysical Research: Oceans*, 108(C3), 2003. doi: 10.1029/2000JC000736.
- [49] Onur Kerimoglu, Dietmar Straile, and Frank Peeters. Role of phytoplankton cell size on the competition for nutrients and light in incompletely mixed systems. *Journal of Theoretical Biology*, 300:330–343, 2012. ISSN 0022-5193. doi: <http://dx.doi.org/10.1016/j.jtbi.2012.01.044>.
- [50] Jennifer L Klug, Janet M Fischer, Anthony R Ives, and Brian Dennis. Compensatory dynamics in planktonic community responses to ph perturbations. *Ecology*, 81(2):387–398, 2000.
- [51] Jamie M. Kneitel and Jonathan M. Chase. Disturbance, predator, and resource interactions alter container community composition. *Ecology*, 85(8):2088–2093, 2004. ISSN 1939-9170. doi: 10.1890/03-3172. URL <http://dx.doi.org/10.1890/03-3172>.
- [52] Marguerite Koch, George Bowes, Cliff Ross, and Xing-Hai Zhang. Climate change and ocean acidification effects on seagrasses and marine macroalgae. *Global change biology*, 19(1):103–132, 2013.
- [53] T. Kohyama. Size-structured multi-species model of rain forest trees. *Functional Ecology*, 6(2):206–212, 1992.

- [54] Julia A. F. Langer, Rahul Sharma, Susanne I. Schmidt, Sebastian Bahrndt, Henriette G. Horn, María Algueró-Muñiz, Bora Nam, Eric P. Achterberg, Ulf Riebesell, Maarten Boersma, et al. Community barcoding reveals little effect of ocean acidification on the composition of coastal plankton communities: Evidence from a long-term mesocosm study in the gullmar fjord, skagerrak. *PloS one*, 12(4):e0175808, 2017.
- [55] Karl-Erich Lindenschmidt and Ingrid Chorus. The effect of water column mixing on phytoplankton succession, diversity and similarity. *Journal of Plankton Research*, 20(10):1927, 1998. doi: 10.1093/plankt/20.10.1927. URL +<http://dx.doi.org/10.1093/plankt/20.10.1927>.
- [56] Silke Lischka, Jan Büdenbender, Tim Boxhammer, and Ulf Riebesell. Impact of ocean acidification and elevated temperatures on early juveniles of the polar shelled pteropod limacina helicina: mortality, shell degradation, and shell growth. *Biogeosciences*, 8(4):919, 2011.
- [57] E. Litchman, C. A. Klausmeier, and K. Yoshiyama. Contrasting size evolution in marine and freshwater diatoms. *Proceedings of The National Academy of Sciences*, 106(8):2665–2670, 2009. doi: 10.1073/pnas.0810891106.
- [58] Elena Litchman, Christopher A. Klausmeier, Oscar M. Schofield, and Paul G. Falkowski. The role of functional traits and trade-offs in structuring phytoplankton communities: scaling from cellular to ecosystem level. *Ecology Letters*, 10(12):1170–1181, 2007. ISSN 1461-0248. doi: 10.1111/j.1461-0248.2007.01117.x.
- [59] Elena Litchman, Paula de Tezanos Pinto, Christopher A. Klausmeier, Mridul K. Thomas, and Kohei Yoshiyama. Linking traits to species diversity and community structure in phytoplankton. *Hydrobiologia*, 653(1):15–28, 2010. ISSN 1573-5117. doi: 10.1007/s10750-010-0341-5.
- [60] Elena Litchman, Kyle F Edwards, Christopher A Klausmeier, and Mridul K Thomas. Phytoplankton niches, traits and eco-evolutionary responses to global environmental change. *Marine Ecology Progress Series*, 470:235–248, 2012.
- [61] Kai T. Lohbeck, Ulf Riebesell, and Thorsten B. H. Reusch. Gene expression changes in the coccolithophore *emiliana huxleyi* after 500 generations of selection to ocean acidification. *Proceedings of the Royal Society of London B: Biological Sciences*, 281(1786), 2014. ISSN 0962-8452. doi: 10.1098/rspb.2014.0003. URL <http://rspb.royalsocietypublishing.org/content/281/1786/20140003>.
- [62] Emilio Marañón. Cell size as a key determinant of phytoplankton metabolism and community structure. *Annual Review of Marine Science*, 7(1):241–264, 2015. doi: 10.1146/annurev-marine-010814-015955.

- [63] Emilio Marañón, Pedro Cermeño, Daffne C. Lòpez-Sandoval, Tamara Rodríguez-Ramos, Cristina Sobrino, María Huete-Ortega, José María Blanco, and Jaime Rodríguez. Unimodal size scaling of phytoplankton growth and the size dependence of nutrient uptake and use. *Ecology Letters*, 16(3):371–379, 2013. ISSN 1461-0248. doi: 10.1111/ele.12052.
- [64] Marcos D. Mateus. Bridging the gap between knowing and modeling viruses in marine systems—An upcoming frontier. *Frontiers in Marine Science*, 3:284, 2017. doi: 10.3389/fmars.2016.00284.
- [65] Kristian McConville, Claudia Halsband, Elaine S. Fileman, Paul J. Somerfield, Helen S. Findlay, and John I. Spicer. Effects of elevated co₂ on the reproduction of two calanoid copepods. *Marine pollution bulletin*, 73(2):428–434, 2013.
- [66] D. J. McGillicuddy, L. A. Anderson, S. C. Doney, and M. E. Maltrud. Eddy-driven sources and sinks of nutrients in the upper ocean: Results from a 0.1° resolution model of the north atlantic. *Global Biogeochemical Cycles*, 17(2), 2003. ISSN 1944-9224. doi: 10.1029/2002GB001987. URL <http://dx.doi.org/10.1029/2002GB001987>.
- [67] Susanne Menden-Deuer and Evelyn J. Lessard. Carbon to volume relationships for dinoflagellates, diatoms, and other protist plankton. *Limnology and Oceanography*, 45(3): 569–579, 2000. ISSN 1939-5590. doi: 10.4319/lo.2000.45.3.0569.
- [68] David J. S. Montagnes and Montagnes Franklin. Effect of temperature on diatom volume, growth rate, and carbon and nitrogen content: Reconsidering some paradigms. *Limnology and Oceanography*, 46(8):2008–2018, 2001. ISSN 1939-5590. doi: 10.4319/lo.2001.46.8.2008.
- [69] David JS Montagnes, Susan A Kimmance, and David Atkinson. Using q₁₀: can growth rates increase linearly with temperature? *Aquatic Microbial Ecology*, 32(3):307–313, 2003.
- [70] CM Moore, MM Mills, KR Arrigo, I Berman-Frank, L Bopp, PW Boyd, ED Galbraith, RJ Geider, C Guieu, SL Jaccard, et al. Processes and patterns of oceanic nutrient limitation. *Nature Geoscience*, 6(9):701, 2013.
- [71] Francois M. M. Morel. Kinetics of nutrient uptake and growth in phytoplankton. *Journal of Phycology*, 23(2):137–150, 1987. ISSN 1529-8817. doi: 10.1111/j.1529-8817.1987.tb04436.x.
- [72] M. Moreno de Castro, M. Schartau, and K. Wirtz. Potential sources of variability in mesocosm experiments on the response of phytoplankton to ocean acidification. *Biogeosciences*, 14(7):1883–1901, 2017.
- [73] Lindsay K. Newbold, Anna E. Oliver, Tim Booth, Bela Tiwari, Todd DeSantis, Michael Maguire, Gary Andersen, Christopher J. van der Gast, and Andrew S. Whiteley. The response of marine picoplankton to ocean acidification. *Environmental Microbiology*, 14(9): 2293–2307, 2012.

- [74] NODC. World ocean atlas, 2009. URL <https://www.nodc.noaa.gov/cgi-bin/0C5/W0A09F/woa09f.pl>.
- [75] Allanah J Paul, Lennart T Bach, K-G Schulz, Tim Boxhammer, Jan Czerny, Eric P Achterberg, Dana Helleman, Yves Trense, M Nausch, Michael Sswat, et al. Effect of elevated CO_2 on organic matter pools and fluxes in a summer baltic sea plankton community. *Biogeosciences*, 12(20):6181–6203, 2015.
- [76] Carolin Paul, Birte Matthiessen, and Ulrich Sommer. Warming, but not enhanced CO_2 concentration, quantitatively and qualitatively affects phytoplankton biomass. *Marine Ecology Progress Series*, 528:39–51, 2015.
- [77] T. Platt, C. L. Gallegos, and W. G. Harrison. Photoinhibition of photosynthesis in natural assemblages of marine phytoplankton. *Journal of Marine Research*, 38:687–701, 1980.
- [78] F. J. Poulin and P. J. S. Franks. Size-structured planktonic ecosystems: constraints, controls and assembly instructions. *Journal of Plankton Research*, 32(8):1121–1130, 2010.
- [79] J.A. Raven. Nutrient transport in microalgae. *Advances in Microbial Physiology*, 21:47 – 226, 1981. ISSN 0065-2911.
- [80] Peter B Reich, Sarah E Hobbie, Tali Lee, David S Ellsworth, Jason B West, David Tilman, Johannes MH Knops, Shahid Naeem, and Jared Trost. Nitrogen limitation constrains sustainability of ecosystem response to CO_2 . *Nature*, 440(7086):922–925, 2006.
- [81] C. S. Reynolds, J. Padisák, and U. Sommer. Intermediate disturbance in the ecology of phytoplankton and the maintenance of species diversity: a synthesis. *Hydrobiologia*, 249(1):183–188, 1993. ISSN 1573-5117. doi: 10.1007/BF00008853. URL <http://dx.doi.org/10.1007/BF00008853>.
- [82] Kenneth A Rose, Gordon L Swartzman, Andrew C Kindig, and Frieda B Taub. Stepwise iterative calibration of a multi-species phytoplankton-zooplankton simulation model using laboratory data. *Ecological Modelling*, 42(1):1–32, 1988.
- [83] A.-S. Roy, S. M. Gibbons, Harald Schunck, S. Owens, J. G. Caporaso, Martin Sperling, J. I. Nissimov, Sarah Romac, Lucie Bittner, M Mühling, et al. Ocean acidification shows negligible impacts on high-latitude bacterial community structure in coastal pelagic mesocosms. *Biogeosciences*, 10(1):555–566, 2013.
- [84] Geraldine Sarthou, Klaas R. Timmermans, Stephane Blain, and Paul Treguer. Growth physiology and fate of diatoms in the ocean: a review. *Journal of Sea Research*, 53(1-2):25–42, 2005. ISSN 1385-1101. doi: <http://dx.doi.org/10.1016/j.seares.2004.01.007>.

- [85] Boris Sauterey, Ben A. Ward, Michael J. Follows, Chris Bowler, and David Claessen. When everything is not everywhere but species evolve: an alternative method to model adaptive properties of marine ecosystems. *Journal of Plankton Research*, 37(1):28–47, 2015. doi: 10.1093/plankt/fbu078.
- [86] D. A. Schlesinger, L. A. Molot, and B. J. Shuter. Specific growth rates of freshwater algae in relation to cell size and light intensity. *Canadian Journal of Fisheries and Aquatic Sciences*, 38(9):1052–1058, 1981. doi: 10.1139/f81-145.
- [87] Kai G Schulz, RGJ Bellerby, Corina PD Brussaard, Jan Büdenbender, Jan Czerny, Anja Engel, Matthias Fischer, Signe Koch-Klavsen, Sebastian Krug, Silke Lischka, et al. Temporal biomass dynamics of an arctic plankton bloom in response to increasing levels of atmospheric carbon dioxide. *Biogeosciences (BG)*, 10:161–180, 2013.
- [88] Anne S. Schwaderer, Kohei Yoshiyama, Paula de Tezanos Pinto, Nathan G. Swenson, Christopher A. Klausmeier, and Elena Litchman. Eco-evolutionary differences in light utilization traits and distributions of freshwater phytoplankton. *Limnology and Oceanography*, 56(2):589–598, 2011. ISSN 1939-5590. doi: 10.4319/lo.2011.56.2.0589.
- [89] Helmut Segner, Me Schmitt, and Sergi Sabater. Assessing the impact of multiple stressors on aquatic biota: The receptor’s side matters. 48, 06 2014.
- [90] Claude E. Shannon. A mathematical theory of communication. *The Bell System Technical Journal*, 27:379–423,623–656, 1948.
- [91] Joy Smith. *The effects of ocean acidification on zooplankton: using natural CO₂ seeps as windows into the future*. PhD thesis, University of Plymouth, 2016.
- [92] Joy N. Smith, Claudio Richter, Katharina E. Fabricius, and Astrid Cornils. Pontellid copepods, labidocera spp., affected by ocean acidification: A field study at natural co₂ seeps. *PloS one*, 12(5):e0175663, 2017.
- [93] S. Lan Smith, Agostino Merico, Kai W. Wirtz, and Markus Pahlow. Leaving misleading legacies behind in plankton ecosystem modelling. *Journal of Plankton Research*, 36(3):613, 2014. doi: 10.1093/plankt/fbu011.
- [94] U. Sommer. A comparison of the droop and the monod models of nutrient limited growth applied to natural populations of phytoplankton. *Functional Ecology*, 5(4):535–544, 1991.
- [95] Ulrich Sommer. Maximal growth rates of antarctic phytoplankton: Only weak dependence on cell size. *Limnology and Oceanography*, 34(6):1109–1112, 1989. ISSN 1939-5590. doi: 10.4319/lo.1989.34.6.1109.

- [96] Ulrich Sommer. An experimental test of the intermediate disturbance hypothesis using cultures of marine phytoplankton. *Limnology and Oceanography*, 40(7):1271–1277, 1995. ISSN 1939-5590. doi: 10.4319/lo.1995.40.7.1271.
- [97] Richard R. Strathmann. Estimating the organic carbon content of phytoplankton from cell volume or plasma volume. *Limnology and Oceanography*, 12(3):411–418, 1967. ISSN 1939-5590. doi: 10.4319/lo.1967.12.3.0411.
- [98] Niousha Taherzadeh, Onur Kerimoglu, and Kai W. Wirtz. Can we predict phytoplankton community size structure using size scalings of eco-physiological traits? *Ecological Modelling*, 360:279 – 289, 2017. ISSN 0304-3800. doi: <http://dx.doi.org/10.1016/j.ecolmodel.2017.07.008>. URL <http://www.sciencedirect.com/science/article/pii/S0304380017303393>.
- [99] Jan Taucher, Mathias Haunost, Tim Boxhammer, Lennart T. Bach, María Algueró-Muñiz, and Ulf Riebesell. Influence of ocean acidification on plankton community structure during a winter-to-summer succession: An imaging approach indicates that copepods can benefit from elevated co₂ via indirect food web effects. *PLOS ONE*, 12(2):1–23, 02 2017. doi: 10.1371/journal.pone.0169737.
- [100] N. Terseleer, J. Bruggeman, C. Lancelot, and N. Gypens. Trait-based representation of diatom functional diversity in a plankton functional type model of the eutrophied southern north sea. *Limnology and Oceanography*, 59(6):1958–1972, 2014. doi: 10.4319/lo.2014.59.6.1958.
- [101] T Frede Thingstad. Elements of a theory for the mechanisms controlling abundance, diversity, and biogeochemical role of lytic bacterial viruses in aquatic systems. 45(6): 1320–1328, 2000.
- [102] Rucheng C Tian. Toward standard parameterizations in marine biological modeling. *Ecological modelling*, 193(3):363–386, 2006.
- [103] D. Tilman. *Resource Competition and Community Structure*. Annual Reviews Inc., 1982.
- [104] Anne E Todgham and Jonathon H Stillman. Physiological responses to shifts in multiple environmental stressors: relevance in a changing world. *Integrative and comparative biology*, 53(4):539–544, 2013.
- [105] Dedmer B. Van de Waal, Jolanda M. H. Verspagen, Jan F. Finke, Vasiliki Vournazou, Anne K. Immers, W. Edwin A. Kardinaal, Linda Tonk, Sven Becker, Ellen Van Donk, Petra M. Visser, et al. Reversal in competitive dominance of a toxic versus non-toxic cyanobacterium in response to rising co₂. *The ISME journal*, 5(9):1438, 2011.

- [106] Rolf D Vinebrooke, David W Schindler, David L Findlay, Michael A Turner, Michael Paterson, and Kenneth H Mills. Trophic dependence of ecosystem resistance and species compensation in experimentally acidified lake 302s (canada). *Ecosystems*, 6(2):0101–0113, 2003.
- [107] Anya Waite, Anne Fisher, Peter A. Thompson, and Paul J. Harrison. Sinking rate versus cell volume relationships illuminate sinking rate control mechanisms in marine diatoms. *Marine Ecology Progress Series*, 157:97–108, 1997.
- [108] B. A. Ward, S. Dutkiewicz, O. Jahn, and M. J. Follows. A size-structured food-web model for the global ocean. *Limnology and Oceanography*, 57(6):1877–1891, 2012. ISSN 1939-5590. doi: 10.4319/lo.2012.57.6.1877.
- [109] Ben A. Ward, Stephanie Dutkiewicz, and Michael J. Follows. Modelling spatial and temporal patterns in size-structured marine plankton communities: top–down and bottom–up controls. *Journal of Plankton Research*, 36(1):31, 2014. doi: 10.1093/plankt/fbt097.
- [110] Kai W. Wirtz. Non-uniform scaling in phytoplankton growth rate due to intracellular light and co2 decline. *Journal of Plankton Research*, 33(9):1325–1341, 2011. doi: 10.1093/plankt/fbr021.
- [111] Kai W. Wirtz. Mechanistic origins of variability in phytoplankton dynamics: Part i: niche formation revealed by a size-based model. *Marine Biology*, 160(9):2319–2335, 2013. ISSN 1432-1793. doi: 10.1007/s00227-012-2163-7.
- [112] Kai W Wirtz and Bruno Eckhardt. Effective variables in ecosystem models with an application to phytoplankton succession. *Ecological Modelling*, 92(1):33–53, 1996. ISSN 0304-3800. doi: [http://dx.doi.org/10.1016/0304-3800\(95\)00196-4](http://dx.doi.org/10.1016/0304-3800(95)00196-4).
- [113] Kai W. Wirtz and Onur Kerimoglu. Autotrophic stoichiometry emerging from optimality and variable co-limitation. *Frontiers in Ecology and Evolution*, 4:131, 2016. ISSN 2296-701X.
- [114] Kai W. Wirtz and Ulrich Sommer. Mechanistic origins of variability in phytoplankton dynamics. part ii: analysis of mesocosm blooms under climate change scenarios. *Marine Biology*, 160(9):2503–2516, 2013. ISSN 1432–1793. doi: 10.1007/s00227-013-2271-z. URL <http://dx.doi.org/10.1007/s00227-013-2271-z>.
- [115] Eckart Zöllner, Hans-Georg Hoppe, Ulrich Sommer, and Klaus Jürgens. Effect of zooplankton-mediated trophic cascades on marine microbial food web components (bacteria, nanoflagellates, ciliates). *Limnology and Oceanography*, 54(1):262–275, 2009.

A

Appendix I

A.1. Equilibrium solution to the size-based multi-species model

According to the resource competition theory, the species with the smallest equilibrium external nutrient concentration (Nut^*) is the winner of resource competition [103]. Equilibrium solutions of similar differential equation systems describing phytoplankton growth with variable internal stores have been presented previously (e.g., [23] and [49]), but as our model slightly differs from those previous models, here we present a steady-state analysis of our model too. The equilibrium nutrient quota is obtained by setting the differential equation of phytoplankton to zero:

$$\frac{dPhy_i}{dt} = \mu_i(Q_i, I)Phy_i - (m + D) Phy_i = 0 \quad (A.1)$$

$$\mu_i(Q^*, I^*) = m + D \quad (A.2)$$

where $i=1, 2, \dots, 29$ is the number of species, Q^* (mol-N mol-C^{-1}) and I^* (W m^{-2}) represent the equilibrium nutrient quota and light intensity; respectively. After substituting growth function (Equation (A.2)) into Equation (A.1) and some rearrangements, we obtained the equilibrium nutrient quota as following:

$$m + D = \left(\frac{\mu_{\max,i} Q_{\max,i}}{Q_{\max,i} - Q_{\min,i}} \right) \left(1 - \frac{Q_{\min,i}}{Q_i^*} \right) \left(\frac{I^*}{K_I + I^*} \right) \quad (\text{A.3})$$

$$Q_i^* = \frac{\mu'_i Q_{\min,i}}{\mu'_i - (m + D)}, \text{ with:} \quad (\text{A.4})$$

$$\mu'_i = \left(\frac{\mu_{\max,i} Q_{\max,i}}{Q_{\max,i} - Q_{\min,i}} \right) \left(\frac{I^*}{K_I + I^*} \right) \quad (\text{A.5})$$

Finally, by setting the quota change over time to zero and substituting the growth function from Equation (A.2) into Equation (A.7), the Nut^* is calculated as:

$$\frac{dQ_i}{dt} = v_i(\text{Nut}, Q_i) - \mu_i(Q_i, I) Q_i = 0 \quad (\text{A.6})$$

$$v_i(\text{Nut}^*, Q_i^*) = \mu_i(Q_i^*, I^*) Q_i^* \quad (\text{A.7})$$

$$\left(\frac{v_{\max,i} \text{Nut}^* A_i}{v_{\max,i} + \text{Nut}^* A_i} \right) \left(\frac{Q_{\max,i} - Q_i^*}{Q_{\max,i} - Q_{\min,i}} \right) = \mu'_i \left(1 - \frac{Q_{\min,i}}{Q_i^*} \right) Q_i^* \quad (\text{A.8})$$

$$\frac{v_{\max,i} \mu'_i Q_i^* - \mu'_i Q_{\min,i} v_{\max,i}}{v_{\max,i} A_i B_i - \mu'_i Q^* A_i + Q_{\min,i} \mu'_i A_i} = \text{Nut}_i^*, \text{ with:} \quad (\text{A.9})$$

$$B_i = \frac{Q_{\max,i} - Q_i^*}{Q_{\max,i} - Q_{\min,i}} \quad (\text{A.10})$$

Employing our model size-based physiological traits (v_{\max} , μ_{\max} , A , Q_{\min} and Q_{\max}) (Di-L0) and physical parameters in the Equation (A.9) always result in the lowest Nut^* , thus, the unconditional dominance of small cells.

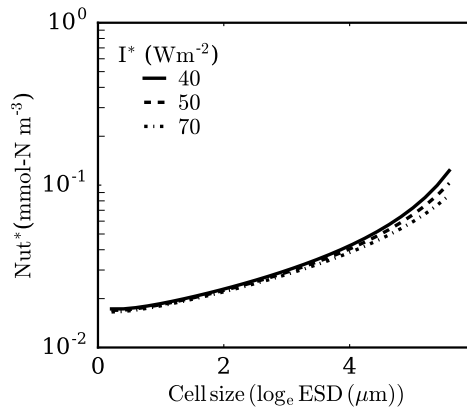


Figure A.1.1.: Equilibrium nutrient concentration over phytoplankton cell size for different values of equilibrium light intensity (Di-L0).

A.2.

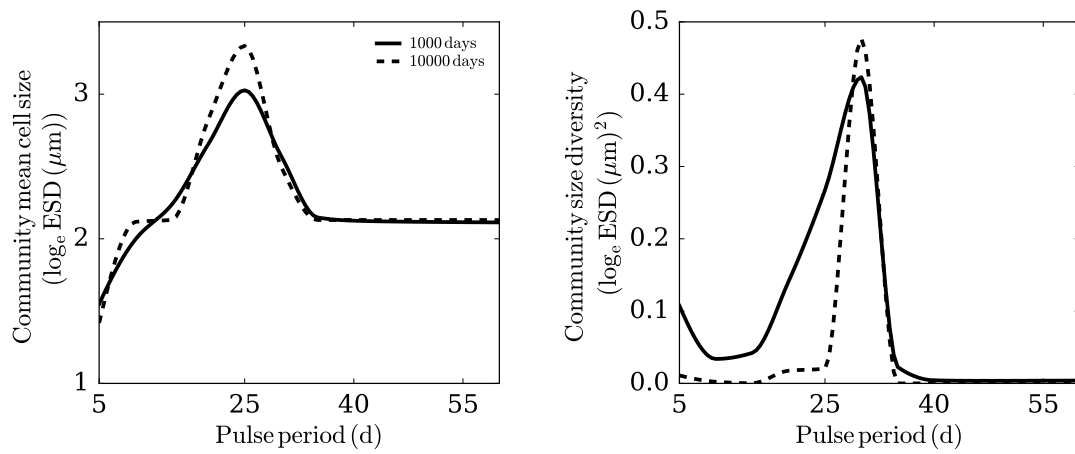


Figure A.2.1.: Comparison between simulation time of 1000 days and long term (10000 days) for change of diatom community mean cell size and size diversity (Di-NL, $Nut_{in} = 60 \text{ mmol-N m}^{-3}$).

A.3.

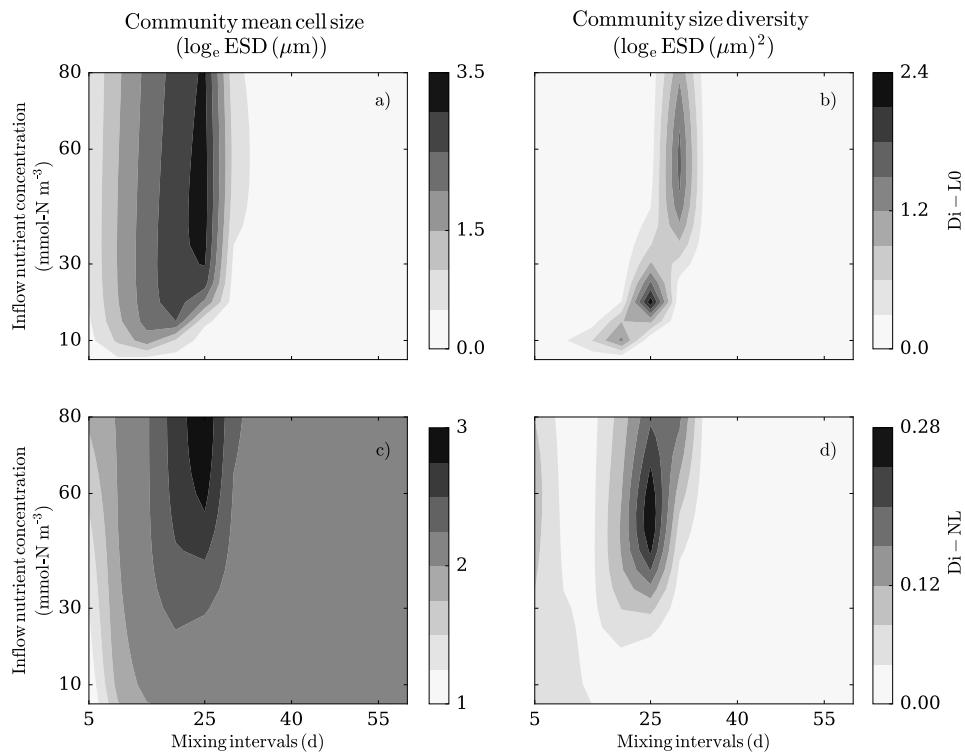


Figure A.3.1.: Change of diatom community mean size (a, c) and size diversity (b, d) over various inflow nutrient concentrations and mixing intervals for the Di-L0 scenario (a-b) and Di-NL scenario (c-d).

B

Appendix II

B.1. Model description

Phytoplankton specific production rate (μ_i) for group “ i ” in the model is a function of light intensity, temperature, internal nutrient quotas and CO_2 (Table B.2, Eq.1). All metabolic rates and remineralization rate of detritus increase with rising temperature following the Q_{10} equation or Van’t Hoff rule, resp., (f_T) (Table B.3, Eq.1) [69]. Nitrogen and phosphorous are in the model regarded as limiting nutrients of primary production and the growth rate dependency on their intracellular stores is defined by the Droop function ($q_{N,i}$ and $q_{P,i}$) (Table B.1, Eq.3-4). Co-limitation by the two nutrients quotas is described by a normalized multiplicative type function (Table B.1, Eq.2) [113]. Light limitation ($f_{\text{PAR},i}$) follows a cumulative one-hit Poisson distribution including photoinhibition [77]. This light response function also depends on cell size, temperature, and CO_2 (Table B.1, Eq.5). The average light intensity ($\overline{\text{PAR}}$) over the mixed layer is obtained by the Lambert-Beer law (Table B.1, Eq.18) resolving the attenuation of light due to background particles and phytoplankton biomass (Table B.1, Eq.17) [45]. Furthermore, the rate limitation by sub-optimal carboxylation ($f_{\text{CO}_2,i}$) is specified by a biophysically explicit description for carbon uptake as a function of cell size adopted from [110] and simplified by [72] (Table B.3, Eq.6).

Table B.1.: Model equations. Auxiliary variables and parameters are described in Table B.2–B.7. The subscript i distinguishes phytoplankton size classes and j the three zooplankton classes.

State variable	Dynamical equation	Unit
1. Phytoplankton biomass	$\frac{d\text{Phy}_i}{dt} = (\mu_i - A - R_i - S_i)\text{Phy}_i - G_i + (\epsilon_m G_{m,i} - \sum_{k=i}^{i^*} G_{m,k})\text{Phy}_i$	mmol-C m ⁻³
2. Cell nitrogen quota	$\frac{dQ_i^N}{dt} = V_i^N - (\mu_i - R_i)Q_i^N$	mol-N mol-C ⁻¹
3. Cell phosphorous quota	$\frac{dQ_i^P}{dt} = V_i^P - (\mu_i - R_i)Q_i^P$	mol-P mol-C ⁻¹
4. Ciliates biomasses ($Z_{j=1,2}$)	$\frac{dZ_{j=1,2}}{dt} = y \sum_{i=1}^n \text{Graz}_{ij} D_j^{\text{reg}} - \text{Graz}_{j3} D_3^{\text{reg}} - m_j Z_j^2$	mmol-C m ⁻³
5. Copepod biomass ($Z_{j=3}$)	$\frac{dZ_{j=3}}{dt} = y \sum_{i=1}^n \text{Graz}_{ij} D_j^{\text{reg}} - m_j Z_j^2$	mmol-C m ⁻³
6. N-content of detritus (Det _N)	$\frac{d\text{Det}_N}{dt} = \sum_{i=1}^n (A \cdot \text{Phy} Q_i^N) - (\phi f_T + \frac{V_d}{\text{MLD}})\text{Det}_N + (1-y) \sum_{i=1}^n G_i Q_i^N + (1-\epsilon_m) \sum_{i=1}^n G_{m,i} Q_i^N + \sum_{j=1}^3 m_j Z_j^2 Q_j^{Z,N} \dagger$	mmol-N m ⁻³
7. P-content of detritus (Det _P)	$\frac{d\text{Det}_P}{dt} = \sum_{i=1}^n (A \cdot \text{Phy} Q_i^P) - (\phi f_T + \frac{V_d}{\text{MLD}})\text{Det}_P + (1-y) \sum_{i=1}^n G_i Q_i^P + (1-\epsilon_m) \sum_{i=1}^n G_{m,i} Q_i^P + \sum_{j=1}^3 m_j Z_j^2 Q_j^{Z,P} \dagger$	mmol-P m ⁻³
8. Nitrogen conc. (N)	$\frac{dN}{dt} = \phi f_T \text{Det}_N - \sum_{i=1}^n (V_i^N \cdot \text{Phy}_i) + \epsilon_N \sum_{j=1}^3 Z_j$	mmol-N m ⁻³
9. Phosphorous conc. (P)	$\frac{dP}{dt} = \phi f_T \text{Det}_P - \sum_{i=1}^n (V_i^P \cdot \text{Phy}_i) + \epsilon_P \sum_{j=1}^3 Z_j$	mmol-P m ⁻³

†These terms are replaced with $(1-y) \sum_{j=1}^2 \text{Graz}_{j3} D_3^{\text{reg}} Q_j^{Z,N}$ and $(1-y) \sum_{j=1}^2 \text{Graz}_{j3} D_3^{\text{reg}} Q_j^{Z,P}$ respectively, where zooplankton is assumed as external forcing, i.e. not dynamically resolved.

Phytoplankton biomass removal is driven by aggregation (A), size dependent respiration (R_i), sinking (S_i), grazing by strict heterotrophs (G_i) and mixotrophic grazing ($G_{m,i}$). Phytoplankton cells and/or detritus particles are assumed to form aggregates that are rapidly exported from the system (Table B.2, Eq.5). The strength of aggregation is in our model controlled by a dimensionless auxiliary variable for the concentration of transparent exopolymeric particles (TEP). Concentration of TEP is here suggested to depend on the temporal derivative of the internal nitrogen quota (\dot{Q}_N) of phytoplankton according to a sigmoid function (Table B.3, Eq.7). This formulation reflects the correlation between TEP formation and carbon overconsumption, the latter being accompanied with a rapid decline in nutrient quotas. The respiratory loss of each size class or species, resp., is proportional to its nutrient uptake rate (Table B.2, Eq.4) [79, 3]. Sinking of individual species is described by a modified Stoke's law function adopted from [111], which takes into account positive buoyancy of larger cells (Table B.1, Eq.6). Size dependent grazing of zooplankton on phytoplankton follows a normal distribution function centered around an optimal prey size (L^*). Furthermore, smaller phytoplankton are assumed to be grazed by mixotrophic phytoplankton with larger cell size (Table B.2, Eq.8).

Table B.2.: Primary production related rates. Parameters are described in Table B.3 – Table B.7.

Description	Rate	Unit
1. Growth rate	$\mu_i = \mu_{\max,i} \cdot f_T \cdot f_{Q,i} \cdot f_{\text{PAR},i} \cdot f_{\text{CO}_2,i}$	d^{-1}
2. N-uptake rate	$V_i^N(N, Q_i^N) = v_{\max,i}^N \cdot f_T \cdot \left(\frac{N \cdot A_i^N}{v_{\max,i}^N + N \cdot A_i^N} \right) \cdot (1 - q_{N,i})$	$\text{mol-N (mol-C d)}^{-1}$
3. P-uptake rate	$V_i^P(N, Q_i^P) = v_{\max,i}^P \cdot f_T \cdot \left(\frac{P \cdot A_i^P}{v_{\max,i}^P + P \cdot A_i^P} \right) \cdot (1 - q_{P,i})$	$\text{mol - P(mol-C d)}^{-1}$
4. Respiration rate	$R_i = R^* V_i^N(N, Q_i^N)$	d^{-1}
5. Aggregation rate	$A = A^* \text{TEP} \cdot \left(\sum_{i=1}^n \text{Phy}_i Q_i^N + \text{Det}_N \right)$	d^{-1}
6. Sinking rate	$S_i = e^{-0.5 \left(\frac{q_{N,i} \cdot q_{P,i}}{0.45^2} \right)^2} \cdot e^{(0.5L_i)} \cdot \frac{v_s}{\text{MLD}}$	d^{-1}
7. Grazing rate	$G_i = \sum_{j=1}^3 \text{Graz}_{ij} \cdot Z_j \cdot D_j^{\text{reg}}$	d^{-1}
8. Grazing on ciliates	$G^{\text{Cil}} = I_{\max,3} \cdot g_3 \cdot \frac{\rho_{c3} Z_{1,2}}{F_3} Z_3 D_3^{\text{reg}}$	d^{-1}
9. Mixotrophic grazing	$G_{m_i} = \Theta(L_i) I_{\max}^m G_m^{\max} \sum_{k=i-\Delta m}^i \frac{\text{Phy}_k}{H_m + \sum_{k=i-\Delta m}^i \text{Phy}_k}$	d^{-1}
10. Switching under low nutrient conditions	$G_m^{\max} = 1 - \left(1 + e^{(-20(\mu_i - 0.02))} \right)^{-1}$	d^{-1}
11. Size limitation for mixotrophic grazing	$\Theta(L_i) = \begin{cases} 1 & \text{if } L_i < 2.8 \\ 0 & \text{else} \end{cases}$	

Internal nutrients pools are filled by nutrient uptake as formulated by the Monod function [71] and reduced because of dilution by growth (Table B.1, Eq.2–3). Nutrient uptake increases with ambient nutrient concentration and is down-regulated when the intracellular pool reaches a maximum (Q_{\max}) (Table B.3, Eq.2–3). Changes in ciliate biomass reflect an imbalance between growth due to grazing on small size phytoplankton and grazing by copepod and density dependent mortality (Table B.1, Eq.4). Copepod biomass in the model increases due to grazing on phytoplankton and reduces as a result of density dependent mortality (Table B.1, Eq.5). Particle aggregation and sloppy feeding of zooplankton fuel the detritus pools, while organic matter is remineralized to inorganic nutrients and removed from the surface ocean by sinking (Table B.1, Eq.6–7). Finally, ambient nutrient pools are reduced because of uptake by phytoplankton and replenished through remineralization of detritus and zooplankton excretion (Table B.1, Eq.8–9). For related functions and parameters value please see Table B.3–B.7.

Table B.3.: Model sub functions and related variable parameters.

Description (Source)	Symbol	Function	Unit
1. Temperature dependency [69]	f_T	$\frac{T - T_{\text{ref}}}{Q_{10}^{10}}$	
2. Co-limitation [113]	$f_{Q,i}$	$\frac{q_{N,i} \cdot q_{P,i}}{0.5(q_{N,i} + q_{P,i})}$	
3. Internal nitrogen quota dependency [22]	$q_{N,i}$	$\frac{Q_i^N - Q_{\text{min},i}^N}{Q_i^N}$	
4. Internal phosphorous quota dependency [22]	$q_{P,i}$	$\frac{Q_i^P - Q_{\text{min},i}^P}{Q_i^P}$	
5. Specific light limitation [77]	$f_{\text{PAR},i}$	$\left(1 - e^{-\frac{\alpha_{\text{PAR}} \overline{\text{PAR}}}{\mu_{\text{max},i} \cdot f_{\text{CO}_2,i} \cdot f_T}}\right) \cdot e^{-\frac{\beta_{\text{PAR}} \overline{\text{PAR}}}{\mu_{\text{max},i} \cdot f_{\text{CO}_2,i} \cdot f_T}}$	
6. CO ₂ dependency [110, 72]	$f_{\text{CO}_2,i}$	$\frac{1 - e^{-a_{\text{CO}_2} \cdot \text{CO}_2}}{1 + a^* e^{(L_i - a_{\text{CO}_2} \cdot \text{CO}_2)}}$	
7. Transparent Exopolymer Particles	TEP	$\text{TEP}_{\text{min}} \frac{1 - \text{TEP}_{\text{min}}}{1 + e^{(B^* Q_N + B_{\text{offs}}^*)}}$	mmol-C m ⁻³
8. Functional response [111]	g_j	$1 - e^{-x_j}$	
9. Food processing ratio [111]	x_j	$\frac{A_{\text{zoo}} \cdot F_j}{I_{\text{max},j}}$	
10. Potential grazing rate of grazer Z_j on prey Phy_i [111]	Graz_{ij}	$I_{\text{max},j} \cdot g_j \cdot \frac{\rho_{ij} \cdot \text{Phy}_i}{F_j}$	d ⁻¹
11. Down regulation [111]	D_j^{reg}	$\left(1 + e^{\frac{\sum_{i=1}^n \text{Graz}_{ij} - G_{\text{min}}}{0.05}}\right)^{-1}$	
12. Optimal ingestion rate [111]	$I_{\text{max},j}^*$	$I_{\text{max},j}^{\circ} f_T \cdot e^{(\alpha + (2-\alpha)L_j^* + (\alpha-3)L_j)}$	d ⁻¹
13. Maximum ingestion rate [111]	$I_{\text{max},j}$	$I_{\text{max},j}^* \cdot e^{-s_j(L_j^* - \langle L' \rangle_j)^2}$	d ⁻¹
14. Effective food concentration [111]	F_j	$\begin{cases} F_{j=1,2} = \sum_{i=1}^n \text{Phy}_i \cdot \rho_{ij} \\ F_{j=3} = \sum_{i=1}^n \text{Phy}_i \cdot \rho_{i3} + \sum_{j=1}^2 Z_j \cdot \rho_{j3} \end{cases}$	mmol-C m ⁻³
15. Average food size [111]	$\langle L' \rangle_j$	$\begin{cases} \langle L' \rangle_{j=1,2} = \sum_{i=1}^2 \text{Phy}_i \cdot \rho_{ij} \cdot L_i / F_{j=1,2} \\ \langle L' \rangle_{j=3} = (\text{Phy}_i \cdot \rho_{i3} \cdot L_i + \sum_{j=1}^2 Z_j \cdot \rho_{j3} \cdot L_j) / F_{j=3} \end{cases}$	log _e ESD (μm)

Table B.4.: Model sub functions and related variable parameters (continue).

Description (Source)	Symbol	Function	Unit
16. Variable MLD	$MLD(t)$	$\frac{0.4 + 0.6}{(1 + e^{(0.2(t-t_{\text{delay}})})})}$	m
17. Background turbidity [45]	k	$\epsilon \cdot \left(\sum_{i=1}^n \text{Phy}_i Q_i \right) + \kappa$	d^{-1}
18. Average light intensity within MLD [45]	\overline{PAR}	$\frac{PAR_0}{MLD} \int_0^{MLD} e^{-k \cdot z'} dz' = \frac{PAR_0}{k \cdot MLD} (1 - e^{-k \cdot MLD})$	$\mu\text{mol m}^{-2} \text{s}^{-1}$
19. Total phytoplankton biomass	Phy_T	$\sum_{i=1}^n \text{Phy}_i$	
20. Community mean cell size	$\langle L \rangle$	$20. \frac{1}{\text{Phy}_T} \sum_{i=1}^n L_i \cdot \text{Phy}_i$	$\log_e \text{ESD} (\mu\text{m})$
21. Community size diversity	δL	$\frac{1}{\text{Phy}_T} \sum_{i=1}^n (L_i - \langle L \rangle)^2 \cdot \text{Phy}_i$	$\log_e \text{ESD} (\mu\text{m})$
22. Variable Copepod body size	$L_{j=3}$	$\frac{0.6 + 0.4}{(1 + e^{(0.2(t-t_{\text{delay}})})})}$	$\log_e \text{ESD} (\mu\text{m})$
24. Chlorophyll a	Chl_a	$\Theta_N \sum_{i=1}^n \text{Phy}_i Q_i^N + \Theta_C \sum_{i=1}^n \text{Phy}_i$	mg-C m^{-3}

B.1.1. Model parameters

Table B.5.: Parameters used in the reference run

Symbol	Value	Unit	Description
L_i		\log_e ESD μm	Phytoplankton cell size
A^*	0.2	d^{-1}	Maximum aggregation rate
B^*	15	$\text{mol-N (mol-C d)}^{-1}$	TEP related coefficient
B_{offs}^*	3.5		TEP related coefficient
TEP_{min}	0.07		TEP related coefficient
R^*	3	mol-C mol-N^{-1}	Respiratory C cost of N assimilation for phytoplankton
v_s	0.05	m d^{-1}	Settling velocity of phytoplankton
α_{PAR}	0.024	$\mu\text{mol phot}^{-1}\text{m}^2\text{d}$	Light absorption
β_{PAR}	0.002	$\mu\text{mol phot}^{-1}\text{m}^2\text{d}$	Coefficient for photoinhibition
a_{CO_2}	0.013	μatm^{-1}	Carbon acquisition
a^*	0.02	μm^{-1}	Carboxylation depletion
$L_{j=1,2}$	2.8,3.8	\log_e ESD μm	Zooplankton body size
$L_{j=3}$	6.2	\log_e ESD μm	Copepod maximum body size
L_j^*	1.2,1.2,3	\log_e ESD μm	Optimal prey size for zooplankton class j
I_{max}^o	173	d^{-1}	I_{max} at $L_j = L^* = 0$
$\alpha_{\text{Im},0}$	0.2		Size scaling exponent of I_{max}^*
α	$\alpha_{\text{Im},0}(L_j + L_j^*)$		Zooplankton maximum ingestion rate related parameter
s_j	2.5,2.,2.2	\log_e ESD $(\mu\text{m})^{-2}$	Selectivity of zooplankton j
ρ_{ij}	$e^{-s_j(L_j^* - L_i)^2}$		Preference of grazer Z_j for prey Phy_i
ρ_{j3}	$e^{-s_3(L_3^* - L_j)^2}$		Preference of grazer Z_3 for prey $Z_{j=1,2}$
A_{zoo}	0.2	$\text{m}^3(\text{mmol-C d})^{-1}$	Grazing affinity for algal food
y	0.3		Zooplankton growth efficiency
R_{zoo}	0.3	mmol-C m^{-3}	Specific activity respiration of grazing
ϵ_m	0.2		Specific C overconsumption/release
I_{max}^m	0.9	d^{-1}	Maximum ingestion rate for mixotrophic grazing
Δm	3		Number of size classes with $L_i \leq L_k$ consumable by species k
$m_{j=1,2,3}$	0.02, 0.02, 0.005	d^{-1}	Zooplankton mortality rate
G_{min}	$\frac{A_{\text{zoo}} \cdot R_{\text{zoo}}}{y}$	d^{-1}	Min. harvesting rate at which grazing starts

Table B.6.: Parameters used in the reference run

Symbol	Value	Unit	Description
T_{ref}	10	$^{\circ}\text{C}$	Reference temperature
κ	0.2	d^{-1}	Background turbidity
ϵ	0.05	$\text{m}^2\text{mmol-N}^{-1}$	Light attenuation due to phytoplankton biomass
ϕ	0.003	d^{-1}	Remineralization rate of detritus
v_d	1	m d^{-1}	Detritus sinking velocity rate
Q_{10}	2 (phy.), 2.4 (zoo.)		Rate increase at 10 $^{\circ}\text{C}$ temperature rise
Q_Z^N	0.3	mol-N mol-C^{-1}	Zooplankton internal nitrogen quota
Q_Z^P	0.03	mol-P mol-C^{-1}	Zooplankton internal phosphorous quota
ϵ_N	0.01	$\text{mmol-N}(\text{mmol-C d})^{-1}$	Zooplankton nitrogen excretion parameter
ϵ_P	0.0001	$\text{mmol-P}(\text{mmol-C d})^{-1}$	Zooplankton phosphorous excretion parameter
Θ_N	1.1	$\text{mol Chl}_a\text{mol-N}^{-1}$	Chl_a to nitrogen ratio
Θ_C	0.006	$\text{mol Chl}_a\text{mol-C}^{-1}$	Chl_a to carbon ratio

B.2. Allometric relationships of physiological traits

Table B.7.: Size scaling of physiological parameters for phytoplankton adapted from [29] and [63]. The subscript 'i' represents each phytoplankton species, V is the phytoplankton cell volume and L the natural logarithm of Equivalent Spherical Diameter.

Description	Parameter	Original Value	Original unit	Final value	Final unit
Min. cell N-quota	Q_{\min}^N	$10^{-9.3} V_i^{0.77}$	pg-N cells ⁻¹	$0.032e^{-0.33L}$	mol-N mol-C ⁻¹
Min. cell P-quota	Q_{\min}^P	$10^{-10.6} V_i^{0.79}$	pg-P cells ⁻¹	$0.002e^{-0.27L}$	mol-P mol-C ⁻¹
Max. cell N-quota	Q_{\max}^N	$10^{-8.5} V_i^{0.9}$	pg-N cells ⁻¹	$0.183e^{0.06L}$	mol-N mol-C ⁻¹
Max. cell P-quota	Q_{\max}^P	$10^{-9.5} V_i^{0.89}$	pg-P cells ⁻¹	$0.018e^{0L}$	mol-P mol-C ⁻¹
Max. N-uptake rate	v_{\max}^N	$10^{-8} V_i^{0.8}$	$\mu\text{mol-N (cell d)}^{-1}$	$0.619e^{-0.24L}$	mol-N (mol-C d) ⁻¹
Max. P-uptake rate	v_{\max}^P	$10^{-9} V_i^{0.8}$	$\mu\text{mol-P (cell d)}^{-1}$	$0.062e^{-0.24L}$	mol-P (mol-C d) ⁻¹
N affinity	A^N	$10^{-7.5} V_i^{0.78}$	L (cell d) ⁻¹	$1.983e^{-0.3L}$	m ³ (mmol-C d) ⁻¹
P affinity	A^P	$10^{-7.8} V_i^{0.78}$	L (cell d) ⁻¹	$0.994e^{-0.3L}$	m ³ (mmol-C d) ⁻¹
Cell carbon content	Q_c	$10^{-0.69} V_i^{0.88}$	pg-C cell ⁻¹	$0.116e^{2.64L}$	mol-C cell ⁻¹
Max. growth rate $V_{\text{cell}} < 500 \mu\text{m}^3$	μ_{\max}	$10^{-0.17} V_i^{0.035}$	d ⁻¹	$0.658e^{0.105L}$	d ⁻¹
Max. growth rate $V_{\text{cell}} > 500 \mu\text{m}^3$		$10^{-0.03} V_i^{-0.02}$		$0.963e^{-0.06L}$	

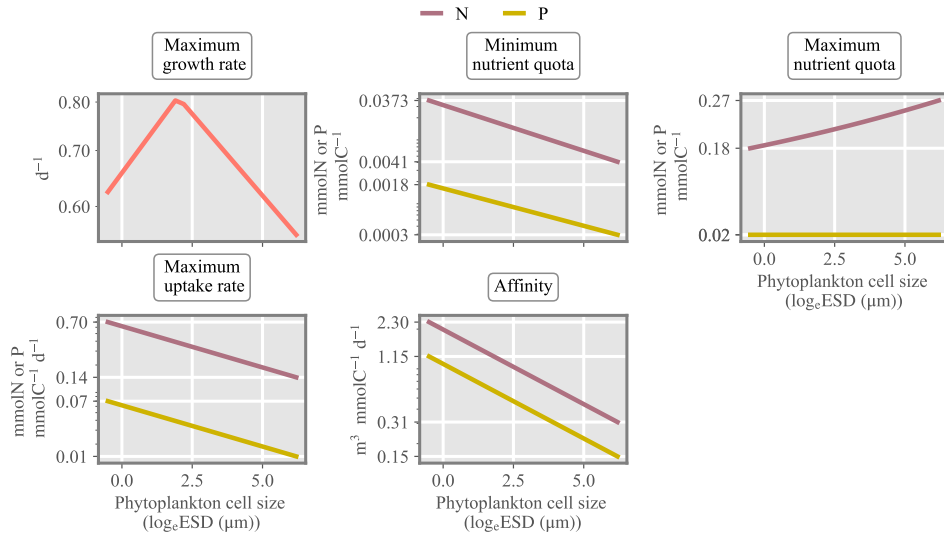


Figure B.2.1.: Allometric relationships used in the model for major growth-nutrient uptake parameters given in Table B.7.

B.3. Multi-stressors effect

B.3.1. Specific multistressor effect size

We here introduce a generic formalism to describe stressor effects in complex systems such as phytoplankton communities or marine food-webs. The formalism specifically aims at relate (known) single stressor effects and trait dynamics to (unknown) multi-stressor effects. For doing so, we pinpoint possible determinants of the non-linear interaction between stressor reactions with special focus on internal re-organization of biological agents, termed adaptive trait dynamics, and the trade-offs ruling that dynamics.

Consider a –sudden– shift in the external variable or stressor, resp., E_n , which triggers a shift in the target variable μ (e.g. growth rate, or biomass) from the unperturbed value μ^0 ($\Delta\mu = \mu - \mu^0$):

$$\Delta_n\mu = \frac{\delta\mu}{\delta E_n}\Delta E_n \quad (\text{B.1})$$

where the differential $\frac{\delta\mu}{\delta E_n}$ formally expresses how sensitive μ reacts to external changes. In case of two simultaneous stressors $\Delta E_n, \Delta E_m$, we write the linear (Taylor) expansion of the total effect:

$$\Delta_{nm}\mu = \frac{\delta\mu}{\delta E_n}\Delta E_n + \frac{\delta\mu}{\delta E_m}\Delta E_m + \frac{\delta^2\mu}{\delta E_n\delta E_m}\Delta E_n\Delta E_m \quad (\text{B.2})$$

While the first terms can be related to single stressor effects which may be known from lab experiments, the last term describing the combined sensitivity to both stressors n and m is in general given neither from theory nor experiments. This sensitivity is here termed the specific multi-stressor sensitivity (SMS) :

$$\text{SMS} = \frac{\delta^2\mu}{\delta E_n\delta E_m} \quad (\text{B.3})$$

Under the (rough) approximation that the observed single stressor shifts $\Delta\mu_n$ and ΔE_n are similar to the respective contributions in the multi-stressor case,

$$\frac{\delta\mu}{\delta E_n} = \frac{\Delta\mu_n}{\Delta E_n} \quad (\text{B.4})$$

we obtain an expression for the specific multi-stressor sensitivity depending on (observed/-known) single-stressor responses $\Delta\mu_n$ and $\Delta\mu_m$:

$$\text{SMS} = \frac{\Delta\mu_{nm} - \Delta\mu_n - \Delta\mu_m}{\Delta E_n\Delta E_m} \quad (\text{B.5})$$

SMS is zero for additive effects, positive for synergistic and negative for antagonistic effects.

B.3.2. Effective interaction traits

The interaction trait x_n with respect to stressor n is defined as the sensitivity of the growth rate wrt the (perturbed) environmental variable E_n

$$x_n = \frac{\partial \mu}{\partial E_n} \quad (\text{B.6})$$

Note the similarity of the trait definition Eq. B.6 to the effect relation Eq. B.1. The first equation *formally* describes how the target variable (here growth rate μ) depends on marginal changes in an ambient factor, while the second quantifies the (again marginal) *realized* effect of μ when shifting that factor. Their respective value must not necessarily coincide because system effects such as compensation, synergies, adaptation will lead to a divergence between the formal dependency $\frac{\partial \mu}{\partial E_n}$ and the phenomenological dependency $\frac{\delta \mu}{\delta E_n}$.

Eq. B.6 in particular offers a simple and reasonable way of how to define effective trait variables. For example, if E_n denotes the grazer pressure, which in turn relates with predator concentration (Z), such that the growth rate includes a mortality term proportional to this concentration ($-g'Z$), x_Z is the negative proportionality factor, thus grazing rate per unit grazer ($-g'$). The factor is in general formulated as the product of edibility and relative ingestion rate, and is here termed the susceptibility to grazing.

In the second case considered in our study, E_m denotes the nutrient concentration ($E_m = N$); however, due to the indirect dependency of growth on N , the formalism gets more complicated. While uptake rate U is an explicit function of the ambient nutrient concentration ($U(N)$), here formulated using the affinity A ,

$$U = \left(U_{\max}^{-1} + (AN)^{-1} \right)^{-1} \quad (\text{B.7})$$

the (carbon based) growth rate depends on the internal and not external nutrient availability apart of the respiration term ($-\zeta U(N)$). Following the rationale outlined by [?], the marginal dependency can be derived by referring to the balance equation, such that we have

$$x_{N,i} \approx \frac{\partial \mu_i}{\partial Q} \frac{dQ_i}{dN} = \frac{\delta \mu_i}{\delta Q} \left[\frac{\partial U_i}{\partial N} - Q_i \frac{\partial \mu}{\partial N} \right] \cdot \left[Q_i \frac{\partial \mu_i}{Q} + \mu \right]^{-1} \quad (\text{B.8})$$

The nutrient usage ability, $x_{N,i}$ or its averaged trait form $x_N = C_T^{-1} \sum_i x_{N,i} C_i$ – with biomass C_i and total community mass C_T – incorporates three types of determinants of how a species or a community can cope with nutrient limitation: (1) The external dependency on nutrient availability that stems from the derivative term

$$\frac{\partial U_i}{\partial N} = U_i^2 (A_i N)^{-2} \cdot A_i \quad (\text{B.9})$$

predicts a diminishing x_N at high nutrient concentration - because of declining relevance of nutrient uptake. (2) The quota dependency of carbon based growth, $\frac{\partial \mu_i}{\partial Q}$, similarly scales down

the relevance of nutrient uptake traits at high internal stores. This physiological determinant reflects a delay moment in the description of nutrient limitation as internal stores may decouple from ambient nutrient level at the scale of hours to weeks. (3) At low nutrient availability with $U_i \approx A_i N$, x_N becomes proportional to the nutrient affinity, which is a classical trait describing nutrient uptake ability.

B.3.3. Cross-over trait sensitivity and trade-offs

A major hypothesis underlying our approach is that the phenomenological dependency $\frac{\delta\mu}{\delta E_n}$ can be approximated at first order by the formal stressor dependency $\frac{\partial\mu}{\partial E_n}$, i.e.

$$\frac{\delta\mu}{\delta E_n} \approx \frac{\partial\mu}{\partial E_n} = x_n \quad (\text{B.10})$$

This relation entirely focusses on the trait mediated response and neglects system feed-backs. However, the approximation allows for a derivation of the specific multi-stressor sensitivity in terms of interrelated changes in trait, which in turn reflect morphological or physiological trade-offs. The SMS follows from combining Eq. B.3 and Eq. B.10 by applying another perturbation ΔE_m and repeat the procedure with a different sequence of stressors, thus perturbing x_m w.r.t. to stressor E_n .

$$\text{SMS} \approx \frac{\delta x_n}{\delta E_m} + \frac{\delta x_m}{\delta E_n} \quad (\text{B.11})$$

This procedure implies that the difference is taken from an already perturbed state instead from the ground value as in the previous formalism. The procedure and its outcome is here denoted as the cross-trait variation (CTV):

$$\text{CTV} = \frac{x_{nm} - x_m}{\Delta E_m} + \frac{x_{mn} - x_n}{\Delta E_n} \quad (\text{B.12})$$

The cross-over terms describe how the effective interaction traits are modified by other stressors such as the possible alteration in susceptibility to grazing due to nutrient stress and the alteration in nutrient usage ability due to grazing. Inherent to these changes are trade-offs, thus relations between different traits. For phytoplankton communities, susceptibility to grazing x_Z is linked to nutrient usage ability x_N since both traits depend on the size structure of the community. Therefore, adaptation in x_N will induce a change in x_Z too. This change will increase with the strength of the trade-off and is inherent to the terms $\delta x_Z / \delta N$ and $\delta x_N / \delta Z$. It is in principle possible to calculate the cross-trait variations based on the formulations underlying the size-based model.

A first major outcome of this study, in mathematical terms, is the similarity between specific multi-stressor sensitivity and cross-over sensitivity in effective traits:

$$\text{SMS} \approx \text{CTV} \quad (\text{B.13})$$

According to this hypothesis, synergistic effects occur at positive cross-variations in traits, thus, when effective traits shift to higher values under application of complementary stressors (e.g., increasing nutrient usage ability under grazing removal). This re-organization within the community will in general require some time so that a second prediction of our theory is a transition from antagonistic to synergistic multi-stressor effects over time.

B.4. Supplementary figures

B.5. Mono species scenario

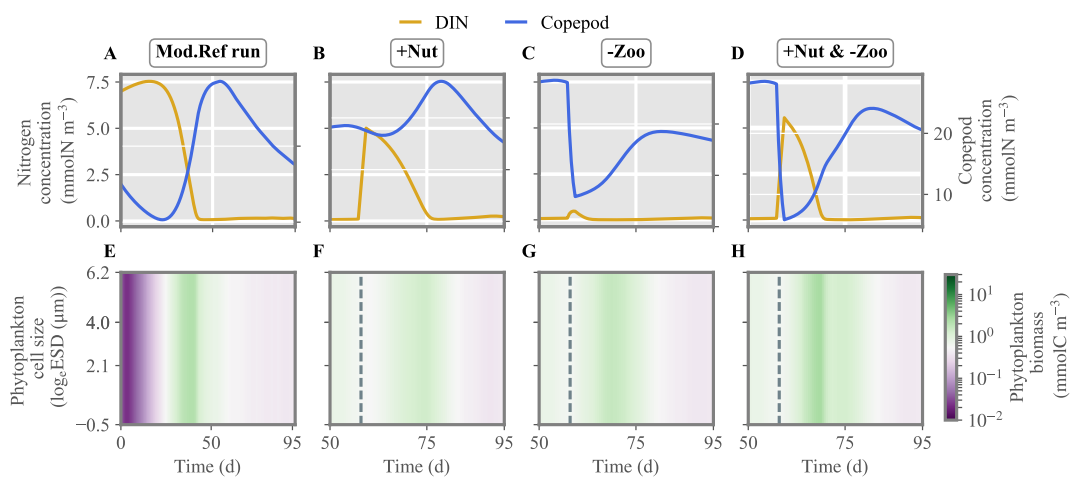


Figure B.5.1.: Nitrogen concentration, copepod biomass and phytoplankton biomass distribution under single / multiple stressors. +Nut and -Zoo represent two stressors corresponding to nutrient enrichment and grazer removal. Dashed lines indicate the time of nutrient injection, zooplankton removal or both.

B.6. Sensitivity analysis

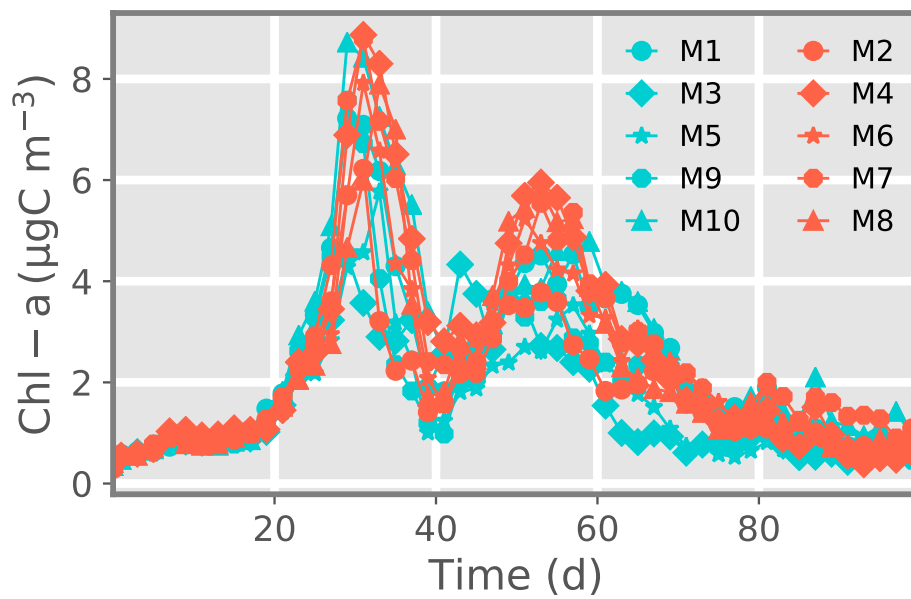


Figure B.6.1.: Measured Chl-a for 10 Kristineberg mesocosms from [5]. Red and blue indicate High CO_2 and low CO_2 conditions respectively.

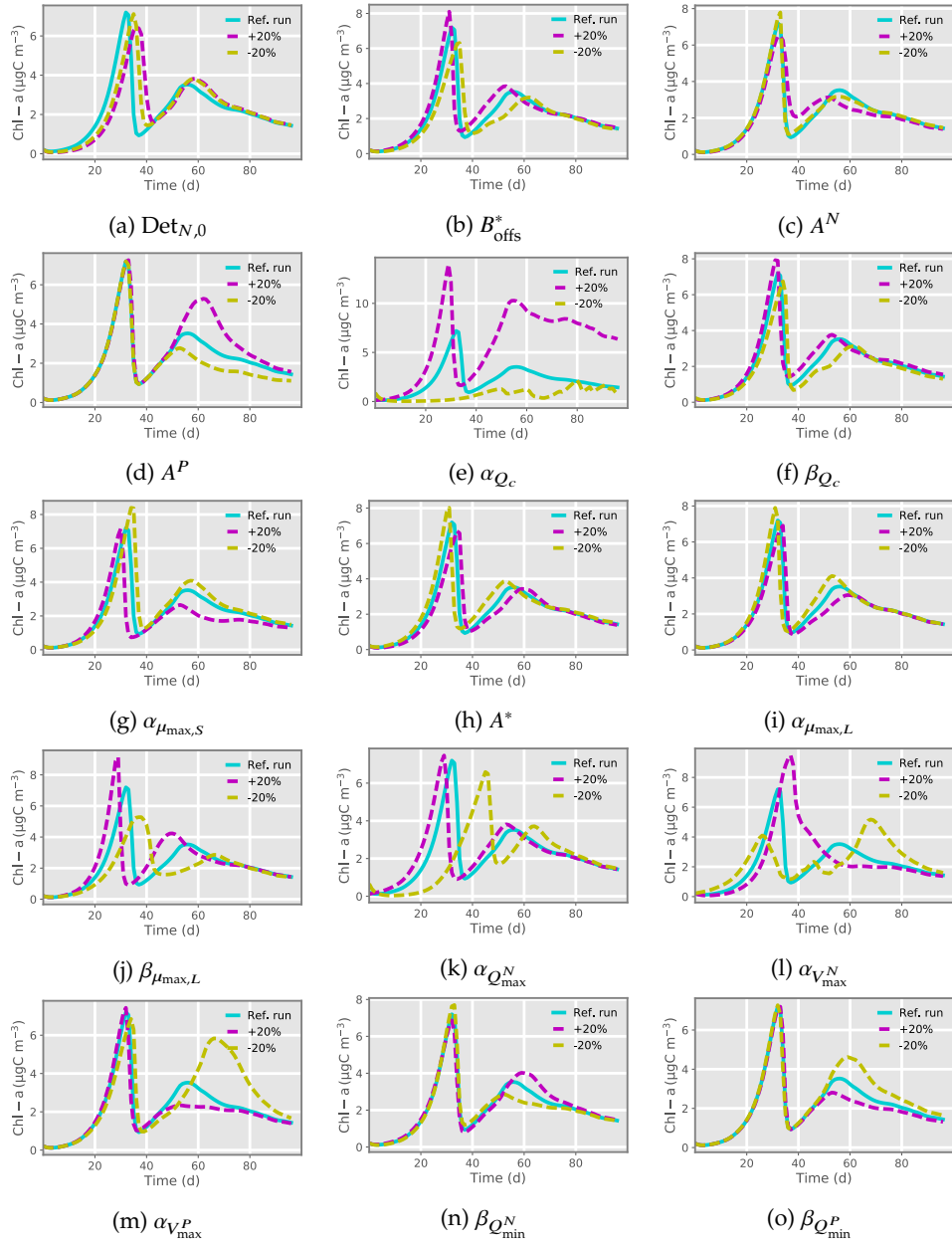


Figure B.6.2.: Sensitivity analysis for Chl simulated in the reference configuration for low $p\text{CO}_2$ condition. Parameters are varied by $\pm\%20$ of their original value. Descriptions and reference values of the parameters are listed in Tables B.7 and B.5.

C

Appendix III

C.1. Individual mesocosms

Even though copepods seems to benefit from CO₂ treatment in the Kristineberg experiments, the connection between copepod abundance and phytoplankton biomass seems to be independent from CO₂. Taking measurements from day 49 and 57 of the experiments, we see a positive correlation between chlorophyll a and copepod abundance. This supports the model results that nutrient excretion by copepods amplifies phytoplankton growth in the post-bloom phase.

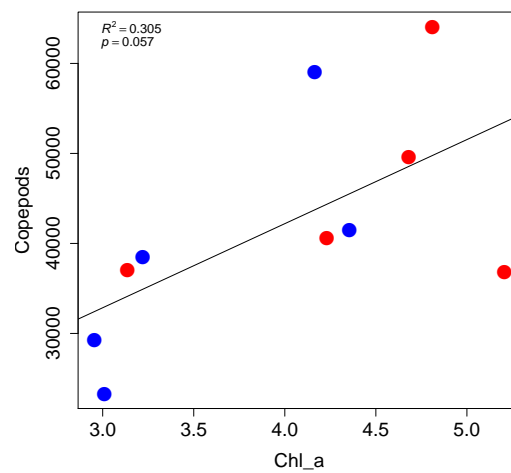


Figure C.1.1.: Mesocosms with high Chl_a show a higher abundance of copepods during the second bloom. Zooplankton abundance data are available for day 49 and 57. We used the mean of both days for copepod abundance and Chl_a (μgC m⁻³). Red dots indicate treated mesocosms, blue dots indicate control mesocosms.

C.2. *Coscinodiscus* dynamic

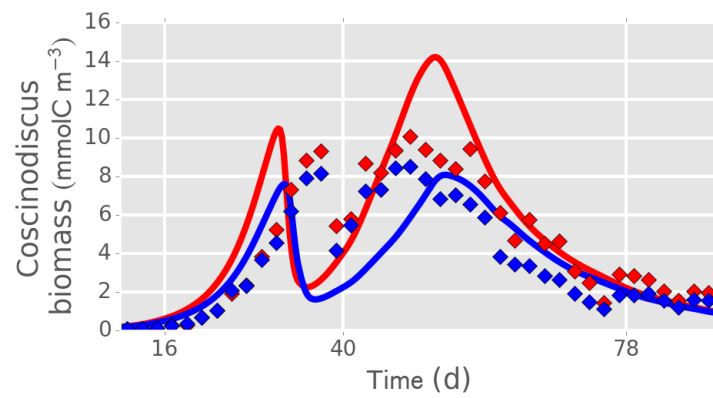


Figure C.2.1.: Comparison between simulated and measured data for treated (red) and untreated (blue) environments. Simulation results indicate all species larger than 200 μm ESD. Solid lines indicate simulated results and diamonds represent measured data.

Curriculum Vitae

Niousha Taherzadeh

nioushatz@gmail.com

Nationality: German-Iranian

Hometown: Munich

Education

Ph.D candidate in Ecosystem Modelling, Nov 2014 - Feb 2018
Ecosystem Modelling group, Institute of Coastal Research
Helmholtz-Zentrum Geesthacht (HZG), Geesthacht, Germany

M.Sc in Environmental Engineering, Apr 2011- Sep 2013
Faculty of Civil, Geo and Environmental Engineering
Technical University of Munich (TUM), Munich, Germany

B.Sc in Environmental Engineering, Oct 2005 – Jan 2011
Faculty of Environmental Engineering
Middle East Technical University (METU), Ankara, Turkey